INTRODUCTION

1.1 Background and Motivation

Underground structures are used for variety of purposes including subways, railways, material storage, sewerage and water transport, culverts, large diameter pipelines and ducts for nuclear power plants. Compared to other kinds of structures, these underground structures have been considered to be relatively safer during the event of earthquakes. This faith is the result of the statistics of good performance records in the past earthquakes. This belief has continued to make its roots in the engineers' mind until the 1995 Hanshin-Awaji earthquake (Kobe earthquake). The Kobe earthquake witnessed severe damage and complete collapse of several subway stations belonging to Kobe metropolitan subway line (An, 1997; Samata et al., 1997; Para-Montesinos et al., 2006). Severe damages have also been reported in 1999 Chi-Chi earthquake and 1999 Kocaeli earthquake (Hashash et al., 2001). These events have not only challenged the engineers belief, but has also raised the serious questions regarding the safety of the underground structures during earthquake, which were once considered to be among the safe structures. Triggered by this event, several researches have been conducted all around the world to access the safety of the underground structures in the event of earthquakes (An, 1997; Samata et al., 1997; Gazetas et al., 2004; Liu and Song, 2005; Nishioka and Unjoh; Para-Montesinos et al., 2006).

In Nepal, some of the underground structures have been constructed and some are underway to construction. The pedestrian Subway at the Bhotahity of the Kathmandu Metropolitan City is a typical example of the underground subway structures constructed in Nepal. Being a mountainous country there is a lot of scope that underground structures are needed to be constructed all around the country for fulfilling various infrastructure needs such as transportation, conveying drinking water, sewerage, and so on.

Recently, the SIKTA Irrigation project has been undertaken. The project consists of one three-chambered underground Reinforced Concrete (RC) Covered Canal for conveying the water from head works to the downstream open irrigation canal. The SIKTA irrigation project is situated in Banke district of the Mid Western Development region. The project would irrigate 34000 hectares of land in the district.

SIKTA Irrigation project is a national project undertaken by the government of Nepal costing billions of rupees. The Nepal government has given high priority to the implementation of the large-scale SIKTA irrigation project. The overall goal of this irrigation project is to contribute to national development objectives of the government and also to improve the living conditions of the people of Banke district. The total financial cost of the project is approximately NRs. 7.3 billions. The importance of the underground RC Box structure of this project can be realized from the fact that this structure is the medium of flow of water from head works to the open canals on the downside of the system. The loss of serviceability of this particular structure makes the entire irrigation system ineffective. As we know that construction of civil infrastructures such as this one costs millions and billions of rupees, we can't afford to build such kinds of structures rather frequently. Thus the safety and serviceability of this structure is a key issue in the successful performance of the whole project during its entire life span.

It is a well-known fact that Nepal lies in one of the world's most seismically active region. The Himalayan range is the youngest mountain range on the earth. It was formed by the convergence of the Indian plate below the Tibetan plate. The Indian plate is constantly moving to the north and converging below the Tibetan plate by 20 mm annually and therefore the building process of the Himalayan range is still under progress. This process of convergence of the two plates is known as the tectonic activity, is the cause of the earthquakes in this region (Upreti, 2001).

All kinds of structures that are to be constructed in Nepal should be designed taking into the effect of earthquakes. In light of the damages that occurred in underground structures in recent times around the various parts of the world, safety of these underground structures has become a prime concern. A detailed investigation of the seismic performance of the structures that is currently underway construction and the structures that are to be constructed in future have to be made.

To access the safety and serviceability of the structure, real structural behavior has to be understood. To access the real structural behavior, traditional linear analysis and design would not suffice. A rigorous nonlinear analysis has to be performed. At least, evaluation of the performance of the traditionally designed structure has to be made

using nonlinear analysis techniques for evaluating its performance so that safety and serviceability can be guaranteed, which is essential for its good structural health. Furthermore, reinforced concrete is a highly nonlinear material. Without the aid of nonlinear analysis tool, we will not be able to access the real behavior of RC structures. These days, due to the development of powerful computing capabilities, nonlinear dynamic analysis has become a powerful tool for simulation and performance assessment of the RC structures in offices (Maekawa et al., 2003).

1.2 Problems and Issues

Owing to the good performance records of underground structures in the past, only limited amount of researches have been conducted in this area. As a result, there is a lack of rational methodology and codes required for the analysis and design of these structures. For this reason, there exist considerable differences among the engineers regarding the design philosophy, loading criteria and methods of analysis (Wang, 1993). In our Indian subcontinent, virtually no such studies have been undertaken. No codes and recommendations are available yet in this region. Until recently, draft code for underground buried pipelines for oil, gas, water, etc, has been prepared by IIT, Kanpur as a part of project GSDMA (Dash and Jain, 2007). A very limited recommendation on seismic design of underground structures have been made in IS 1893:2002. The IS 1893 (Part I): 2002, clause No. 6.4.4, recommends to take design horizontal acceleration spectrum value as half of the design horizontal seismic coefficient Ah for the underground structures and foundations at depths greater than or equal to 30 meters. It further instructs to linearly interpolate the value for the acceleration spectrum value for the structures and foundations placed in between the ground level and 30 meters depth. Also, though the IS 1893:2002 code have been split into five parts, none of the parts deals specifically with the underground structures. Similarly, NBC 105: 1994 code provisions are limited to buildings up to 90 meters in height and elevated water tanks p to 2000 cubic meters capacity. The code is not intended for application in other civil engineering structures. Therefore, it could be concluded that we do not yet have any comprehensive code provisions and documents to deal with the underground structures in our Indian subcontinent. However, with regards to the complete collapse of the underground structures in Japan during 1995 Kobe earthquake and the construction of the underground structures being undertaken

recently in our region also, we are in a urgent need for studying and evaluating the effect of earthquake in these kind of structures.

1.3 Objectives and Scope of the study

1.3.1 Overall Objective

The main aim of carrying out this research work is the performance assessment of underground RC structures subjected to severe ground motion due to earthquakes. The research work is limited to analysis of Covered Canal. The study considers the tunnels constructed at shallow depths only. Similarly, the hydrodynamic effects have not been considered in the analysis.

1.3.2 Specific Objectives

The specific objectives of this research work are as follows:

1. Evaluate the performance of RC Covered canal subjected to strong ground motion due to earthquakes.
2. To investigate the coupled effect of various conditions of water level, viz. full, empty and partially full, and earthquake force on the behavior of the intended structure.
3. To investigate the performance of the covered canal on the multi-layered soil profile.
4. Identification of the critical location in the covered canal.

1.4 Methodology

The nonlinear dynamic finite element analysis of RC-Soil system under the seismic excitation was carried out using the software WCOMD. Through nonlinear analysis taking into account the soil-structure interaction in time domain, the effect of earthquake ground motion on the intended structure has been carried out. Accordingly, to achieve the specified objectives following tasks has been carried out:

1. Covered Canal of SIKTA irrigation project is taken as the case for carrying out the intended study.

2. The necessary loading data, geotechnical investigation reports and drawings are collected from the project office, department of irrigation, Jawalakhel, Lalitpur, Nepal.
3. A number of coupled nonlinear analysis of the RC-Soil system was then carried out to determine the lateral extent of the soil mass to be considered for simulating the semi-infinite soil mass.
4. After having determined the extent of the soil mass to be considered in the analysis, the coupled nonlinear analysis of the RC-soil system model was prepared.
5. With the basic model prepared, the effect of the various conditions of the water levels, viz., full, empty and partially full was investigated. Altogether six different conditions of water level were considered.
6. To further investigate the performance of the covered canal, the analysis was performed for different combinations of the soil profiles. The number of soil layers and the soil properties taken was both limited to three, equal to that of the original case for all combinations of the soil profiles. Altogether eleven different conditions of soil profiles have been generated for the intended study.
7. The critical locations in the covered canal were also determined.

1.5 Organization of the thesis

The contents of this thesis have been divided into seven chapters as follows.

Chapter 1 presents the introduction to this research work. The motivation and scenario behind this research work is explained in this chapter. Similarly, the scope, objectives and limitations of are also listed. The methodologies used are also described in this chapter.

Chapter 2 provides the literature review related to the past researches on underground structures and description of soil-structure interaction problems. The chapter also discusses the various issues in finite element modeling of the soil-structure system and discusses various methodologies used by different authors for finite element modeling of soil-structure interaction problems.

Chapter 3 describes the dynamic finite element analysis of the coupled RC-Soil system. The constitutive model for soil that has been adopted in the analysis is

explained in this section. Also, the constitutive model for joint element is presented here.

Chapter 4 is concerned with the numerical analysis of the covered canal. The geological profiles, geometry of the structure, material properties, input static & dynamic loads and different analysis cases, all are described in this chapter.

Chapter 5 presents the results of various parametric studies that have been conducted during the research work.

Chapter 6 presents the conclusions drawn after carrying out the research and also presents the interpretation of the obtained results.

Chapter 7 gives the list of topics that can be considered for the future research works.

2 LITERATURE REVIEW

2.1 Soil - Structure Interaction

(Rosenblueth, 1980; Kramer, 1996; Kausel, 1983)

If the motion at any point on the soil structure interface differs from the motion that would occur at the same point in the free field if the structure was not present, there is an interaction between the soil and the structure and is referred to as soil-structure interaction. There are two reasons for this difference in the motion. First reason is the inability of the structure (substructure) to comply with the free field deformation. The second reason is that the dynamic response of the structure itself will also induce the deformation of the supporting soil. There are in general two approaches to analysis of soil-structure interaction effects: the direct approach (Single Step) and the multi step approach. In the direct approach (often referred to as total solution), the entire soil-structure system is modeled and analyzed in a single step. The analysis may be done in time domain or frequency domain. In the time domain analysis, the system of differential equation is solved directly through step-by-step integration with respect to time. In frequency domain analysis, transfer function of any desired effect is obtained by solving at each frequency. System of algebraic equations and time history response is then computed through the use of Fourier transforms. The time domain analysis allows the treatment of nonlinear behavior of the material whereas the frequency domain analysis is limited to linear problems only. In the multi step approach, the analysis is divided into two parts: kinematic interaction and inertial interaction. The total solution is then obtained by the superposition of the two effects. As the method relies on the superposition principle it is limited to linear problems only.

2.2 Seismic Bed Rock

(Tadanobu, 2000)

Bedrock is a relatively hard solid rock that underlies softer rocks, sediments and soils. The location of this bedrock can be at the depths of few kilometers to several hundreds of kilometers from the ground surface. While conducting the soil-structure interaction analysis we need to locate the bedrock. But consideration of this bedrock at the actual depths is not practical because it is very difficult to investigate the properties of the soil layers at these large depths. Further, when conducting the

analysis using the numerical techniques such as FEM, it is practically not possible to construct huge mesh incorporating such depths. For this reason, a simple concept of the seismic bedrock has been developed. This seismic bedrock does not necessarily coincide with the geological bedrock. Several proposals have been developed for setting the seismic bedrock. However, there is a lack of uniformity in the treatment of the seismic bedrock. The deepest seismic bedrock has been set at the layer of granite experiencing a shear wave velocity of 3 kilometers per second. Similarly, the shallowest seismic bedrock has been set for a layer having N value of about 50 (Japanese SPT value). The consideration of this seismic bedrock is also dependent on the objective of the investigation that is to be carried out. The philosophy behind the setting of the seismic bedrock is quite simple. Seismic bedrock is a physical boundary that separates the effect of the localized soil conditions at the point of observation from the other factors affecting the ground motion. In conclusion, we can say that the setting of the seismic bedrock depends in the objectives of the analysis, analytical model used, importance of the structure and other engineering considerations.

2.3 Finite Element Modeling Issues

Today, finite element technique is the most widely used numerical technique for solving various kinds of structural problems including underground structures. The two and three-dimensional dynamic response analysis and the soil-structure interaction problems are usually carried out using the dynamic finite element analysis (Kramer, 1996). Despite of its wide use, extreme care has to be exercised during the formulation of the problem for arriving at the acceptable solution. Further, the solution is always approximate and is subject to careful interpretation. While dealing with underground structures which has to take into account the soil-structure interaction effects, factors such as size and shape of the elements, modeling of the internal damping of energy dissipation and reproduction of semi-infinite soil mass through the use of appropriate boundary condition in a finite domain of finite elements have to be considered (Kramer, 1996; Kausel, 1983; Maekawa et al., 2003).

Discretization Considerations (Kramer, 1996; Kausel, 1983): The use of coarser mesh can result in the filtering of high frequency components whose short wave length cannot be modeled by widely spaced nodal points. However, it is possible to use

larger elements far away from the region of interest at a considerable distance from the structure.

Far field Effect (Rosenblueth, 1980; Kramer, 1996; Kausel, 1983; Maekawa et al., 2003): Determination of lateral extent of soil mass and selection of appropriate boundary condition to simulate the behavior of semi-infinite soil domain with a finite domain of finite element mesh is an important factor that should be considered in the analysis of soil-structure system. The lateral extent of the soil mass should be such that there is a considerable length of soil beyond which free field deformations are recovered. This fact is clearly depicted in the figure 2.1 (Rosenblueth, 1983).

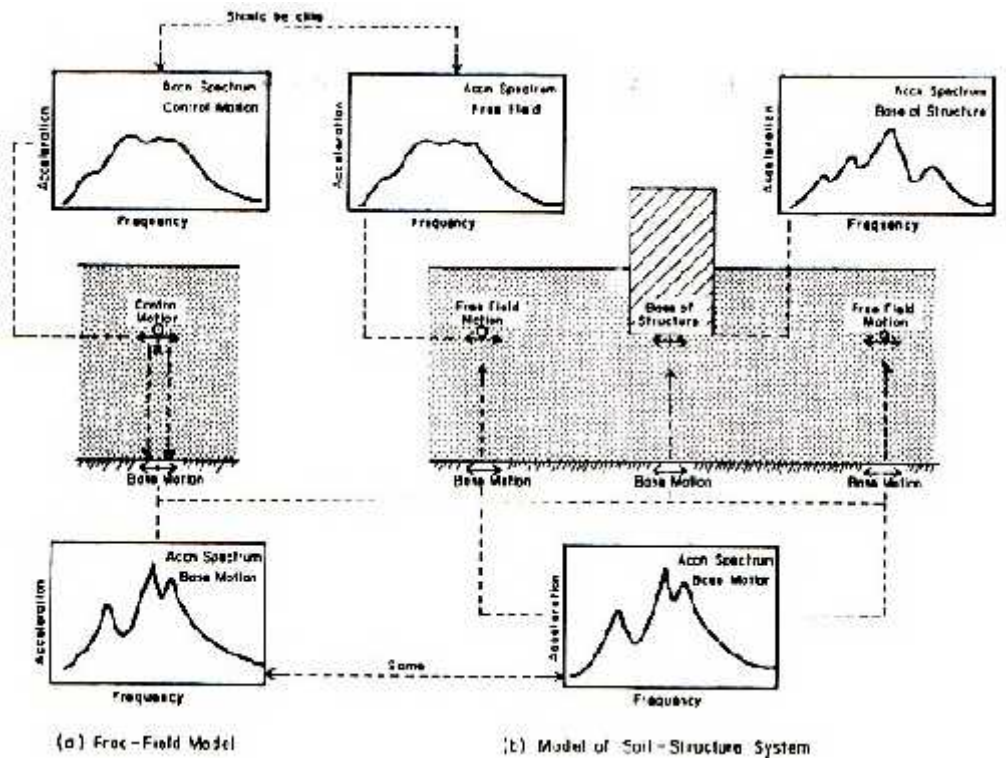

Figure 2.1: Soil- Structure Interaction Model

Regarding the type of boundary to be used, conventionally there is a tradition to use hinge or roller support at the lateral boundaries. These supports do not correctly represent the transmitting boundary. Transmitting waves are perfectly reflected back into the domain after reaching the supports and no energy is transmitted out of the domain. There is a tendency to neglect this factor by asserting that the effect may be neglected by placing the boundary far away from the structure. Adopting this strategy,

although the effect gets reduced as the domain becomes larger, this often leads to a very large mesh demanding a tremendous amount of computer speed and memory. To solve this problem Wolf proposed the superposition boundary where the total solution is decomposed into symmetric far field boundary and anti symmetric far field boundary. The soil-structure system needs to be analyzed twice for each of the two different boundary conditions. An (1996) used this approach for the analysis of the underground subway stations, the Daikai and Kamisawa station located in Kobe using the software WCOMD. To make the problem computationally efficient, An (1996) developed a strategy of overlapping of two narrow boundary zones with complementary boundary condition corresponding to the symmetric and anti symmetric far field boundary conditions. The system was installed in the software WCOMD. The boundary condition is depicted in figure 2.2.

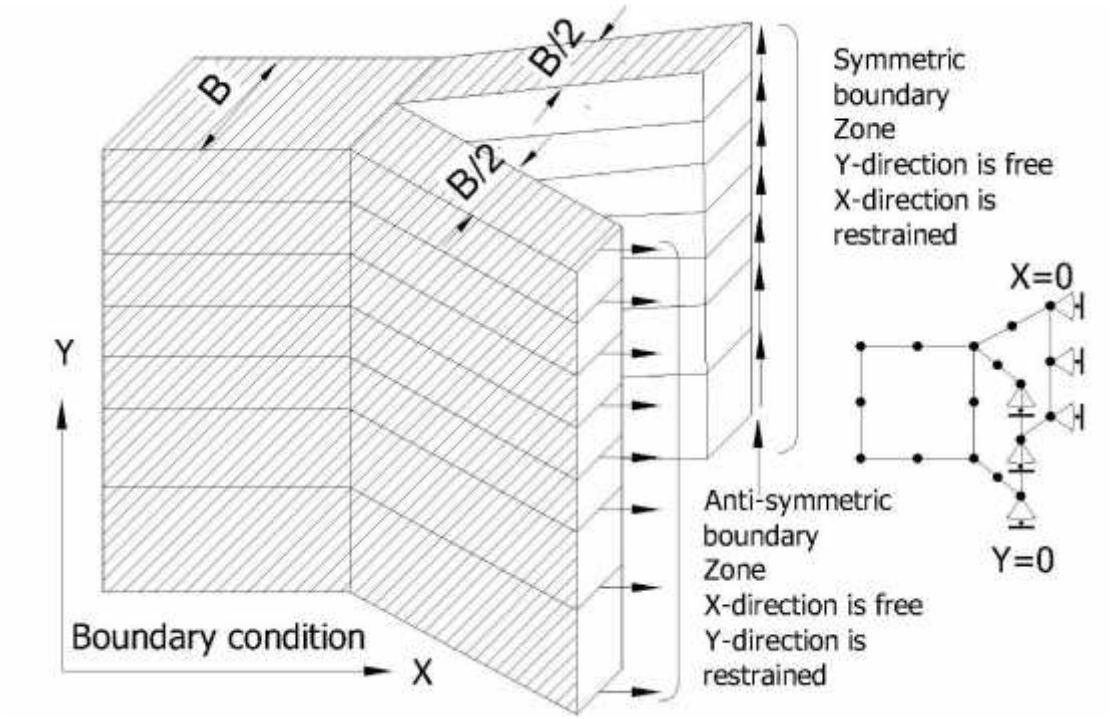

Figure 2.2: Mixed Artificial Boundary condition attached to the main mesh

This boundary condition was attached to the main mesh of the soil-structure system. Each boundary zone has got half of the total stiffness and mass. The wave that propagates from the main mesh enters the two boundary zones simultaneously. After reflection at the artificial boundary the amplitude of the waves reflected back to domain will have same magnitude but opposite sign and thus cancel each other. This

results in zero energy transmitted back to the main mesh simulating the far field boundary condition roughly. The total length of the domain is checked so that the whole domain can dissipate almost all of the energy from the main mesh to the far field.

2.4 The physics of the Symmetric and anti symmetric lateral boundary condition

Consider a wave pulse advancing along the string with one end free and other end fastened at the rod (support). If the support is fixed, the wave pulse must remain at rest at the support. The wave pulse arriving at the support then exerts a force; the result is that the reaction force kicks back on the string and sets up a reflected pulse traveling in opposite direction. The nature of the reflected pulse is shown in the figure 2.3 (a). Similarly, if the support is free to move in transverse direction (the string is tied to a light ring that slides on a smooth rod), the wave pulse arriving at the support causes the end to overshoot and sets up the reflected wave in opposite direction (Sears et al., 1985). The nature of the pulse is shown in the figure 2.3 (b).

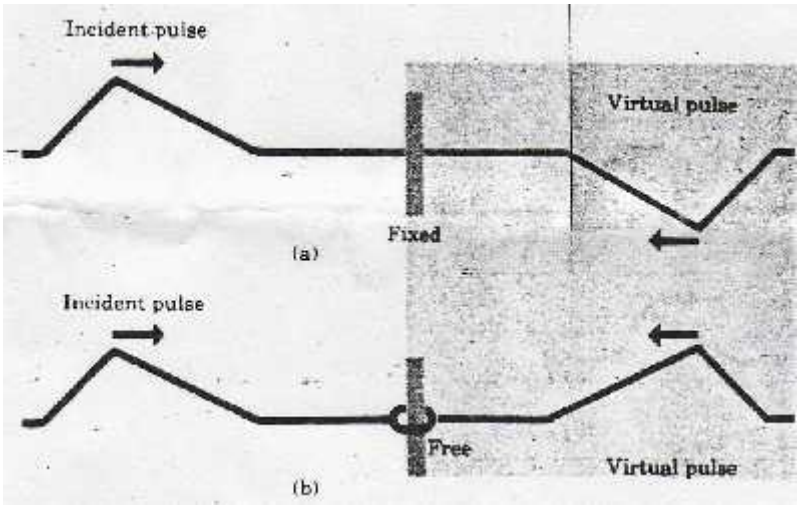

Figure 2.3: Nature of the pulse (a) at a fixed end of a string, and (b) at a free end, in terms of imaginary virtual pulse

It is evident from the figure that the nature of the reflected pulse in the two cases is exactly opposite. Thus when the two reflected waves are superposed, they cancel out each other, the result being no wave pulse traveling back along the string.

Wolf proposed this kind of strategy for evaluation of soil-structure interaction problems (Maekawa et al., 2003). This strategy has been adopted by An (1996), and employed in the software WCOMD as explained in section.

2.5 Soil-Structure Interface

(Tadanobu, 2000; Maekawa et al., 2003)

The soil and structure have got different nonlinear behavior and stiffness characteristics. During the static loading conditions, the soil and structure are in complete contact due to horizontal earth pressure that exerts on the structure. However, during the earthquakes, due to differences in the characteristics of soil and structure these two do not displace equally. Thus, complete contact at the interface is not ensured. The sliding and separation between the soil and structure occurs along the interface. In order to account for this phenomenon, model for RC-Soil interface is required. Various kinds of interface elements have been developed. These interface elements expresses the relationship between the stresses transmitted at the interface and relative displacement.

2.6 Joint Element

(Tadanobu, 2000; Maekawa et al., 2003)

The soil-structure interface can be modeled using the joint elements. Shear springs having a spring constant Ks and normal spring having a spring constant Kn are used to express the characteristics of these elements. The ideal constitutive relationship of the joint elements is shown in figure 2.4. Similarly, the constitutive relationship used for joint element used in the numerical analysis is shown in figure 2.5. In the ideal relationship both Ks and Kn become infinite and henceforth, the numerical computation becomes infinite. Thus, for carrying out the numerical computation, the values of these spring constants have to be set finite and as large as possible. The normal stress/strain relationship is assumed to be bilinear for opening/closure mode. The normal stress is zero incase of separation and when the soil and structure is in contact a large value of the stiffness is sufficient to avoid overlap of elements is assigned.

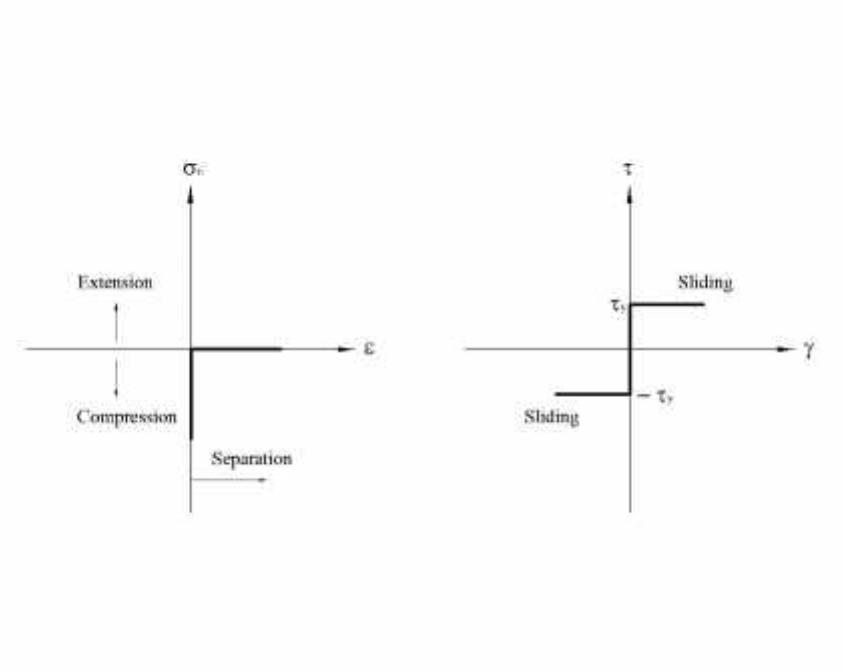

Figure 2.4: Ideal Constitutive relationship of Joint element

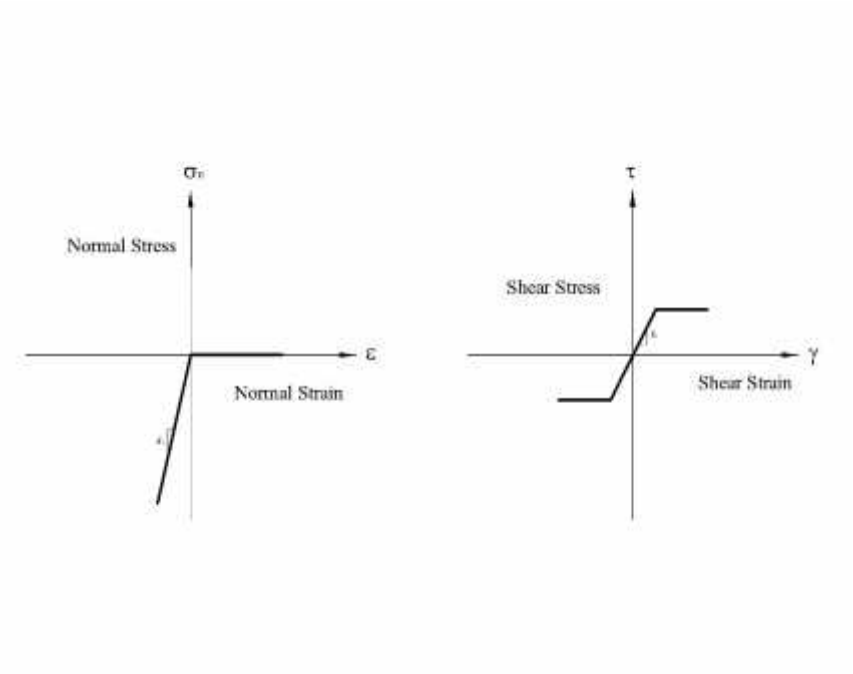

Figure 2.5: Constitutive relationship of Joint element used in numerical analysis

The shear stress/strain relationship is expressed by a linear relationship representing the sliding mode in which also large value of shear stiffness is assigned.

2.7 Past Research on Underground RC Structures

An (1996) conducted nonlinear dynamic finite element analysis for determining the cause of the collapse of Daikai subway station and Kamisawa subway station during the 1995 Kobe earthquake. Nonlinear finite element software WCOMD-SJ was used for carrying out the study. Before this earthquake there were no records of such kind of complete collapse, although many of the underground structures have sustained some damages. Along the Kobe subway line, the Daikai subway station collapsed whereas the adjacent tunnel section was intact. The cause of collapse was failure of the intermediate column, as a result of which the top slab collapsed. The Kamisawa station is the two storey RC Box structure with intermediate columns. During the earthquake, the intermediate columns of the upper deck collapsed.

The soil profile around the Daikai station and tunnel sections consists of soft soil layers of clay, sand and gravels having SPT-N below 20. Similarly, the soil profile around the upper deck of Kamisawa station consists of soft sand and clay layers with SPT-N not exceeding 20, while the soil layers around the lower deck are somewhat stiff layers of sand and clay with SPT-N up to 45.

For the study of Daikai station, three different kinds of earthquake waves that were measured at different locations during the 1995 Kobe earthquake have been used. These three waves are the waves measured at Kobe Meteorological Observatory, Higashi-Kobe Bridge and Amagasaki City close to the station. Out of these three waves, the Daikai station collapsed under the Kobe Wave measured at Kobe Meteorological Observatory. Similarly, the Kamisawa station was also studied under three different waves, namely, waves measured at Kobe meteorological Observatory, artificial seismic wave generated for Koutouen area and Amagasaki wave. The station failed under both Kobe and Koutouen wave while, it survived under Amagasaki wave. These numerical analysis results confirmed the collapse of these stations during the event. The main cause of collapse of these stations was the collapse of the intermediate columns. The intermediate columns of Daikai station failed with maximum normalized displacement of 1.5 % and maximum shear stress of 16 kgf/cm2. The tunnel section survived with the maximum normalized displacement of 1.0 % and maximum shear stress of 7 kgf/cm2. Similarly, the upper columns of the

Kamisawa station failed with the maximum normalized displacement of 0.8 % and maximum shear stress of 18 kgf/cm2. The lower columns had induced shear stress of only 12 kgf/cm2. In Daikai station, it was found out that the induced shear stress of Amagaski wave was about two times than that of Higashi-Kobe wave although the peak acceleration in both cases is almost equal. This shows that the shear stress not only depends on the maximum acceleration but also on the characteristics of the wave. The response of the column was found to be dependent on the variation of the compressive stress induced in the column. This variation of the compressive stress was in turn dependent on the vertical component of the earthquake wave. To investigate this the analysis of the section was carried out by applying only horizontal acceleration. The analysis showed that this vertical component has little to do with the failure mode and dynamic response and hence is not the primary cause of collapse. However, ductility of the structure increased when vertical component was ignored. To further investigate the effect of the induced compressive stress on the ductility of the structure interaction diagram of the axial force versus ductility was plotted by analyzing a single RC column and the whole structure under statically applied combination of compression and shear. The dynamic responses were also plotted in the diagram. The plot showed that for section A, dynamic response reached the capacity envelope of the structure whereas for section B the response was well within the envelope. The results show that increase in the compressive stress reduces the ductility. To investigate the inter-relation between the compression capacity, shear capacity and ductility, three parametric studies were conducted: by increasing both flexure and shear capacity, by increasing shear capacity, and by decreasing flexural capacity & increasing shear capacity. The study showed that increase in the main reinforcement is not the suitable method as it decreases ductility of the overall structure. Increasing web reinforcement is the effective way of increasing the shear capacity and ductility. And, decrease in flexural capacity while increasing the shear capacity is the most economical way of increasing ductility.

It has been pointed out in this research that combination of the horizontal and vertical acceleration may change the dynamic response of the structure such as failure location. The effect of the soil profile has also been addressed to some extent in this research. It has been deduced that the softer foundation can cause larger shear damage. In conclusion, this research revealed that the level of the seismic excitation

the underground stations experienced was beyond the expected design values of the earthquake loads considered during the design. The structural ductility and energy absorbing capacity of the intermediate columns were found to be insufficient. In addition to shear capacity and ductility, the compression capacity also plays an important role in the safety of the underground structure.

Gazetas, et.al (2005) have carried out the response studies of the three metro underground structures in Athens that were subjected to 1999 Parnitha earthquake. The three underground structures are: just completed cut-and-cover Sepolia station, tunneled station of Monastiraki and temporary prestressed-anchor piled wall of the abandoned Kerameikos station. An accelerograph recorded the ground surface motion at the Monastiraki station. Similarly, two numbers of accelerograph recorded the free field and the station-base motion at the Sepolia station. The temporary prestressed-anchor piled wall produced a record of seismic displacement at its top. By utilizing these available records, numerical analysis were carried out to study the response of these underground structures, which performed well during the earthquake. During the study particular emphasis was given to Sepolia station. The Sepolia station experienced peak accelerations of 0.18g at its base and 0.45g at the roof, which were almost exactly equal to design accelerations. Similarly, the successful performance of two temporary structures in Monastiraki and Kerameikos, which were not designed for earthquake loads also have been investigated. These structures have experienced accelerations of order 0.5g during the earthquakes. The records of the accelerographs at the Sepolia and Monastiraki stations are used for determining the base motion of the respective stations through inverse analysis procedure known as deconvolution. The rock outcrop KEDE record is used as the base motion for the analysis of retaining wall of Kerameikos station. The accelerograph records at the Monastiraki station showed a very high PGA of order 0.51g in one direction. The record has very low dominant period of 0.08 to 0.17 seconds. In spite of this high value of PGA recorded at the station, smaller degree of damage was seen in the vicinity of the station. It was suspected that the presence of a deep shaft of an underground construction, heavy-walled shallow tunnel of the old metro line and 5m deep open archaeological excavation may have influenced the peak ground acceleration at the record station. Confirmation to this behavior was made by carrying out an inverse procedure (deconvolution) using the finite element method, with the record under investigation

being the target surface motion. The soil profile comprises of stiff sandy clays and highly weathered rock formations down to at least up to 60 m depth. Equivalent linear soil properties were assigned to the soil elements. One dimensional equivalent linear wave propagation analysis was performed taking into account the decrease of the shear modulus and increase in material damping with increase in the amplitude of shear strain. Then two-dimensional wave propagation analysis was conducted using the equivalent strain compatible soil parameters obtained from the 1D analysis. The typical soil profile at Sepolia station comprises of 6.7 m thick sandy to silty clay layer followed by 6 – 8 m thick stiff sandy clay layer with gravels and then followed by 10 –13 m thick layer of locally fractured conglomerate/ Anthenian schist. An inverse procedure similar to the one used for Monastiraki station was employed here also. The analysis was validated by comparing the recorded the computed accelerogram. The lateral boundaries were placed as far as computationally possible to simulate the semi-infinite soil mass. The results indicated that the Sepolia station was severely shaken during the earthquake. The roof acceleration was found to be 0.45g and the station base acceleration to be 0.19g. These computed accelerations were found to be almost equal to the design accelerations, which is as matter of fact, just a coincidence. Although the structure experienced high value of acceleration, the internal forces developed to be significantly lower than the capacity of the structure. It has been deduced that the soil-structure interaction has affected the response of the structure. The results have been compared with the results of the Daikai station that collapsed in 1995 Kobe earthquake. The good performance of this station has been attributed to a number of factors. The seismic loading is of lower order. The soils of the Sepolia stations have SPT value from 15 to 50, i.e., the soils are stiffer. The station has only 1 m of the overburden. Further, Daikai station was not designed as per modern capacity design method whereas this station has been designed as per capacity design approach.

The temporary prestressed-anchor plied wall of Kerameikos station also performed well in the event. The good performance of this wall can be attributed to the combination of the flexibility of this wall and the stiffer retained soil leading to minimal dynamic earth pressure. The maximum dynamic axial forces in the anchors were also found to be small. Further, high frequency content of the ground motion has also played significant role in the good performance.

Montesinos, et.al (2006) also conducted nonlinear finite element analysis for the investigation of cause of collapse of Daikai subway station during the 1995 Kobe earthquake. The analysis concentrated on the evaluation of the soil-structure interaction effects, calculation of drift demands imposed on the subway and calculation of drift capacity of the columns that collapsed during the event. The study found out that the difference in the geometrical characteristics of the Daikai main station and the running tunnel sections was the cause of the collapse of the Daikai main station. The main station has a wider section than the running tunnel section. The columns of the main station section hence carried larger axial force than the tunnel section. Further, due to larger dimension of the main station decreased the relative stiffness between the soil and the structure compared to the tunnel section. This induced larger deformation on the main station section contributed to damage of the section. The central columns which collapsed had very limited drift capacity due to large spacing of the transverse reinforcement combined with the moderate axial load it carried as a result of overburden soil. Thus these columns were unable to sustain the large drift demands and shear stress demands induced during the earthquake loading. To avoid these kinds of catastrophic collapses in future, the study suggests taking into account the relative stiffness between structure and the degrading soil properly. Further, the frictional characteristics of the interface between the structure and ground has also to be taken into account properly. The study also recommended providing large degree of ductility in critical member locations particular for structures inside the softer soils.

Liu and Song (2005) studied the response of large underground structures in liquefiable soils subjected to both horizontal and vertical earthquake motions. Fully coupled dynamic finite element analysis was conducted using the modified version of DYNA Swandyne II. The study revealed that large underground structures might be damaged due to earthquake induced soil liquefaction. However, the in plane seismic response of underground structure was found to be similar to those in non-liquefiable soil except the liquefaction induced uplift. The study found that the increase in the buried depth increases the safety of the underground structures. It was also found out that the effect of vertical earthquake excitation depends on the characteristics of the excitation used. The use of grouting underneath the underground structure to mitigate the effect of floatation proved to be effective according to the analysis results.

Wang, J. N. (1993) developed a monograph on Seismic Design of Tunnels. A rational and consistent methodology for seismic design of lined transportation tunnels has been developed. Seismic design criteria have been developed by comparative study of seismic design philosophies of other civil engineering structures. A review of the current seismic design methodology for both circular mined tunnels and cut-and-cover rectangular tunnels has also been made in the monograph. A simple method for evaluation of ovaling effect on circular lining due to earthquakes has been developed. Similarly, simplified frame analysis model has also been developed for evaluating the racking effect in cut-and-cover rectangular tunnel due to earthquakes. The method for evaluating the ovaling effect was developed from the theory used by mining/underground engineers and considers soil-structure interaction effects. For the development of methodology for rectangular tunnels, large number of dynamic finite element analysis was conducted considering soil-structure interaction effects and using wide range of structural, geotechnical and geological parameters.

Hashah, et.al (2001) presents the summary of the current state of seismic analysis and design of underground structure. The approaches used by engineers in quantifying the seismic effect on an underground structure are described. Deterministic and probabilistic hazard analysis approaches are reviewed. The development of the appropriate ground motion parameters, including peak accelerations and velocities, target response spectra and ground motion time histories are briefly described. Special design issues, including the design of tunnel segment joints and joints between tunnels and portal structures are also discussed. Examples of seismic design of underground structure are also presented.

Samata, et.al (1997) also carried out the analytical studies for the investigation of underground subway structures which suffered significant damage during 1995 Hanshin-Awaji (Kobe) earthquake. The damage sustained by the box culvert structure with middle columns at the Kamisawa station, Kobe city municipal subway was studied. Three series of analytical studies were conducted. In the first study, ground response analysis was conducted using equivalent linear response analysis using a computer program based on multi-reflection theory. In the second study, soil-structure interaction analysis was carried out using two-dimensional computer program. In the third study, three-dimensional FE static nonlinear analysis was conducted to

investigate the failure mechanism of the damaged structure subjected to earth pressure load. The ground response analysis indicated that with soil deposit thickness taken into account, a larger displacement response was predicted in the section where heavier damage occurred. The soil-structure interaction analysis indicated that the response of present underground structure was governed by the ground displacement dependent on soil deposits. It was found out that the imposed shear force on the top story middle column exceeds the specified shear strength in the case of structures that sustained significant damage. The three dimensional FE nonlinear analysis predicted the shear failures at both top story middle column. The research indicated that significant member ductility need to be ensured for prevention of brittle shear failure against imposed ground displacement.

Nishioka and Unjoh presented a simplified seismic design method for underground structures based on the shear strain-transmitting characteristics from surrounding ground to structures. The seismic performance is estimated by the shear deformation. It is deduced that the structure-ground shear ratio is the hyperbolic function of the ground-structure stiffness ratio and thus an analytical method to estimate the seismic shear deformation using the shear strain transmitting characteristics has been proposed.

2.8 Past Research on Finite Element Modeling

Montesinos, et.al (2006) used plane strain elements for modeling the soil-structure system. A free boundary condition was adopted at the lateral sides of the mesh. The bottom of the discretization was placed at 58 meters from the surface corresponding to the top of the gravel layer in Port Island. Fixed boundary condition was adopted at the bottom of discretization. The finite element model is shown in figure 2.6.

The lateral boundary on the both sides of the structure was placed far enough from the structure so that they have negligible effects on the response of the structure. This was confirmed by carrying out several numbers of simulations by placing the boundaries at different distances from the structure. The location was accepted when there was a region of soil between the boundary and the structure where the free field soil

deformations were recovered. Free field deformations were previously obtained by running a large mesh without the structure. This resulted in the overall mesh length of 1000 meters.

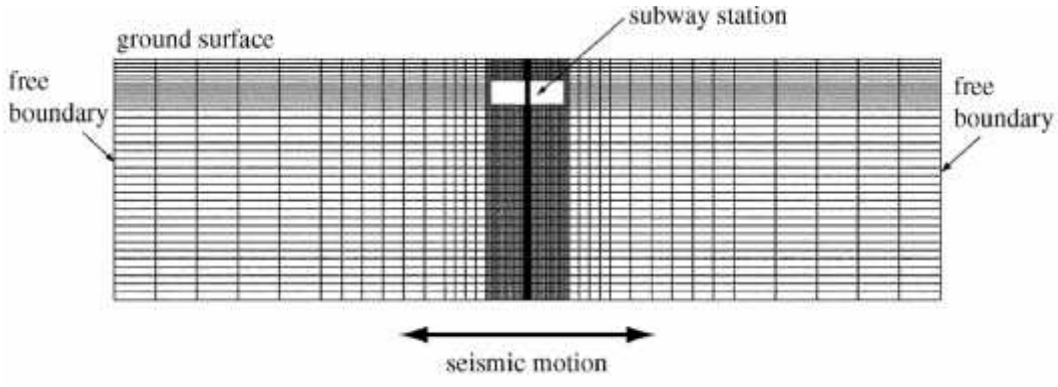

Figure 2.6: Finite Element model used in soil-structure numerical analysis of Daikai subway station

Nishioka and Unjoh modeled the soil as plane strain element and structure as beam elements. The lateral boundaries adopted at the sides were free in horizontal direction and fixed in vertical direction. The finite element model is shown in figure 2.7.

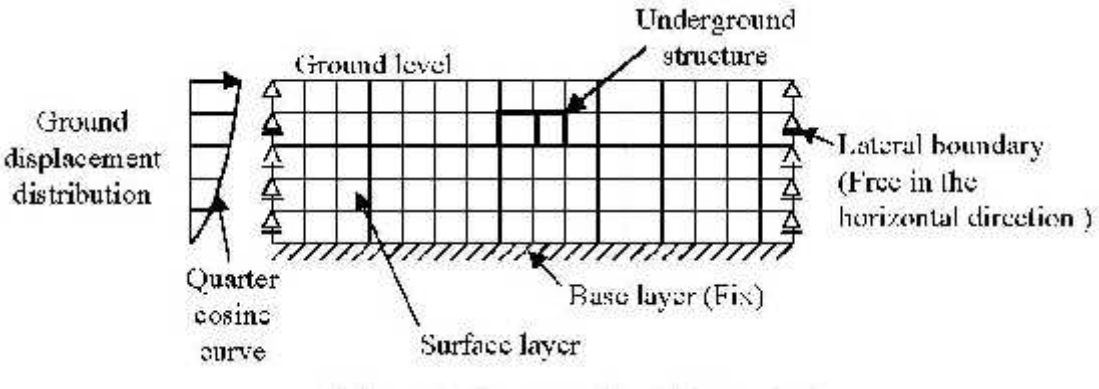

Figure 2.7: Finite element model used for analysis of strain transmitting characteristics of underground structure

Horizontal distance between the structure and the lateral boundaries was set approximately three times longer as the thickness of the surface layer on both sides of the structure. Fixed boundary condition was adopted at the bottom of the dicretization. The thickness of surface layer taken in the analysis is 25.2 m.

Liu and Song (2005) used plane strain elements to model the soil-structure system. The thickness of the element was judged based on the adequate transmission of the seismic wave applied at the base. To simulate the far field boundary condition in the FEM model, tied node feature available in DYNA Swandyne-II was used at the sides of the mesh. This feature allows the horizontal and vertical displacements at the two boundaries to be restrained so as to have the same value. The distance between the lateral boundaries were fixed based on the two factors: a) the distance between the free field zone and the underground structure, and b) the vibration reflection from the lateral boundary. Between the two factors, the second factor was found to be the governing one. This is owing to the fact that the tied boundaries are not energy absorbing and therefore the distance from the underground structure to the tied boundary must be large enough so that the dynamic behavior of the underground structure and the area close to it is not affected by the reflection of the waves from these lateral boundaries. The analysis resulted in the overall length of 300 meters. This was confirmed by analyzing a larger mesh with additional 50 meters on each side of the original one. Elements inside the range of the original domain were exactly same as those of the smaller mesh. Lateral displacement at the upper right corner of the subway was compared in the two cases. Other variables such as uplift displacement, acceleration and inertial forces in the underground structure was also compared and found to be negligibly different. The boundary between the soil deposit and bedrock was assumed fixed in both horizontal and vertical direction. The depth of the analyzed domain, i.e., the thickness of the assumed soil deposit is 70 meters. The finite element model is shown in figure 2.8.

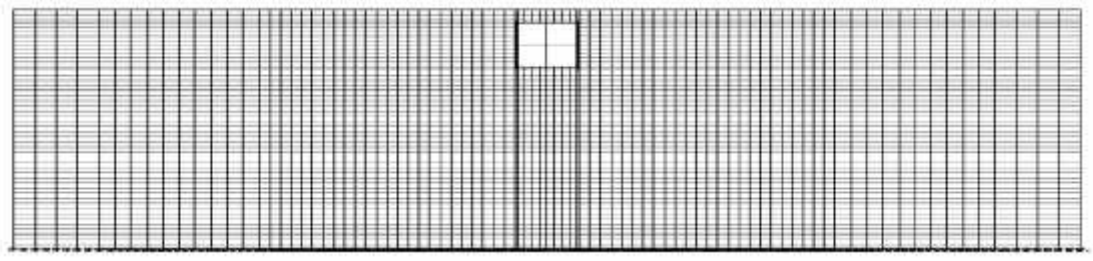

Figure 2.8: The finite element Mesh used for soil-structure interaction of large underground structure in liquefiable soil

An (1996) used plane strain elements to model the soil-structure system. Two extreme sides of the finite element analysis domain have mixed artificial boundary condition to simulate the far field boundary of the soil layer. The total length of the soil layer was checked to get the minimum appropriate length that can present the entire domain and dissipate the energy from finite element analysis domain to the far field. This resulted in the overall length of 555 meter in case of Kamisawa station. The bottom of the discretization was adopted at the top of the soil layer, which has larger stiffness enough for assuming it as the engineering base rock. In case of Daikai station, the bottom of the discretization was maintained at the depth of 17.25 meters from the ground surface. In case of Kamisawa station, the bottom of discretization was maintained at the depth of 20.25 meters from the ground surface. The finite element mesh in case of Daikai station is shown in figure 2.9.

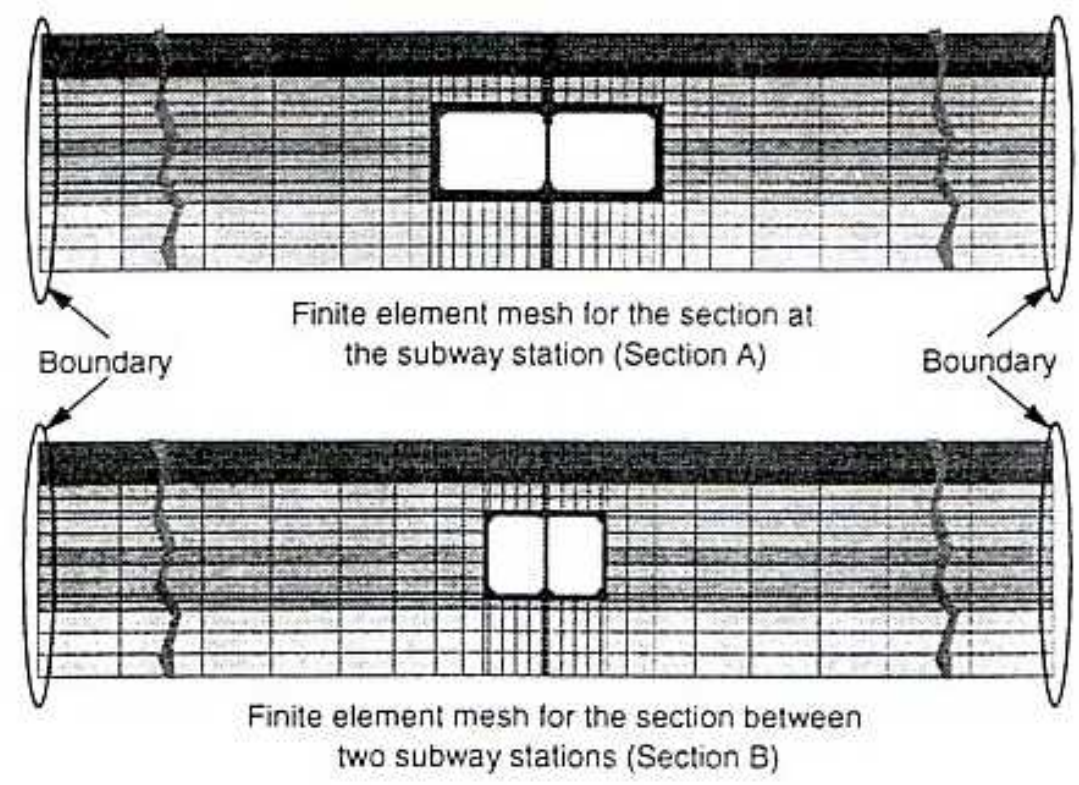

Figure 2.9: Finite element mesh used for investigation of collapse of Daikai Subway Station

Sarigul (1997) conducted parametric studies in achieving the converged solutions on locating the vertical boundary in the dynamic finite element analyses of the structures on semi-infinite foundations. Two parametric studies were conducted. In the first study the structure was embedded in a linear elastic foundation. In the second study, a

surface structure was supported by a saturated nonlinear clay foundation. Two dimensional plane strain elements were used. At first, one dimensional soil-column analysis was performed for the given uniform base acceleration time history to obtain the free field response of the foundation soil. Then the resulting relative accelerations of the soil-column analysis were applied at the vertical boundaries of the global system as known values by using a penalty formulation in the code. The first parametric study was carried out using the computer program CTU. Only one half of the system was analyzed owing to symmetry. The second parametric study was carried out using the computer program MODYS.

In the first parametric study the vertical boundaries were placed at 85.3 ft, 102 ft, 277.3 ft and 320 ft from the half width of the foundation (i.e. origin). Spectral acceleration at the origin were calculated for the four models and compared. Between the last two models, it was found that the solutions were not much different and hence was accepted as the correct solution. Similarly, in the second parametric study the vertical boundaries were placed at distances of 213.4 ft, 554.6 ft and 640 ft. between the last two cases solutions were found to be negligibly different and hence the last solution was accepted as the correct solution. It was found out that convergent solution could be obtained by placing the vertical boundaries sufficiently far from the structure in both cases of linear and nonlinear soil-structure problems. Furthermore, the results at the origin were found to be practically unaffected when the boundary is placed beyond certain location. It has been pointed out that the boundary conditions should be modeled appropriately in order to study soil-structure interaction. As the real system is semi-infinite, the size of the finite element mesh should be large enough to reduce the possible reflections at the boundaries. The general nonlinear and multiphase character of soil behavior and randomness of the earthquake acceleration complicates the problem necessitating a step-by-step time domain analysis to follow the deformation and failure mode of the system under time dependent loading conditions. Further, soil parameters may change with the depth as well. Considering these facts it has been concluded that finite element method is the most suitable method of analysis for carrying out soil-structure interaction analysis.

Choi, Lee and Kim (2002) presented an analytical method for evaluating the soil-structure interaction, which takes into account the sliding and the separation that

occurs at the soil-structure interface. The method employs a hybrid approach that combines a linear SSI code KIESSI-2D in frequency domain and a general purpose commercial software ANSYS for obtaining the nonlinear dynamic response in the time domain. This analytical method is then applied to study the response of a 2D underground box structure. For the analysis, nonlinear time varying interface characteristics and the material non-linearity of the concrete has been taken into account. The phenomenon of sliding and separation at the interface has been modeled using the contact elements and target elements available in ANSYS. If one surface is stiffer than the other one, the softer surface is chosen as contact surface. Therefore, at the interface, the contact elements are used for soil and target elements for concrete. The mohr-coloumb failure criterion is employed for defining the constitutive relationship of contact and target elements. The earthquake wave motion recorded at the ground surface of the Hualian site in Taiwan on May 1 1995 has been used as the input wave motion. The acceleration record has been scaled to 0.5g PGA. The input earthquake wave motion is modeled by the control motion at ground surface of the free field soil layer. The results of the analysis show that the response of the 2D concrete box structure with provision of sliding and separation at the interface is quite different from the one, which assumes perfect bond between the soil and structure. It has been found out that lesser seismic load is transmitted to the structure when separation and sliding at the interface is taken into account. The sliding at the interface increases the relative displacement and decrease in confining pressure in the soil at the interface and hence plays role in dissipating energy induced by the earthquake. The results show that stress is reduced up to 60% and plastic strains up to 27%. The research suggests that the sliding and separation at the soil-structure interface should be taken into account properly.

3 DYNAMIC FEM ANALYSIS OF RC – SOIL SYSTEM

3.1 The Computational Simulation Tool: WCOMD

When real behavior of the RC structure has to be accessed, engineers generally have two choices, either to conduct experiment in laboratories or to carry out computer simulation. Although, the actual result is obtained by conducting experiment in laboratories, it is limited to particular and standard cases only. On the other hand, the computer simulation has practically got no limits in its application. The computer simulation has emerged as a Virtual Testing Center with which we are able to solve structural problems of complex nature, tackle nontraditional problems and also find out optimal solutions. Other interesting applications include assessment of the remaining life of the existing structures and investigation of damage and failures of structures. The tool employed for simulation of real behavior of the RC structures is the finite element based nonlinear analysis techniques (Okamura and Maekawa, 1991; Cervenka, 2002; Maekawa et al., 2003).

Lots of software has been developed around the world to carry out the nonlinear analysis of the RC structures. ATENA and WCOMD are two of the software among many.

WCOMD is software developed by University of Tokyo, Japan (Okamura and Maekawa, 1991). It is the software developed for nonlinear analysis of RC structures for two dimensions. Figures 3.1 and 3.2 shows the graphical user interface of the UC-win/ mesh and UC-win/ WCOMD. UC-win/ mesh is the program used to generate the finite element mesh. The type of materials, material plate properties, boundary conditions and mesh geometry are all defined in this module. Six kinds of materials are available in UC-win/ mesh: Concrete, Steel, Elastic, Soil, RC joint and Universal joint. For carrying out nonlinear analysis, the mesh file is then exported to UC-win/ WCOMD. WCOMD is the solver where nonlinear calculations are made. The static and dynamic loads are defined in this module. Three types of loading patterns are available in UC-win/ WCOMD: Dead weight, Static load and Dynamic load. The elements used in the WCOMD software are eight noded quadrilateral isoparametric elements.

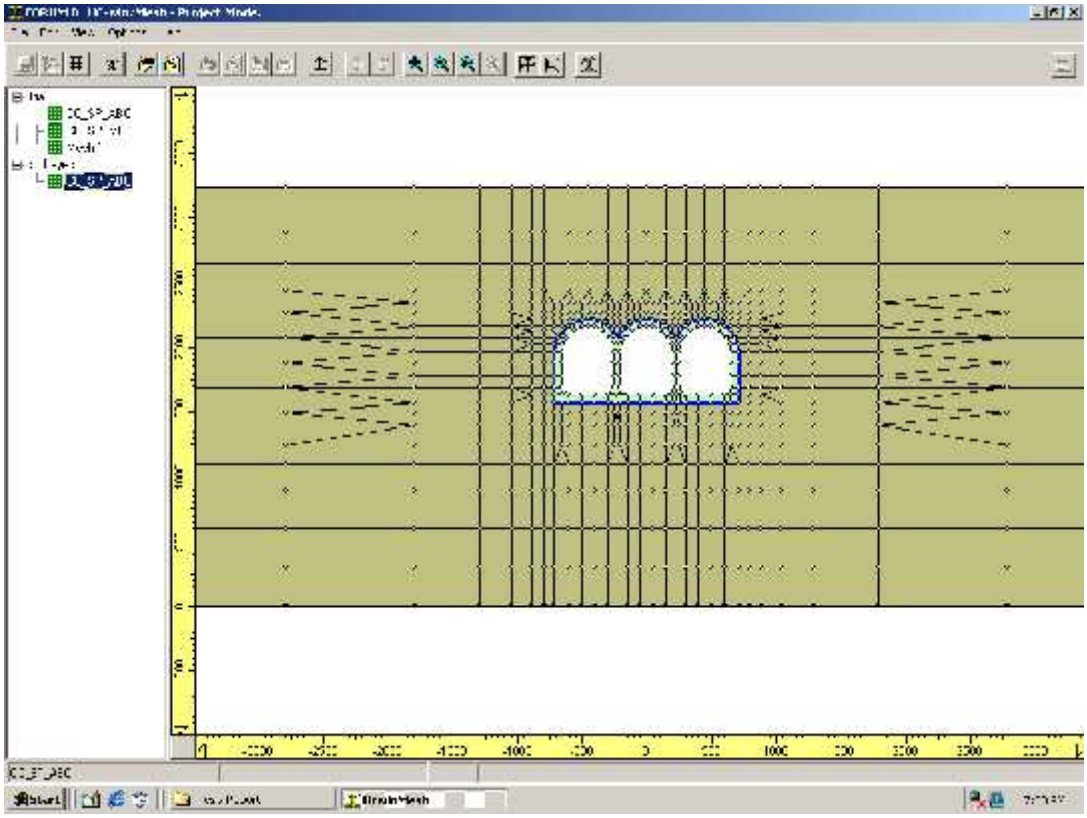

Figure3.1: UC-win/ Mesh Window

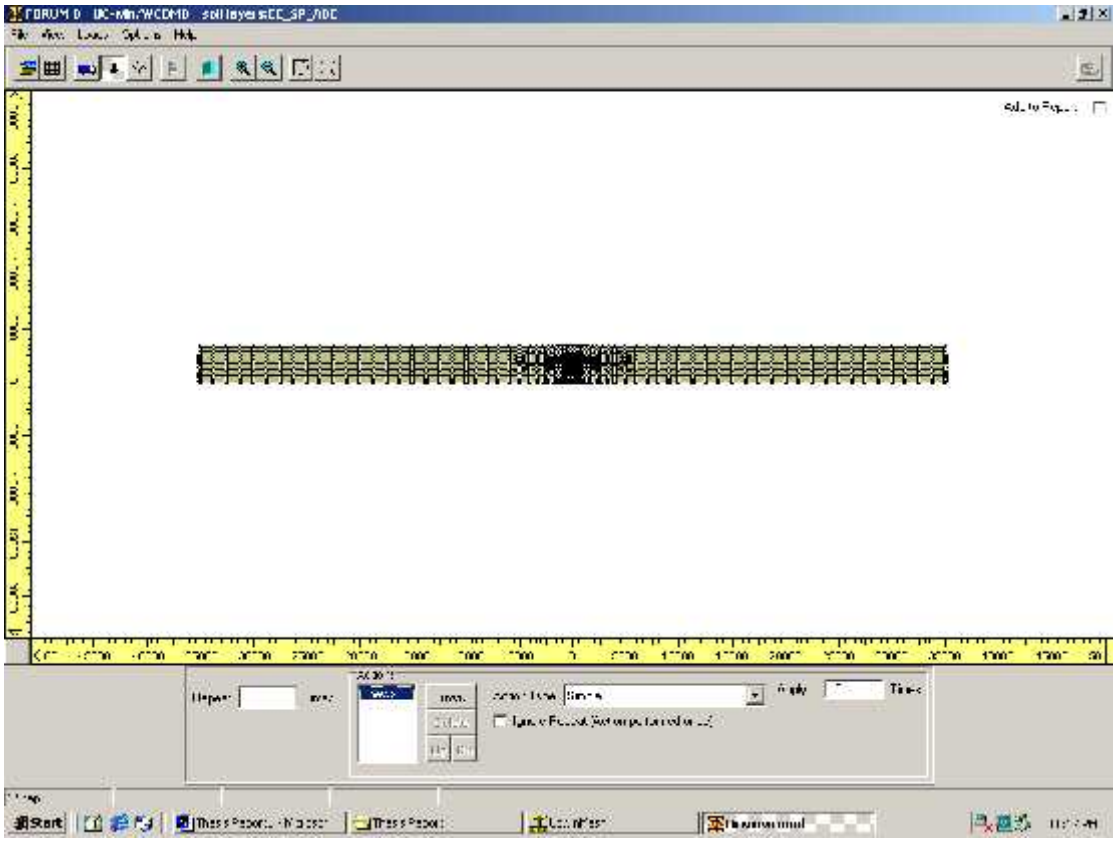

Figure3.2: UC-win/ WCOMD Window

Special constitutive models for finite element based nonlinear analysis for RC has been incorporated in WCOMD. Constitutive model for soil material has also been incorporated in the software, thus enabling us to carry out the analysis of soil-structure interaction system. For modeling of interface between the RC elements and soil elements, RC joint element and universal joint element models have also been incorporated in the software. The material models for cracked concrete and reinforcing bars in concrete have been developed based on test results of reinforced concrete specimens subjected to uniaxial loadings. Combined material models and reinforced concrete plate element has been developed. The multidirectional smeared crack model has been employed. In this model, the material models are expressed as average stress and average strain relationships. The smeared crack model has been used to describe the overall behavior of a member. However, the smeared crack model is not suitable for regions where large discontinuities occur. For such cases, discrete crack model have been employed. The joint element has been developed for the purpose. The joint element model is shown in figure 3.3.

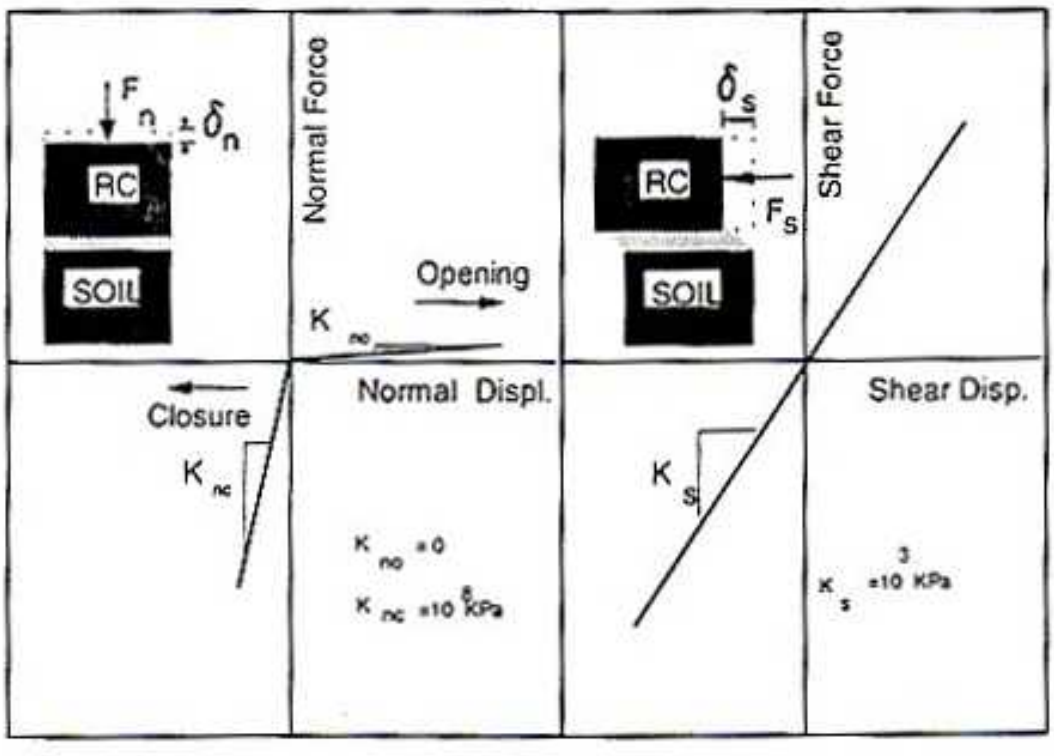

Figure 3.3: Constitutive relationship for RC/ Soil interface model

The joint element is a one-dimensional element having zero thickness. It expresses the relationship between the normal force and normal displacement and shear force and shear displacement.

3.2 Modeling of RC-Soil System

For analysis of underground structures, coupled analysis of the complete RC-soil system is necessary. For this nonlinear path dependent constitutive model of both soil and structure is needed. This is mandatory for dealing with the kinematic and inertial interaction between the soil and the structure under seismic excitation.

The Ohsaki's soil model is used as a constitutive model for soil in WCOMD. The Ohsaki model describes the relationship between the shear strain and shear stress with the aid of three parameters, Go, Su and b. The relationship is as follows:

$$\gamma = f(\tau) = \frac{\tau}{G_0}\left(1 + a\left|\frac{\tau}{S_u}\right|^b\right)$$

For hysteretic behavior, the soil is assumed to obey the Masing rule, which is as follows:

$$\frac{\gamma - \gamma_0}{2} = f\left(\frac{\tau - \tau_0}{2}\right)$$

Here,

□□= shear strain

□□= shear stress (N/mm2)

□□□= shear strain at turning point

□□□= shear stress at the turning point (N/mm2)

Go = initial shear modulus

Su = maximum shear strength

b = soil type factor: 1.6 for sand

1.5 for sand and clay

1.4 for clay

a > 0: a = (Go/100Su – 1) ; Go/Su > 100

When the shear stress of the soil exceeds Su, the soil enters in the plastic range. The liquefaction of the soil is not considered in the model.

The initial elastic shear modulus (Go) is related to initial elastic normal modulus (Eo) and Poisson's ratio as

Go = Eo/2(1+ □)

Generally, only SPT – N value is obtained from the standard penetration test during the geotechnical investigation of the soil. Hence, all the other soil properties are obtained by using the empirical equations based on SPT N. The following empirical equations are used to obtain the different soil properties:

Go = 11.76 N0.8 (N/mm2)

Su = Go / 600 (N/mm2) : for clay

Su = Go / 850 (N/mm2) : for sand and clay

Su = Go / 1100 (N/mm2) : for sand

Shear Velocity is calculated using the following formula:

$$V_s = \frac{1}{100}\sqrt{980\,(cm/sec^2)\,G_0\,(N/cm^2) \Big/ \gamma\,(kN/cm^3)} \quad (m/sec)$$

4 NUMERICAL ANALYSIS

4.1 Geological Profile at Sikta Irrigation Project

The Sikta irrigation project is located at Agaya village in Kanchanpur VDC of Banke district. The intake of the canal lies in the Siwalik foothills. The head works lies in the quaternary deposits. The deposits consist of alternating beds of dense sandy gravels underlain by very stiff to hard silty soil. The bedrock is not found at least up to the depth of 40 meters. The intake is quite away from the Main Frontal thrust and major active fault located in the north. The main canal alignment runs through a mega fan formed by the merger of two more than 10 kilometers wide alluvial fans of Muguwa khola and Khari khola and other small fans formed by other streams. It has been proposed to run the main canal through the gravel and sand beds of fan deposits with about 20 meters deep cutting. A covered canal (underground RC box structure) has been proposed in this deep cutting zone. The geotechnical investigation works has been carried out for the head works area only. Four boreholes were made along the two banks of the river (two on each bank). The investigation was carried out for a depth of 27 meters from the ground surface. The soil profile at the head works is broadly divided into three layers. The layers comprises of very dense sandy gravel with cobbles and boulders up to 12.2 metes average thickness underlain by medium dense sandy silt of 3.8 meters average thickness and stiff to hard loamy silty soil of 11 meters average thickness. The static ground water is at 0.7 meters below the ground level. In the deep cutting zone, where the construction of covered canal has been proposed, it has been estimated that few cemented conglomerate beds could be encountered.

4.2 Geometry of Covered Canal

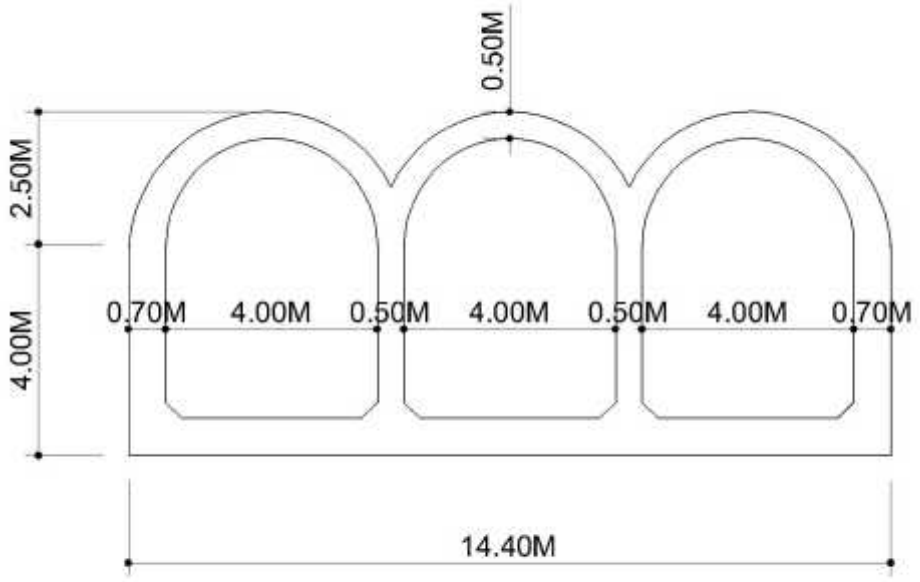

Figure 4.1: Geometry of the Covered Canal

4.3 Layout of Reinforcements

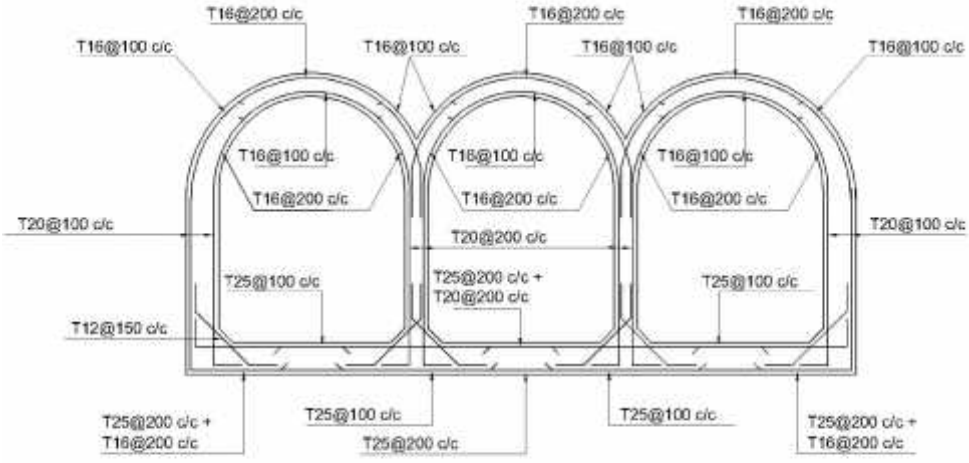

Figure 4.2: Reinforcement details in Covered Canal

4.4 Soil Profile used in Computation

No geotechnical investigation has been conducted in the area where the construction of the covered canal is proposed. Only the geotechnical investigation of the head works area has been carried out. As the covered canal is close to the head works, the soil database for the head works have been used here as the input parameter. For this research, the soil database of bore log 1 has been adopted. There is a presence of a very stiff layer of gravely sand at a depth of 22.2 m from the bank of river (which is also the base level of the covered canal). This stiff layer has been taken as the seismic bedrock. This resulted in overall depth of the soil to be 32.45 meters including the 10.25 meters depth of overburden. The simplified soil profile to be used in the computation is shown in figure 4.3 below.

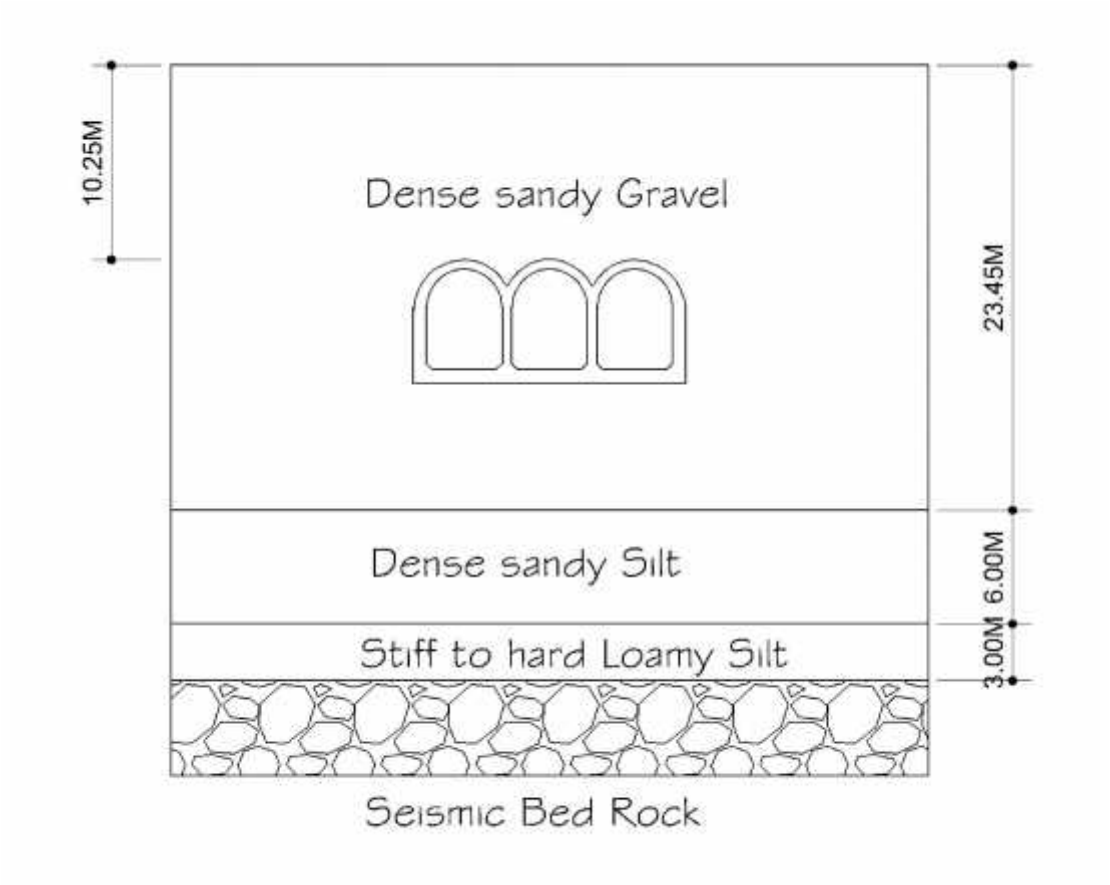

Figure 4.3: Soil Profile considered in Computation (Base Case)

4.5 Material Properties

4.5.1 Structural Material Properties

The covered canal is yet to be constructed. For this reason, the structural properties, which were used in the design, is used here as well for the analysis.

Grade of Concrete = M20 = 20 N/mm2

Grade of Steel = Fe415 = 415 N/mm2

4.5.2 Soil Material Properties

The different properties of the three soil types of soil used in the analysis are tabulated in table 1 below.

Parameters	Unit	Layer I	Layer II	Layer III
Layer Thickness	Meters	23.45	6.00	3.00
Soil Type		Dense Sandy Gravel	Dense sandy silt	Stiff to hard loamy silt
SPT N		30	25	35
Weight density	N/cm3	0.02	0.02	0.02
Poisson Ratio		0.43	0.49	0.49
Go	N/cm2	17869.17	15443.98	20214.44
Eo	N/cm2	51105.83	46023.06	60239.03
Su	N/cm2	16.24	14.04	33.69
Shear Velocity	m/s	295.90	275.23	314.72

Table 1: Soil Profile and its characteristics

4.6 Far Field Boundary Condition

To simulate the effect of far field boundary condition in the finite element model mixed artificial boundary condition used by An. X (1996) is employed. The boundary condition is shown in figure 4.4.

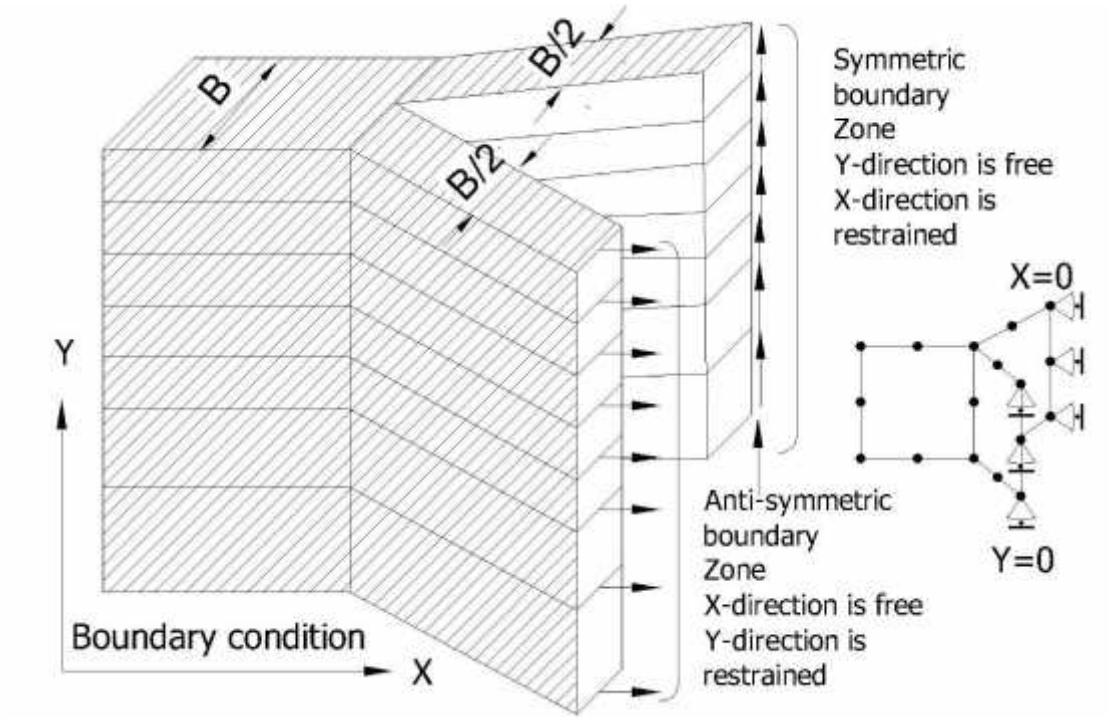

Figure 4.4: Mixed Artificial Boundary

For the purpose of finding out the lateral extent of soil mass to be considered in the analysis, a number of analyses are carried out with different length of the soil mass. The lateral displacement, acceleration, stress and strain values at the inner side of the bottom right corner of the structure was compared. The length of soil mass was accepted when the difference in these values in the last two consecutive analysis became negligible. From the analysis it is found that a length of 700 meters is adequate to represent the semi-infinite soil mass.

4.7 Input Earthquake Wave motion

The records of strong ground motions are not available in the vicinity of the site. For this reason, the earthquake wave motion recorded at the Kobe Meteorological Observatory is chosen as the input wave for this research. Besides, the subway structures of the Kobe metropolitan subway line is the first documented case of complete collapse during earthquakes. This wave has got very high horizontal ground acceleration (0.83g). The earthquake wave is shown in the figure 4.5.

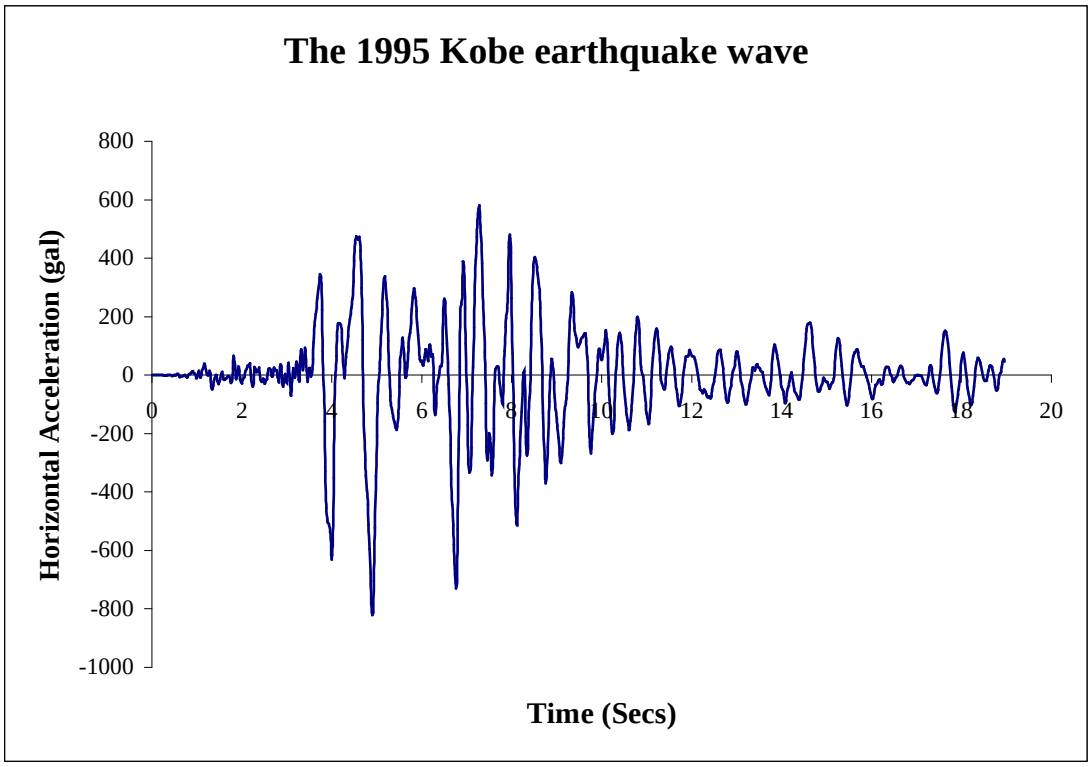

Figure 4.5: Input Earthquake Wave

As the time history analysis is a very time consuming task; to reduce the analysis time the duration of the time history has been truncated to 16 seconds for the analysis of the water cases and 12 seconds for the soil profile cases. This has been achieved by removing the extra steps that do not affect the overall structural behavior and the initial noise data. Also, only the N-S component of horizontal acceleration has been considered in the analysis.

4.8 Water Pressure Loads

The static water pressure loads are applied on the inner walls of the covered canal. The loads are applied on the walls as nodal forces. The nodal forces are computed on the basis of tributary areas. The hydrodynamic effect has not been considered in the analysis.

4.9 Finite Element Mesh

Figure 4.6 shows the finite element mesh of the soil-structure interaction analysis model of the Covered Canal.

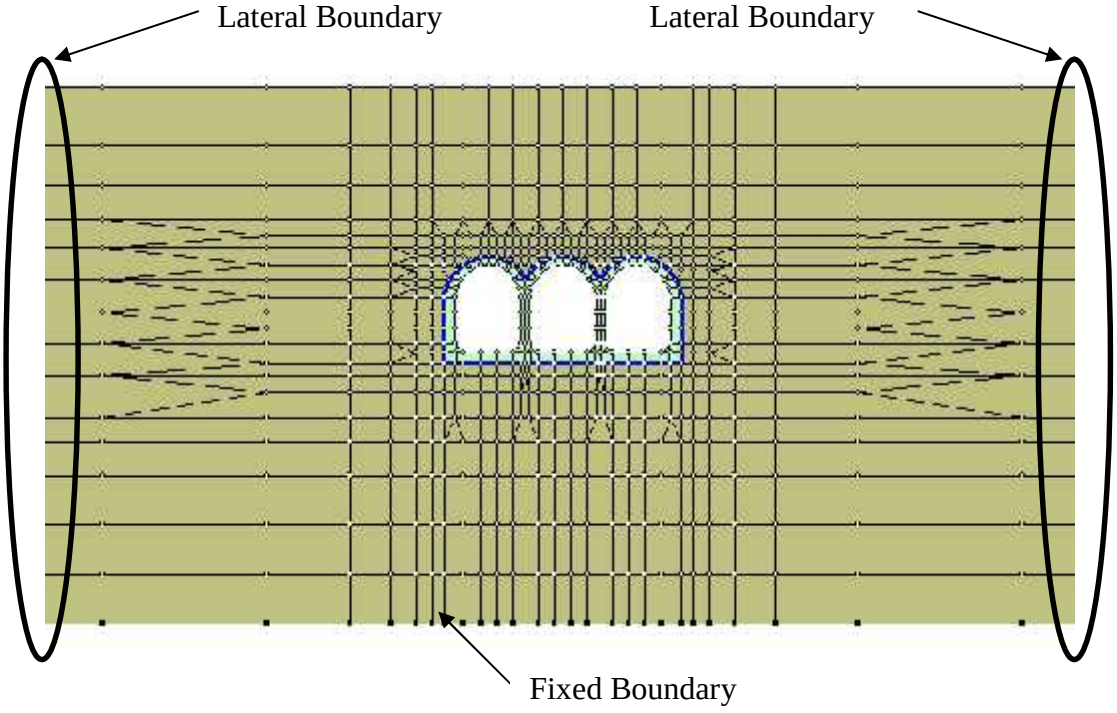

Figure 4.6: Finite Element Mesh

Figure 4.7 shows the enlarged view of the lateral boundary condition used for simulating the far field boundary condition. The skewed dotted lines on top of the elements at the right side of the mesh in figure 4.7 are the overlapping plates. This overlapping plate represents the two different plates in depth direction. Figure 4.8 shows the enlarged view of Covered Canal. The green colored elements are RC elements; light brown colored elements are soil elements and the blue lines between the RC & Soil elements are joint elements.

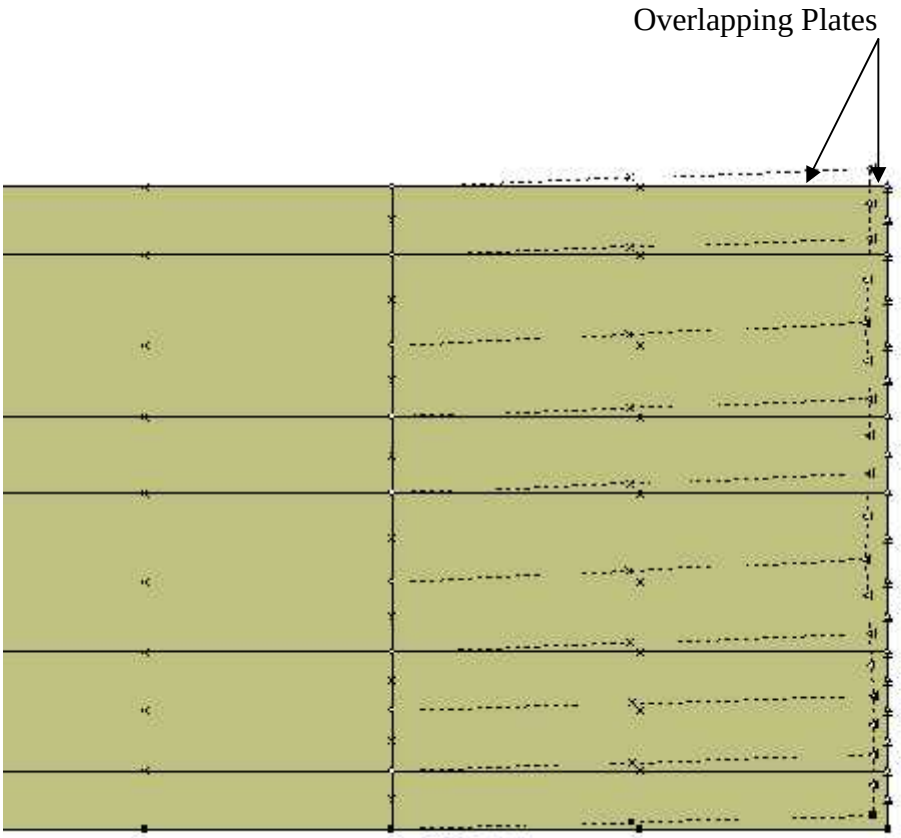

Figure 4.7: Overlapping Plates at the Lateral Boundary

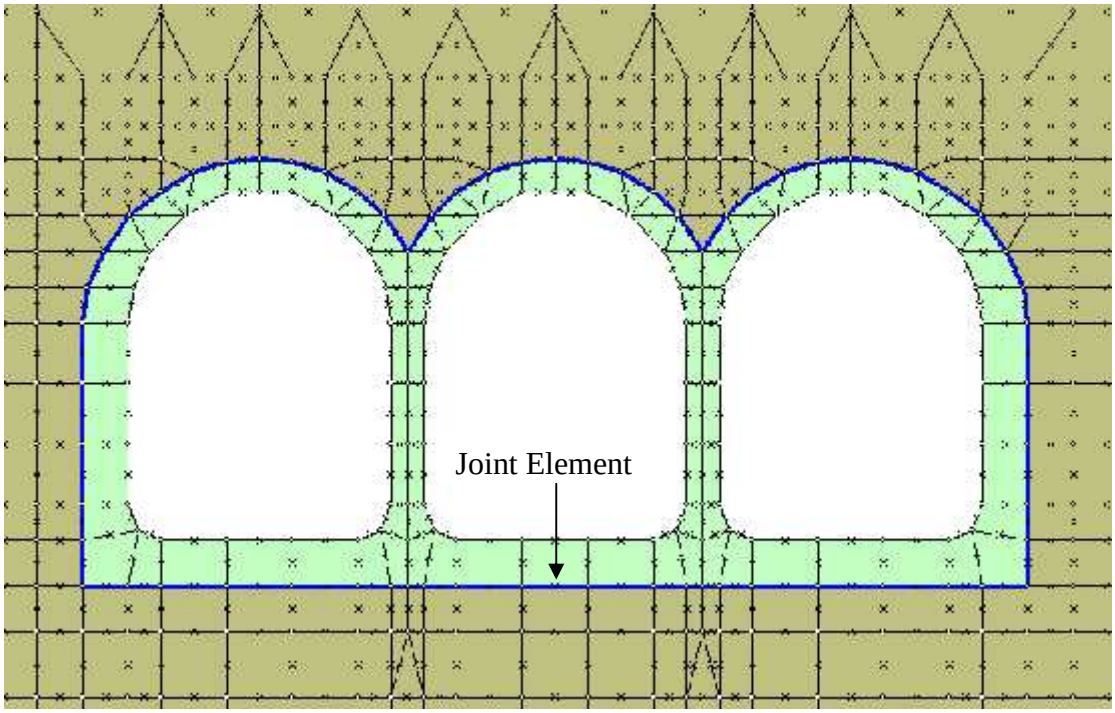

Figure 4.8: Enlarged view of finite element mesh of the Covered Canal

4.10 Analysis Cases

Altogether 17 finite element models are constructed using the software WCOMD.

4.10.1 Six Conditions of Water Level

For the purpose of numerical simulation of the response of the covered canal, it is intended to consider six conditions of the water level. These six cases are given in the figure 4.9.

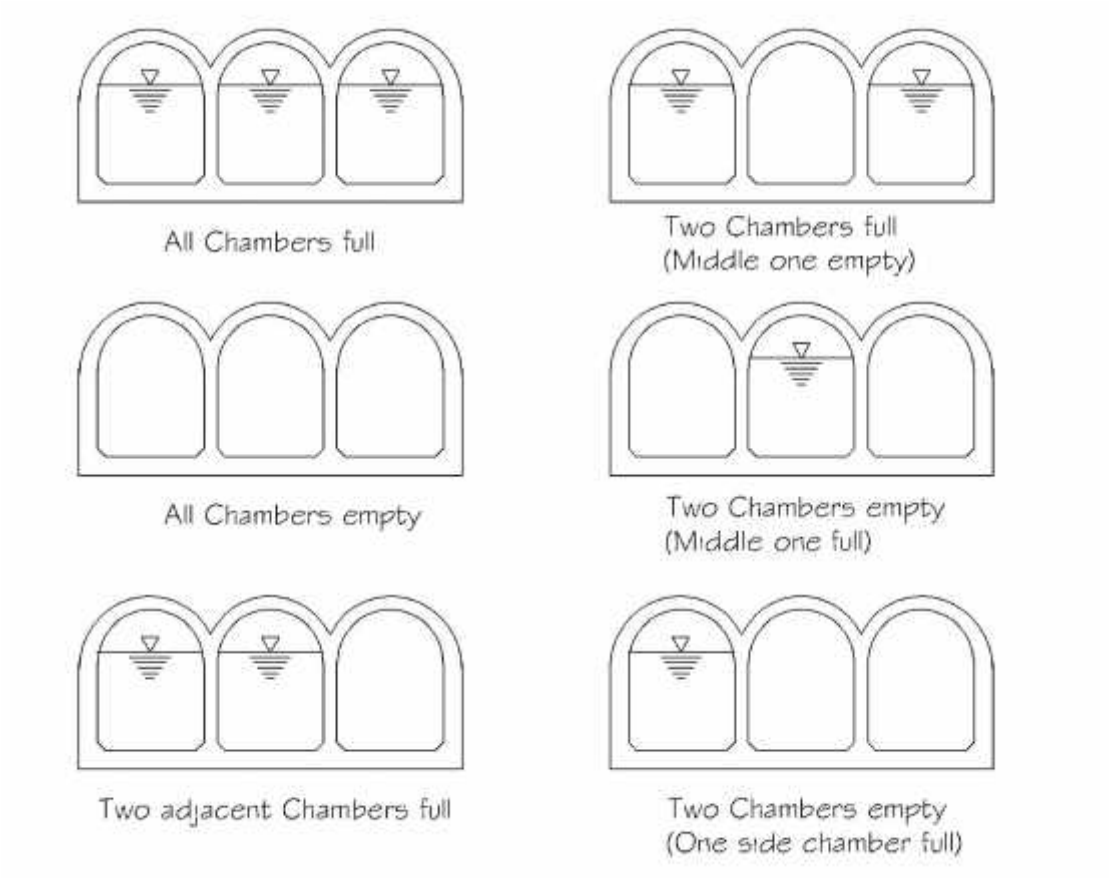

Figure 4.9: Six Conditions of Water Level

4.10.2 Eleven Cases of Soil Profiles

For accessing the performance of the Covered canal, apart from six models of water cases, eleven models of different soil profiles is also constructed. These soil profiles are given in figure 4.10. The letters A denotes dense sandy gravel, B denotes dense sandy silt and C denotes stiff to hard loamy silt. Figure 4.10 (a) shows the soil profiles

formed by the combination of soil properties A, B and C. Figure 4.10 (b) shows the three single layered soil profiles having soil properties A, B and C with thickness of soil layer equal to the total height of the soil domain respectively. Figure 4.10 (c) shows the soil profile having soil properties A, B and C with the thickness of soil layers made equal. Figure 4.10 (d) shows the soil profile having soil properties A, B and C with the smaller thickness middle layer sandwiched between the two larger thickness soil layers.

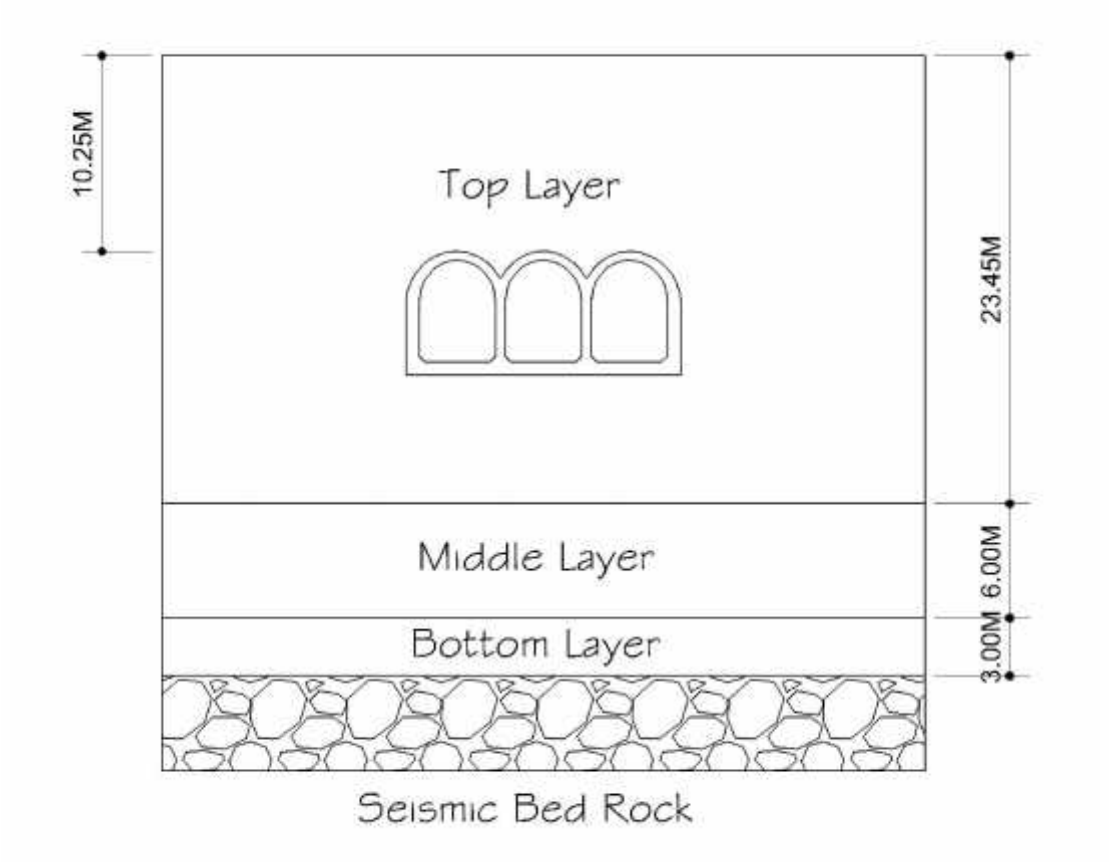

Soil Layer	Various Combination of Soil profiles					
Top Layer	A	A	B	B	C	C
Middle Layer	B	C	A	C	A	B
Bottom Layer	C	B	C	A	B	A

Figure 4.10 (a): Soil profiles with six possible combinations of soil properties A, B and C

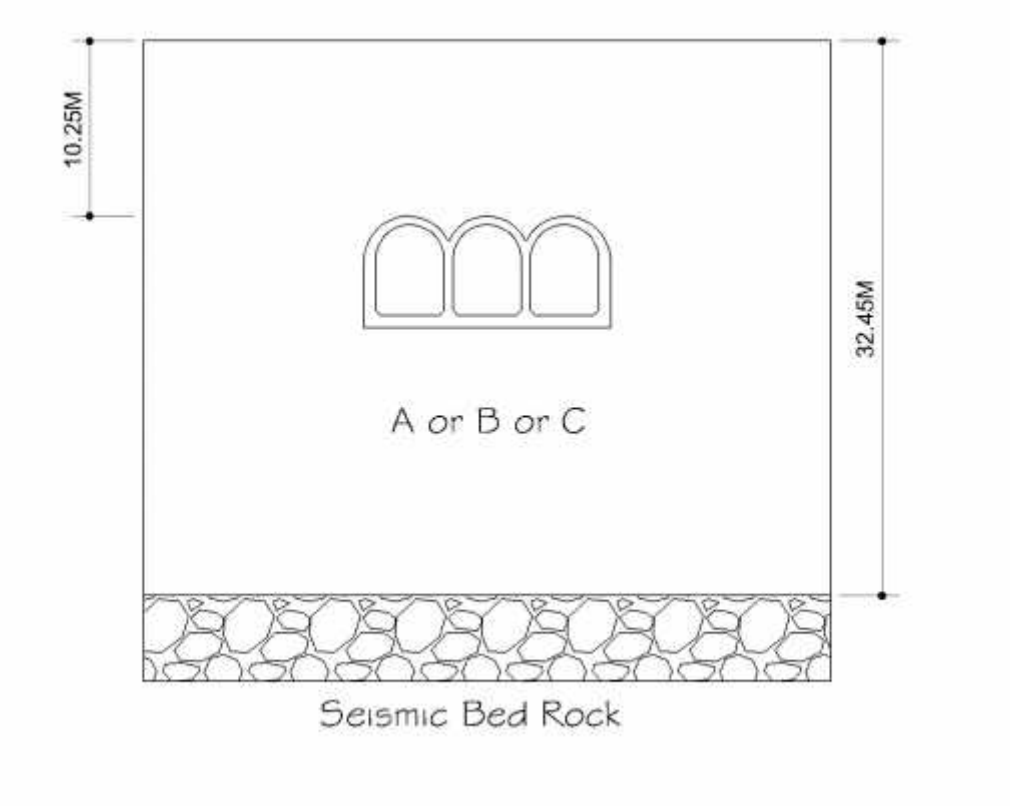

Figure 4.10 (b): Soil profile having only single layer of soil A or B or C of total height of soil domain

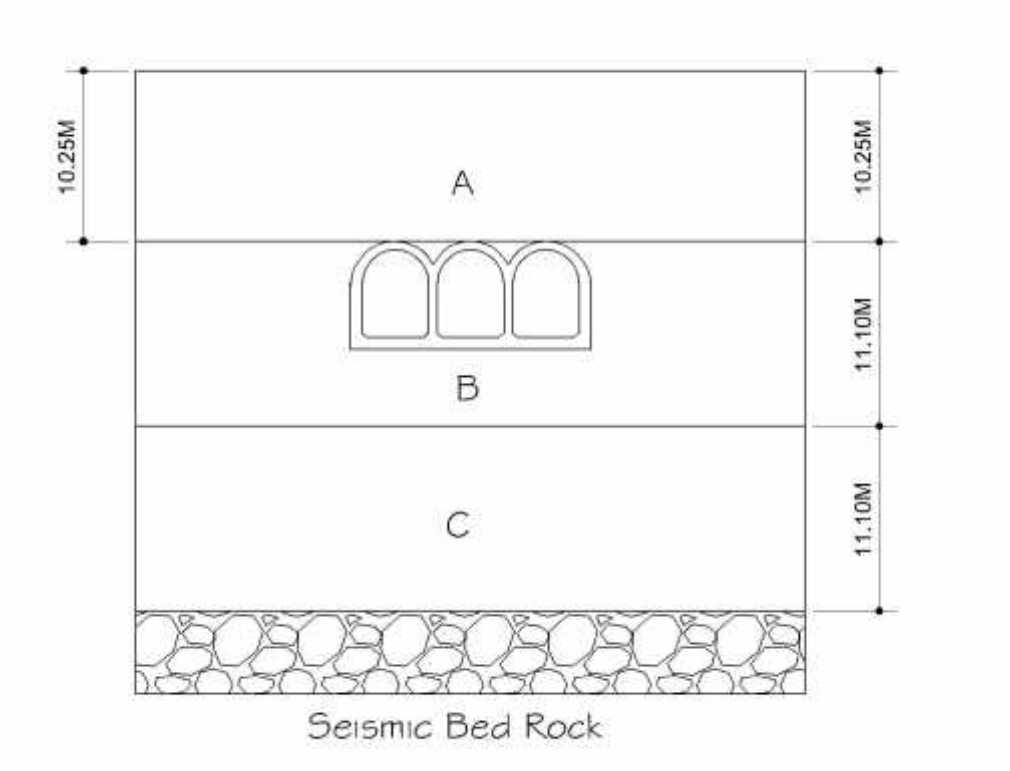

Figure 4.10 (c): Soil Profile with almost equal thickness soil layers with soil properties identical to base case

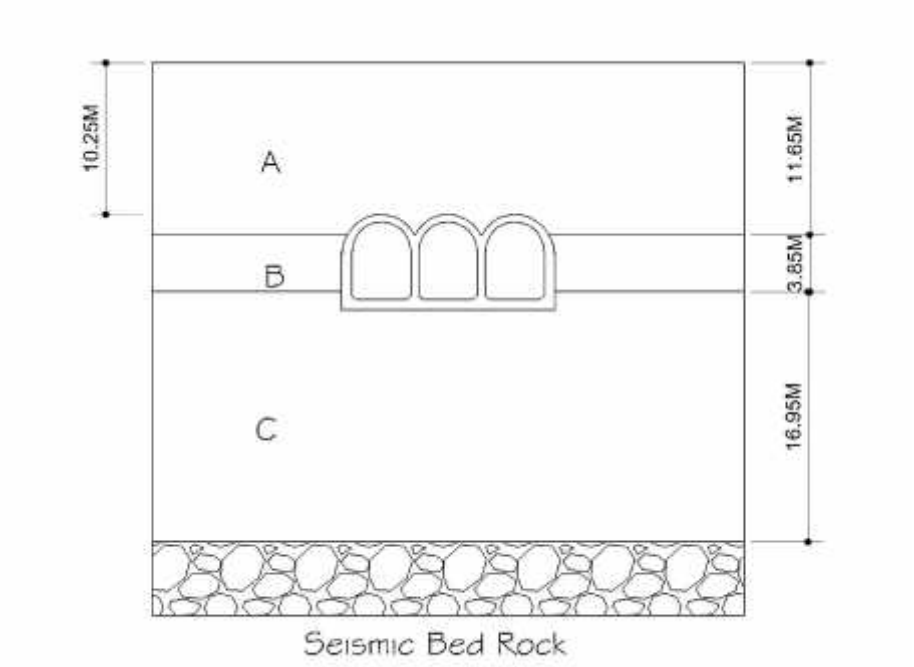

Figure 4.10 (d): Soil profile with smaller middle layer sandwiched between two large layers with soil properties identical to base case

4.10.3 Designation of Models

The details of these seventeen models along with their designation are listed in the Table 2 below.

In the model designation of different conditions of water level, the first two letters denote Covered Canal, next two letters denote Water Level and the last three letters denote the different conditions of water level. For example, CC_WL_ALF denoted Covered Canal with Water Level All chambers Full.

In the model designation of different soil profiles, the first two letters denote Covered Canal, next two letters denote Soil Profile and the last three letters denote the different soil profiles. The designation of soil profiles ABC, ACB, BAC, BCA, CAB and CBA, first letter denotes top layer soil, second letter denotes middle layer soil and the third letter denotes the bottom layer soil. For example, in soil profile CC_SP_BCA, B is the top layer soil, C is the middle layer soil and A is the bottom layer soil. Further, the soil profiles CC_SP_A, CC_SP_B and CC_SP_C are the soil profiles having only one layer of soil of A or B or C with total height of 32.45 meters respectively. The second

last soil profile CC_SP_ABC_ET is similar to soil profile CC_SP_ABC with a difference that the soil layers are of equal thickness. The last soil profile CC_SP_ABC_MLST is also similar to soil profile CC_SP_ABC but having the thickness of the middle soil layer B much smaller than the other two soil layers.

MODEL DESIGNATION	REMARKS
CC_WL_ALF	Covered Canal with Water Level All chambers Full
CC_WL_ALE	Covered Canal with Water Level All chambers Empty
CC_WL_2AF	Covered Canal with Water Level 2 Adjacent chambers Full
CC_WL_2SF	Covered Canal with Water Level 2 Side chambers Full
CC_WL_1MF	Covered Canal with Water Level 1 Middle chamber Full
CC_WL_1SF	Covered Canal with Water Level 1 Side chamber Full
CC_SP_ABC	Covered Canal with Soil Profile ABC (Original)
CC_SP_ACB	Covered Canal with Soil Profile ACB
CC_SP_BAC	Covered Canal with Soil Profile BAC
CC_SP_BCA	Covered Canal with Soil Profile BCA
CC_SP_CAB	Covered Canal with Soil Profile CAB
CC_SP_CBA	Covered Canal with Soil Profile CBA
CC_SP_A	Covered Canal with Soil Profile A
CC_SP_B	Covered Canal with Soil Profile B
CC_SP_C	Covered Canal with Soil Profile C
CC_SP_ABC_ET	Covered Canal with Soil Profile ABC of Equal layer Thickness
CC_SP_ABC_MLST	Covered Canal with Soil Profile ABC having Middle Layer of Smaller Thickness sandwiched between two larger thickness layers

Table 2: Designation and details of the seventeen FE models

5 RESULTS AND DISCUSSION

5.1 General

All together seventeen analyses were conducted. Among them six of them are related to different conditions of water level. Rest of them is related to different cases of soil profile. The results of these analyses are presented in this section. The performance of the covered canal is evaluated in terms of mean inelastic strain, the damage criteria and the deformation of the structure. For the evaluation of the results they have been grouped into two categories. First category consists of the results of six different conditions of water level. Second category consists of the results of eleven different cases of the soil profiles. The number of different soil properties and number of layers considered in the analysis is both limited to three, which is equal to that of the original one.

5.2 Mean Inelastic Strain

(An, 1996; Maekawa et al., 2003)

Mean Inelastic Strain is used to represent the damage level of the whole RC structure. It is an index, which shows qualitatively the amount of damage incurred in the structure and the remaining amount of residual deformation after an earthquake. The first strain invariant (I1) or the volumetric change of an element is closely related to the crack occurrence and expansion of the in-plane element. Thus, the first strain invariant (I1) represents the damage level that occurs in an element. The mean inelastic strain (I) is defined as the spatial average of the first strain invariant (I1) of all RC elements. The value is zero for elastic shear behavior under which no residual deformation exists. Hence, the mean inelastic strain is adopted here to represent the damage intensity of the whole RC structure. The first strain invariant and the mean inelastic strain are computed using the following equations:

$$I1 = \varepsilon_{xx} + \varepsilon_{yy} = \Delta V/V \qquad \text{Local}$$

$$I = \int I1\,(x, y)\,dx\,dy/A \qquad \text{Global}$$

Where □xx and □yy are the 2D principal strains at (x, y) and A is the total area of the RC in-plane elements.

5.3 Damage Criteria

Three types of damage criteria have been developed for judging the degree of damage: Failure criteria, Considerable damage criteria and Light damage criteria.

Failure: It is a state when reached, the structure cannot be repaired and the only alternative left is to demolish the structure. Failure is reached if any one of the following strain conditions is reached at any gauss point of a RC element:

Maximum tensile strain normal to crack, □t = 3%

Maximum compressive strain parallel to crack, □c = 1%

Maximum shear strain parallel to crack, □sh = 2%

Considerable damage: It is a state of the structure where the structure can be repaired/ retrofitted. Considerable damage occurs when the peak compressive strain at any gauss point in RC element reaches the value equal to the uniaxial compressive strength of the concrete multiplied by the magnification factor, i.e.,

□c = □ □peak

The following relation gives the value of the □peak,

□peak = 447.2 √fc’ (N/mm2) X 10-6

The value of □ is taken as 1.5

Light damage: It is also a state of the structure in which the structure can be repaired/ retrofitted. Light damage occurs when the peak tensile strain normal to the crack reaches a value of 0.1%, i.e.,

□t = 0.1%

5.4 Results of Water Cases

To evaluate the performance of the covered canal, six different cases of water levels were considered (Figure 4.9). The case with all chambers empty has been chosen as the base case. The performance is expressed in terms of mean inelastic strain level, damage level and variation of stress & strain in time domain.

5.4.1 Mean Inelastic Strain

The mean inelastic strain in time domain is plotted for the six cases of the water level. Figure 5.1 (a)-(f) are the plots.

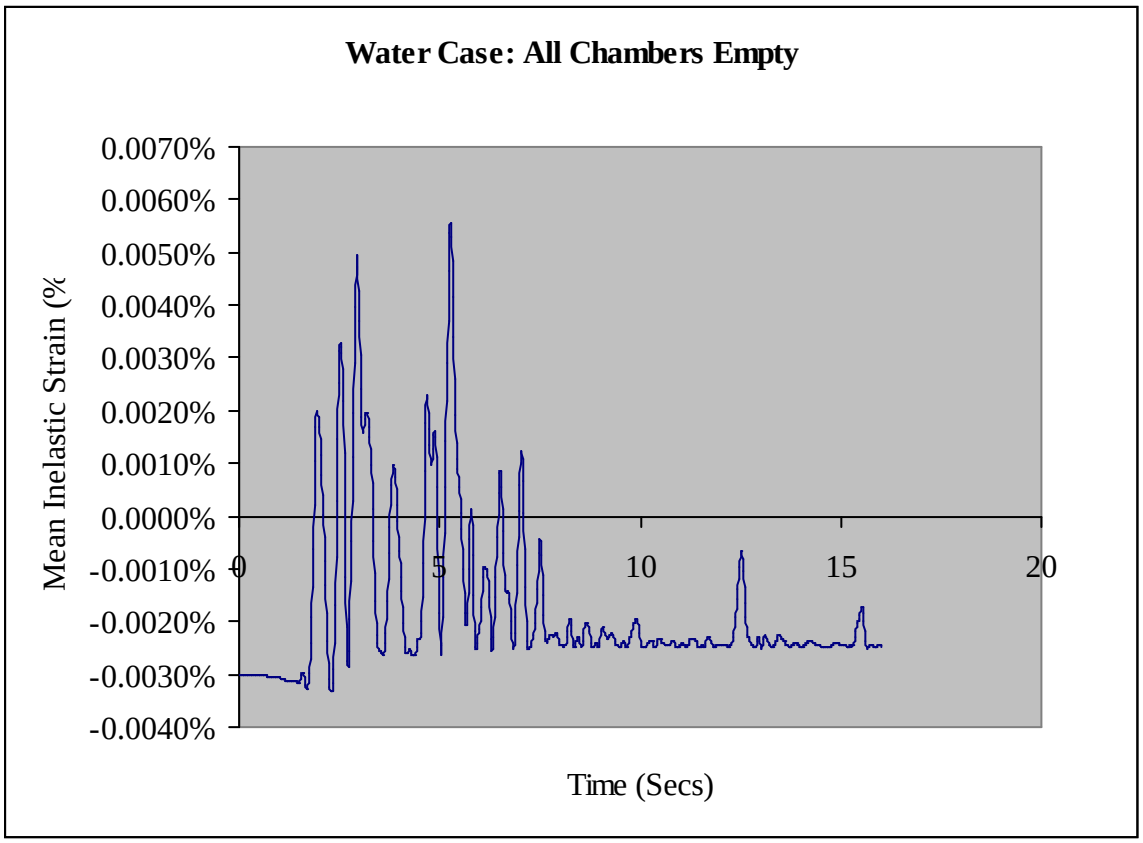

5.1 (a)

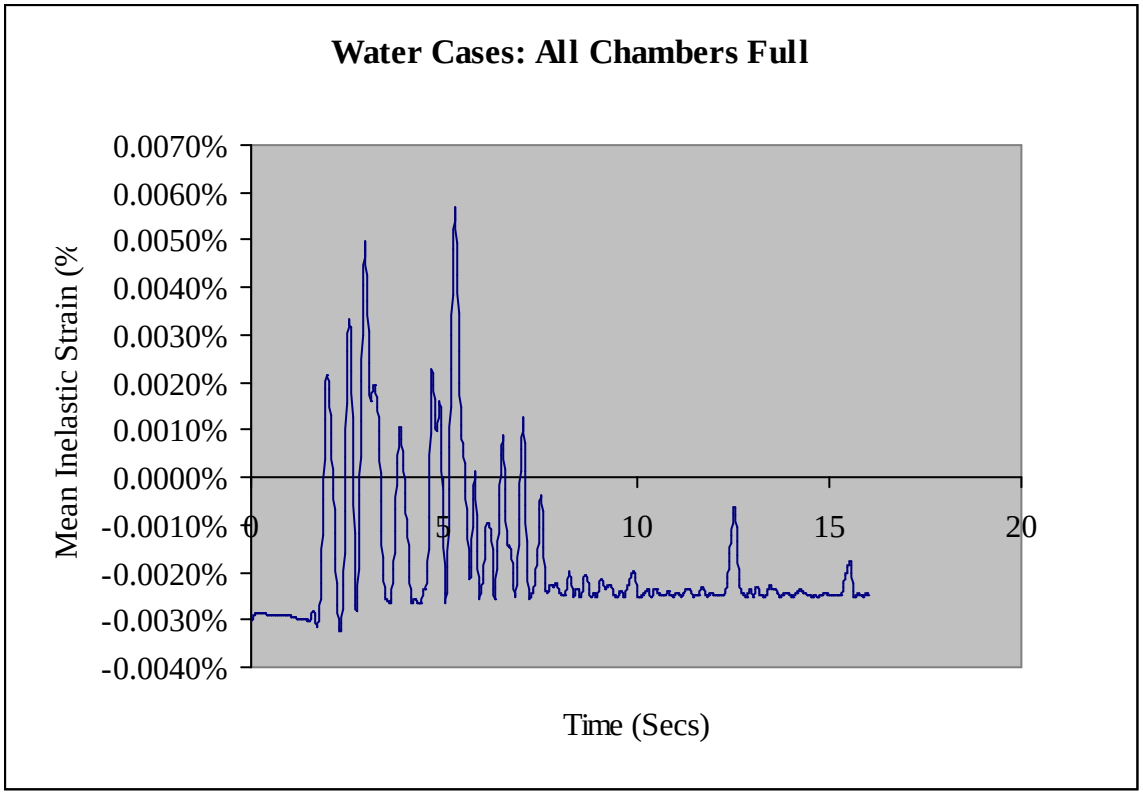
Water Cases: All Chambers Full
Mean Inelastic Strain (%
0.0070%
0.0060%
0.0050%
0.0040%
0.0030%
0.0020%
0.0010%
0.0000%
-0.0010%
-0.0020%
-0.0030%
-0.0040%
0
5
10
15
20
Time (Secs)

5.1 (b)

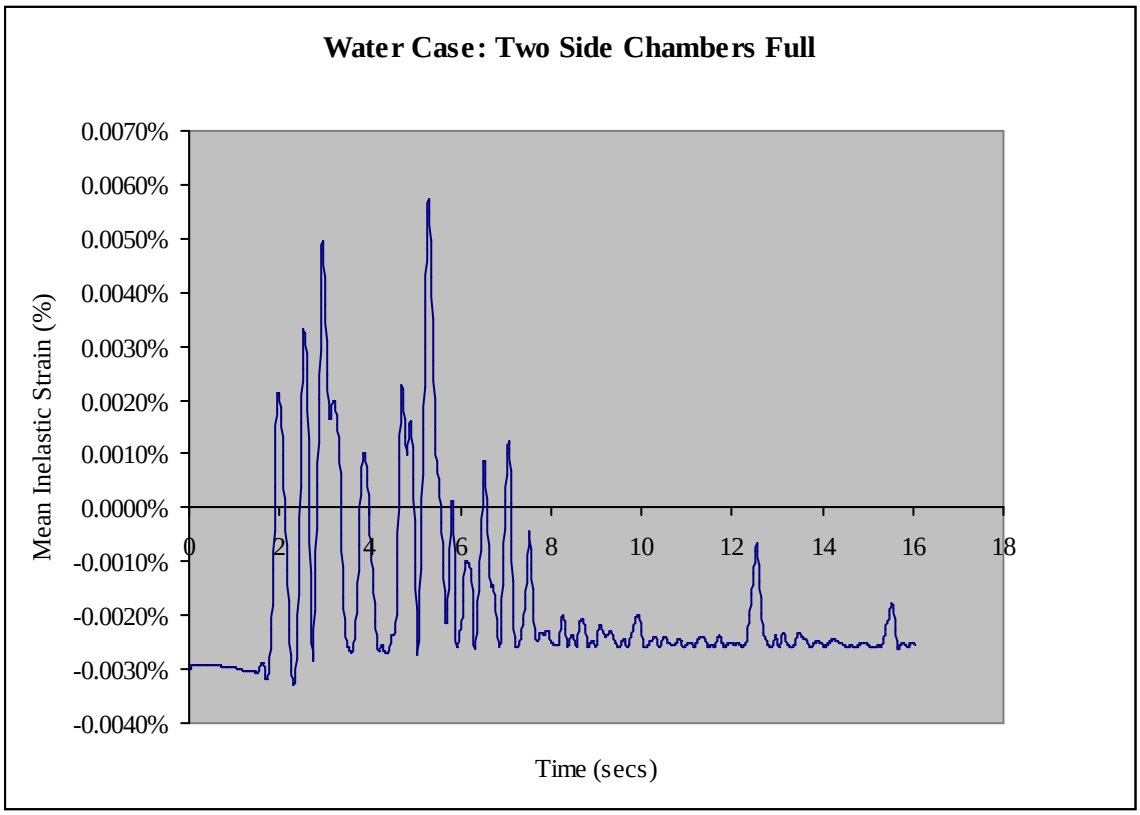
Water Case: Two Side Chambers Full
Mean Inelastic Strain (%)
0.0070%
0.0060%
0.0050%
0.0040%
0.0030%
0.0020%
0.0010%
0.0000%
-0.0010%
-0.0020%
-0.0030%
-0.0040%
0
2
4
6
8
10
12
14
16
18
Time (secs)

5.1 (c)

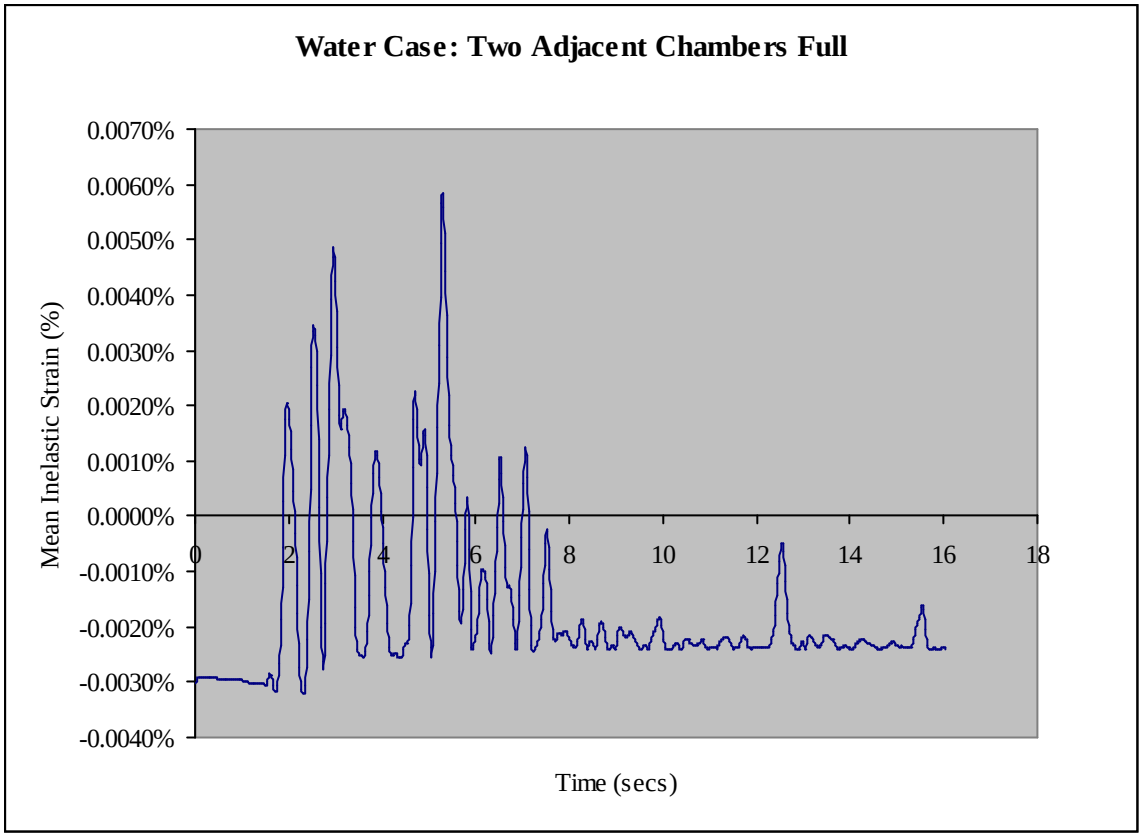
Water Case: Two Adjacent Chambers Full
Mean Inelastic Strain (%)
0.0070%
0.0060%
0.0050%
0.0040%
0.0030%
0.0020%
0.0010%
0.0000%
-0.0010%
-0.0020%
-0.0030%
-0.0040%
0
2
4
6
8
10
12
14
16
18
Time (secs)

5.1 (d)

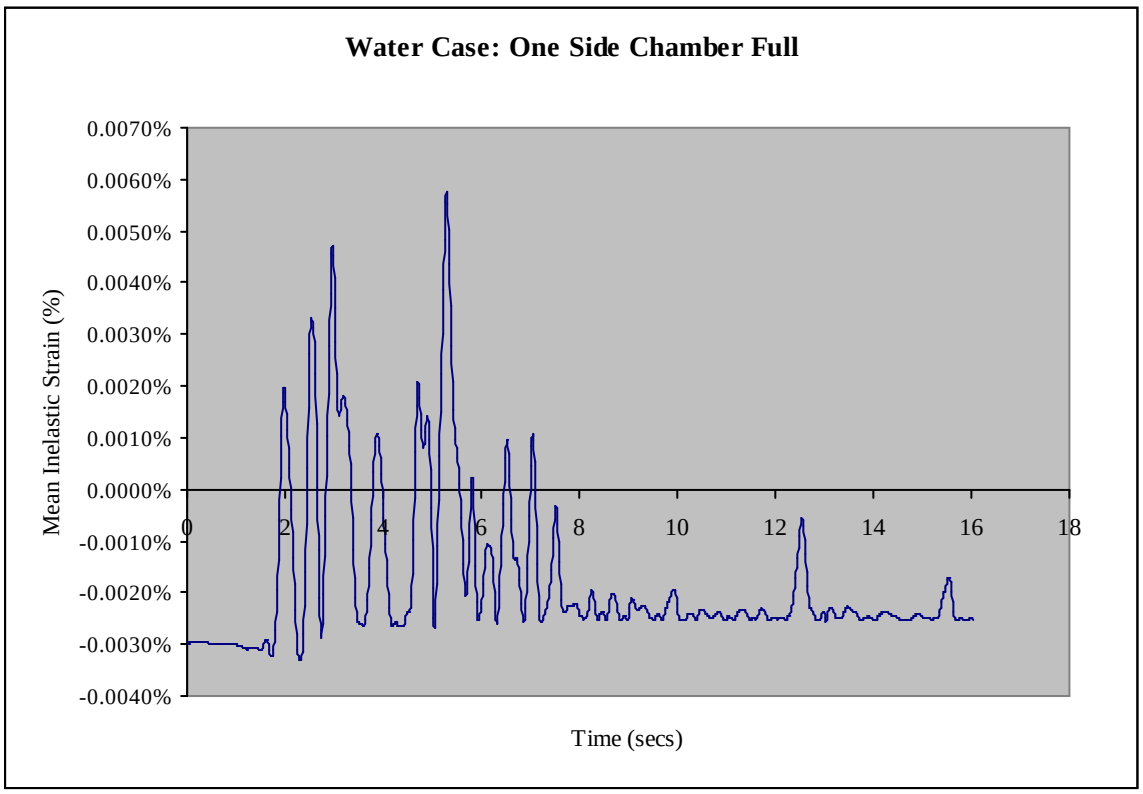
Water Case: One Side Chamber Full
Mean Inelastic Strain (%)
0.0070%
0.0060%
0.0050%
0.0040%
0.0030%
0.0020%
0.0010%
0.0000%
-0.0010%
-0.0020%
-0.0030%
-0.0040%
0
2
4
6
8
10
12
14
16
18
Time (secs)

5.1 (e)

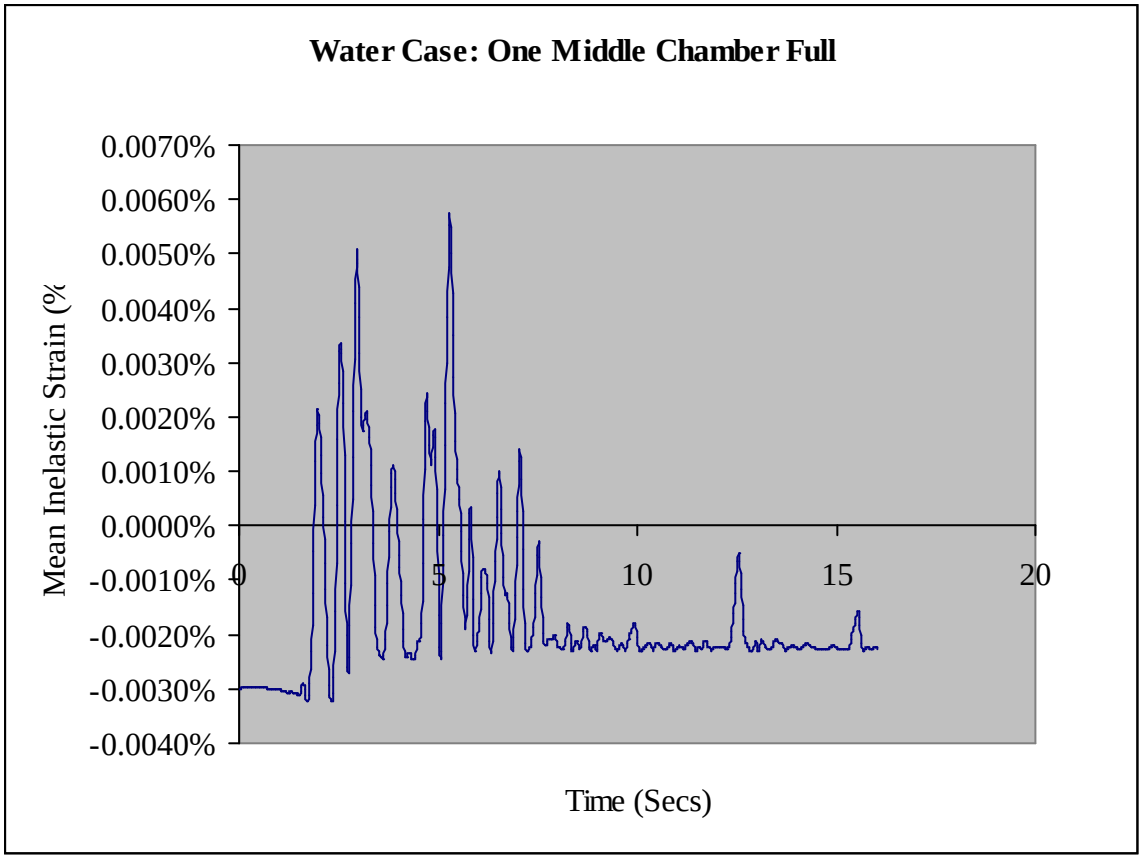

5.1 (f)

Figure 5.1 (a)-(f): Mean inelastic strain in time domain for various water cases

From the plots we can see that the mean inelastic strain levels are very low around 0.006 %. The structure did not fail during the entire history of the earthquake loading.

5.4.2 Damage Level

In all of these six conditions, the structure experienced only light damage during the entire history of the earthquake loading and didn't sustain any residual damage. The damage locations are almost identical in all conditions of water level. The peak damage along with the damage location is shown in figure 5.2.

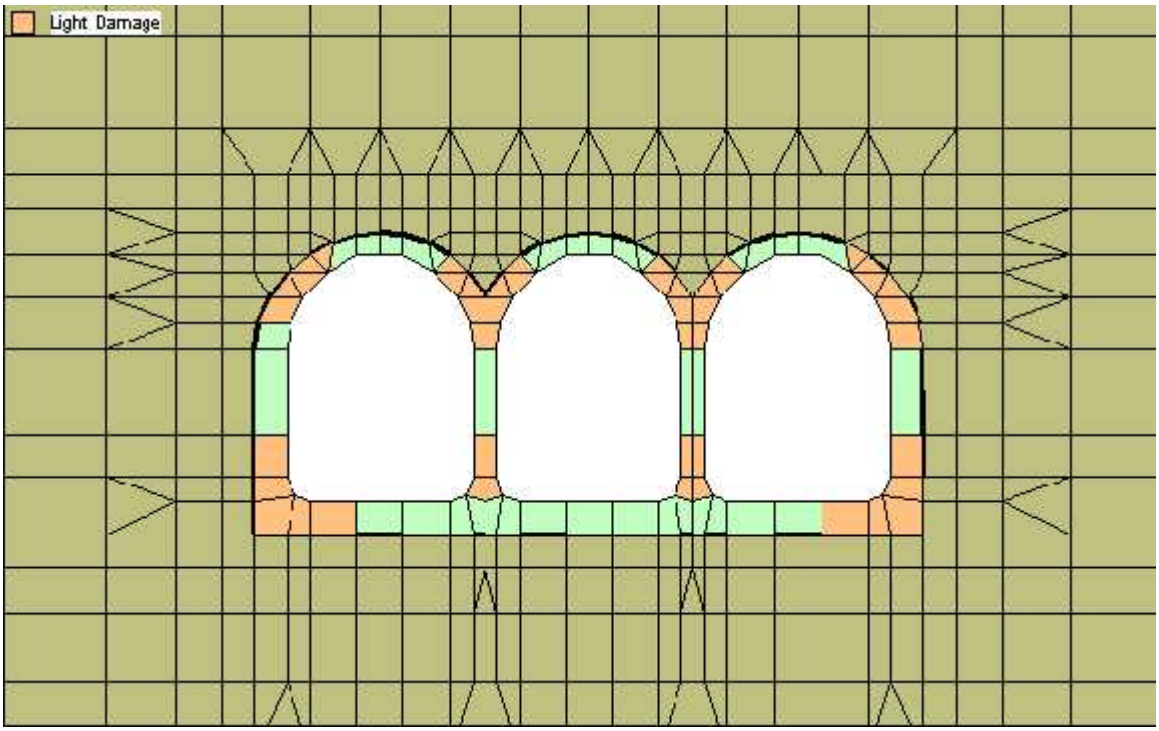

Figure 5.2: Damage location in the Covered Canal

5.4.3 Deformation, Crack Pattern and Yield Locations

Figure 5.3 shows the maximum deformation profile of the base case model. In the figure we can clearly see the separation between the soil and the structure at various interface locations along the periphery of the structure. Figure 5.4 shows the crack pattern of the structure at the maximum deformation. From the figure it is seen that the first crack occurred at very early stage of loading at 58 steps, i.e., at 1.16 seconds. We know that cracks are the major source of non-linearity in reinforced concrete structures. This clearly explains why traditional linear analysis would not suffice and nonlinear analysis has to be carried out. Similarly figure 5.5 shows the yield locations in the structure at the end of entire history of earthquake loading.

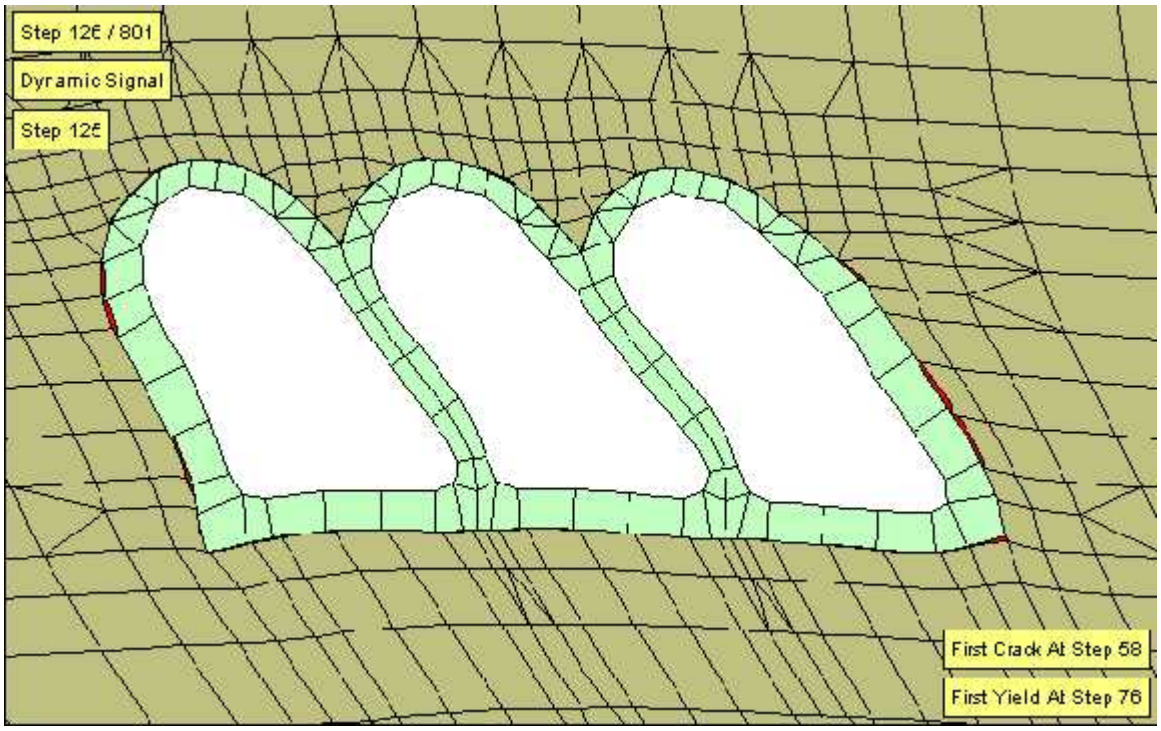

Figure 5.3: Maximum Deformation Profile (Exaggerated View; not to scale)

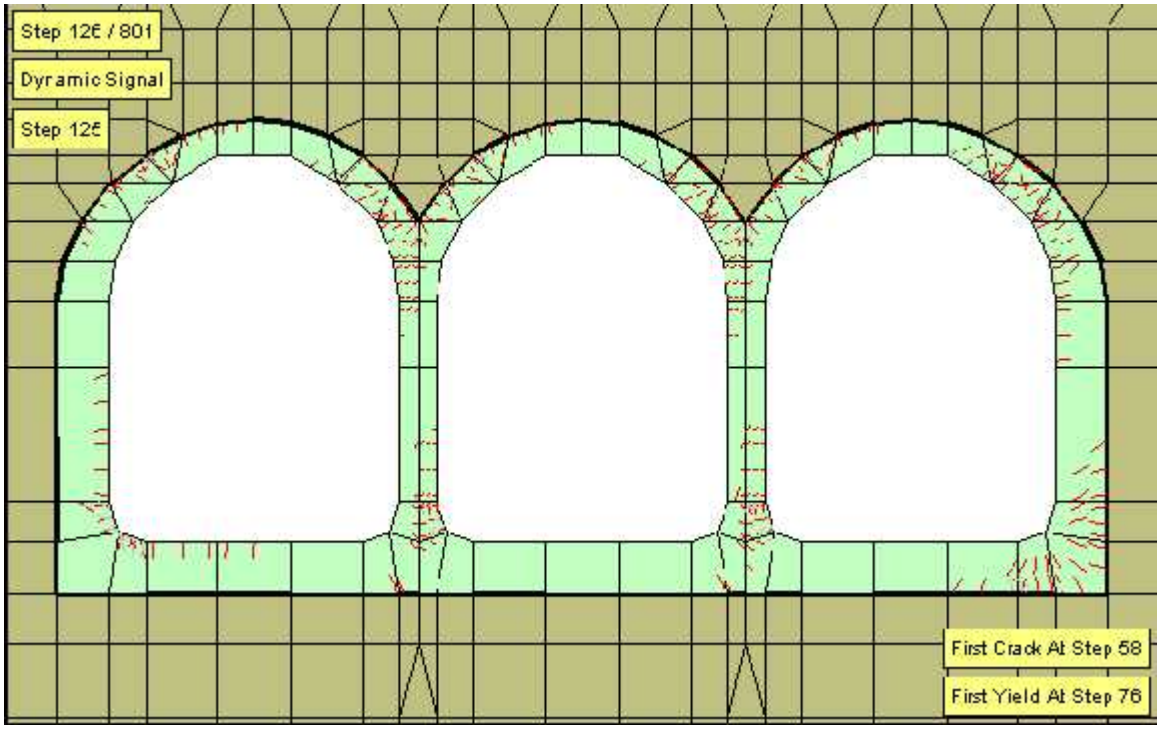

Figure 5.4: Crack Pattern at maximum deformation

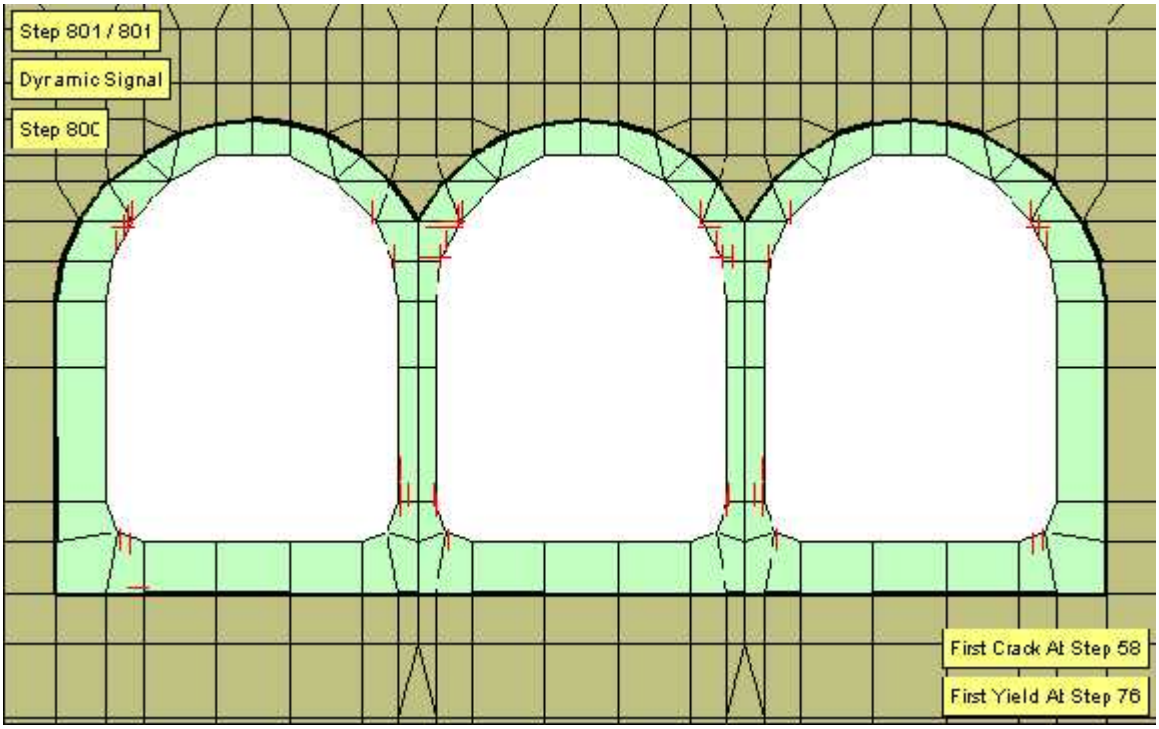

Figure 5.5: Yield Locations in the structure

5.4.4 Variation of Stress and Strain in time domain

In order to investigate the variation of the stress and strain parameters in time domain, an element, which experienced light damage, has been chosen. Accordingly, element 499 has been chosen. Maximum value occurred at gauss point 31 of that element. The element 499 lies at the bottom of the inner wall right to the axis of symmetry of the covered canal. The element 499 along with the gauss point 31 is shown in figure 5.6 (a). Figure 5.6 (b) shows the plot of peak tensile strain of various conditions of water level. From the figure 5.6 (b), we see that the peak tensile strains varied for all the cases. The case with one-middle chamber water full has got the lowest strain value among the six cases. And, the case with two-side chambers water full has got the highest strain value among the six cases.

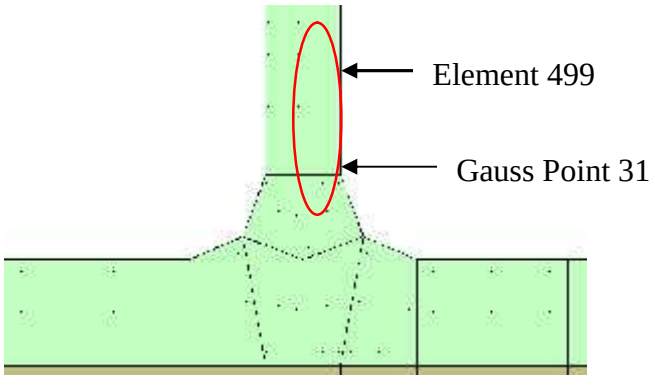

Figure 5.6 (a): Element 499 along with gauss point 31

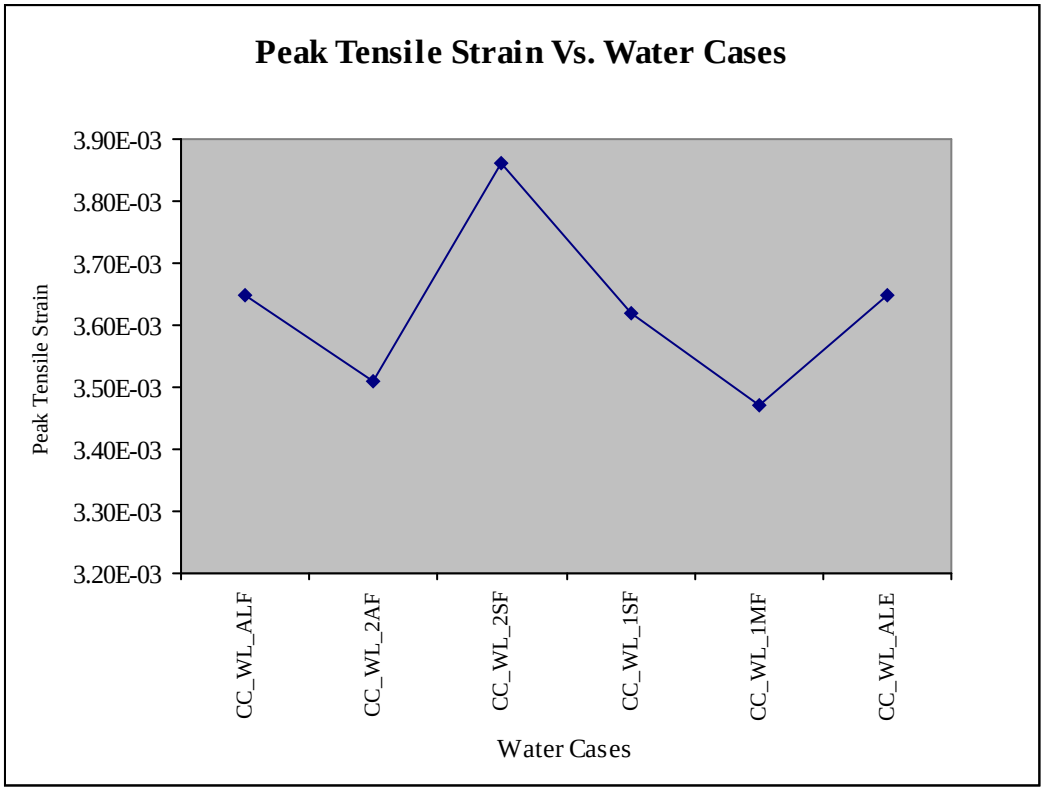

Figure 5.6 (b): Peak tensile strain for various water cases

The water cases with all chambers full and all chambers empty have got almost equal values of peak tensile strains.

The results show that the Covered Canal is safer under 1995 Kobe earthquake for the given soil profile. However, it will be inappropriate at this stage to conclude and generalize that the Covered Canal is safer in the earthquakes. From these results, we can also notice that when hydrodynamic effects are not considered, the different conditions of water level in the covered canal has got little effect on the overall performance of the covered canal.

5.5 Results of Soil Profile Cases

The geotecnical investigation has not been carried out in the area where the covered canal is to be constructed. The analysis for the water cases was carried out using the database of the bore log 1 of the head works area. From the results of the preceding analysis, we cannot conclude that whether the covered canal is safer or not in the event of the earthquake, though it is found to be safer in the preceding analysis. So, it

is deemed to be necessary to access the performance of the covered canal in various kinds of soil profiles. For this purpose, eleven models have been developed (Figure 4.3 and 4.10). These eleven models are grouped into three sets. First set consists of the three models having only one layer of soil each. Second set consists of six models with thickness and number of soil layers identical to original base case and varying the profiles by combination of soil properties. Third set consists of two models apart from base case with soil properties and number of soil layers identical to the base case and varying the thickness of the soil layers. These sets are tabulated below:

Set 1	Set 2	Set 3
CC_SP_A	CC_SP_ABC	CC_SP_ABC
CC_SP_B	CC_SP_ACB	CC_SP_ABC_ET
CC_SP_C	CC_SP_BAC	CC_SP_ABC_MLST
	CC_SP_BCA	
	CC_SP_CAB	
	CC_SP_CBA	

Table 3: Grouping of the eleven soil profiles results into three sets

The performance is expressed in terms of mean inelastic strain level, damage level and variation of stress & strain in time domain.

5.5.1 Mean Inelastic Strain

Soil profiles A, B, and C

Figure 5.7 (a)-(c) shows the plots of mean inelastic strain for soil profiles CC_SP_A, CC_SP_B and CC_SP_C. Soil profile CC_SP_B has got lowest mean inelastic strain level and the soil profile CC_SP_C has got highest mean inelastic strain level among the three. The mean inelastic strain level of CC_SP_C is almost double than that of the other two profiles. These results indicate that when the structure is embedded in clay type of soil, it sustains more damage.

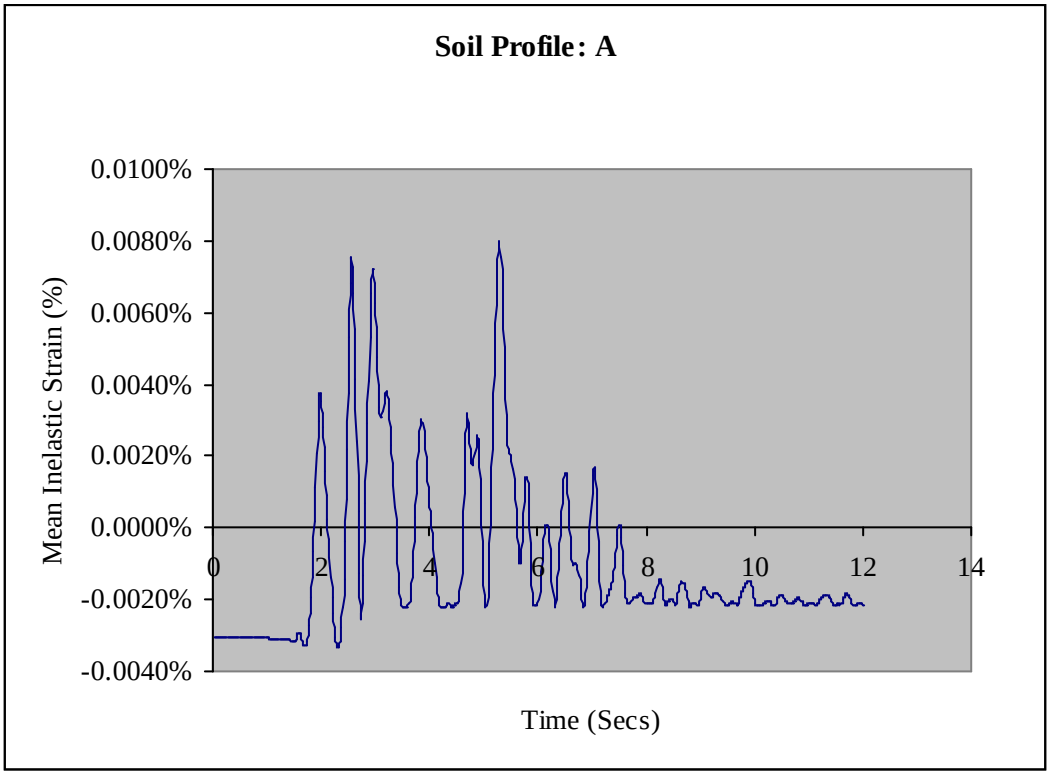
Soil Profile: A
0.0100%
0.0080%
0.0060%
0.0040%
0.0020%
0.0000%
-0.0020%
-0.0040%
Mean Inelastic Strain (%)
0
2
4
6
8
10
12
14
Time (Secs)

5.7 (a)

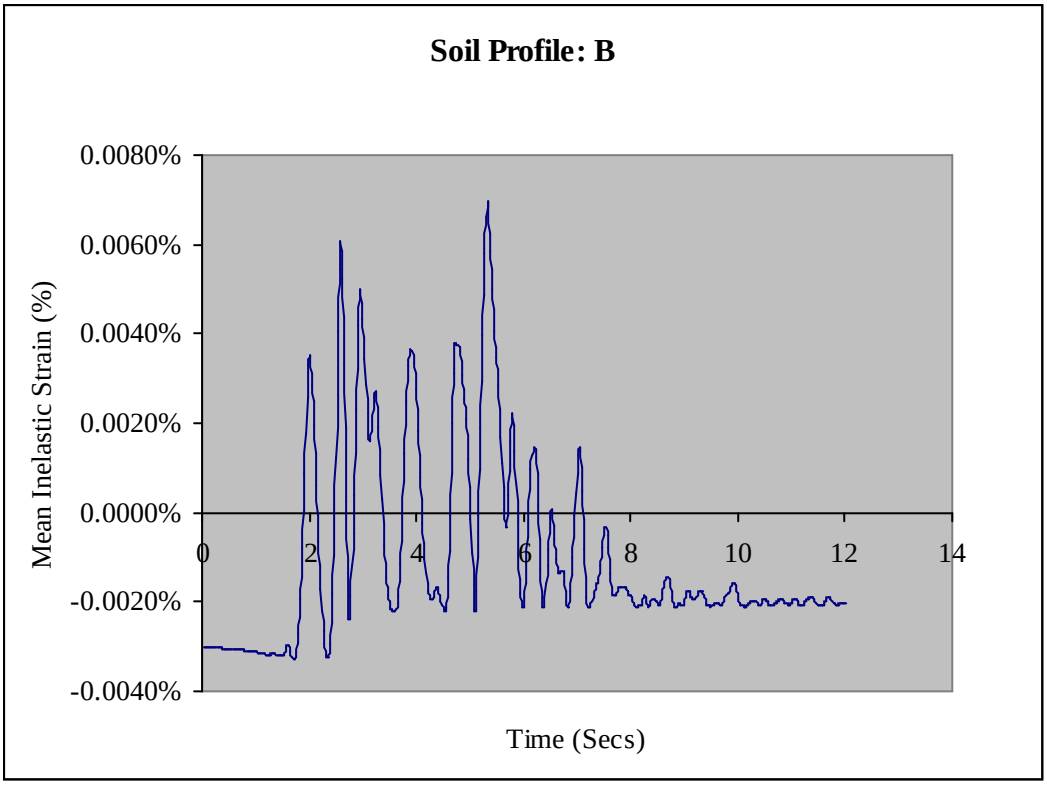
Soil Profile: B
0.0080%
0.0060%
0.0040%
0.0020%
0.0000%
-0.0020%
-0.0040%
Mean Inelastic Strain (%)
0
2
4
6
8
10
12
14
Time (Secs)

5.7 (b)

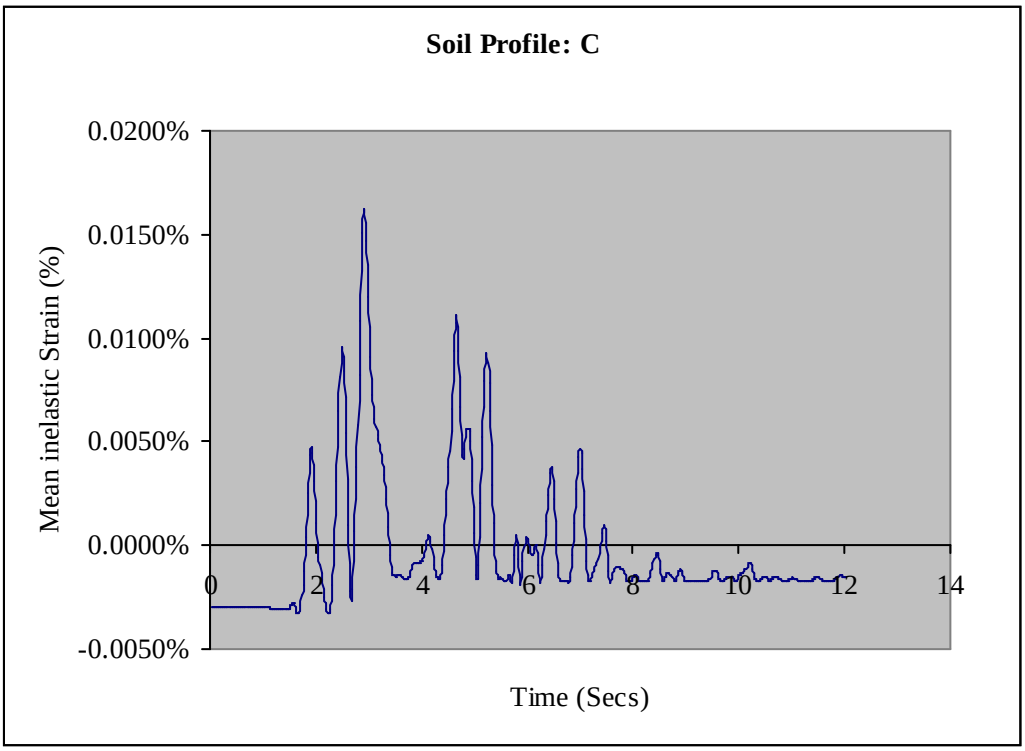

5.7 (c)

Figure 5.7 (a)-(c): Mean inelastic strain in time domain of soil profiles consisting of single layer soil

Soil profile: Combination of A, B and C

Figure 5.8 (a)-(f) shows the plots of mean inelastic strain for soil profiles CC_SP_ABC, CC_SP_ACB, CC_SP_BAC, CC_SP_BCA, CC_SP_CAB and CC_SP_CBA.

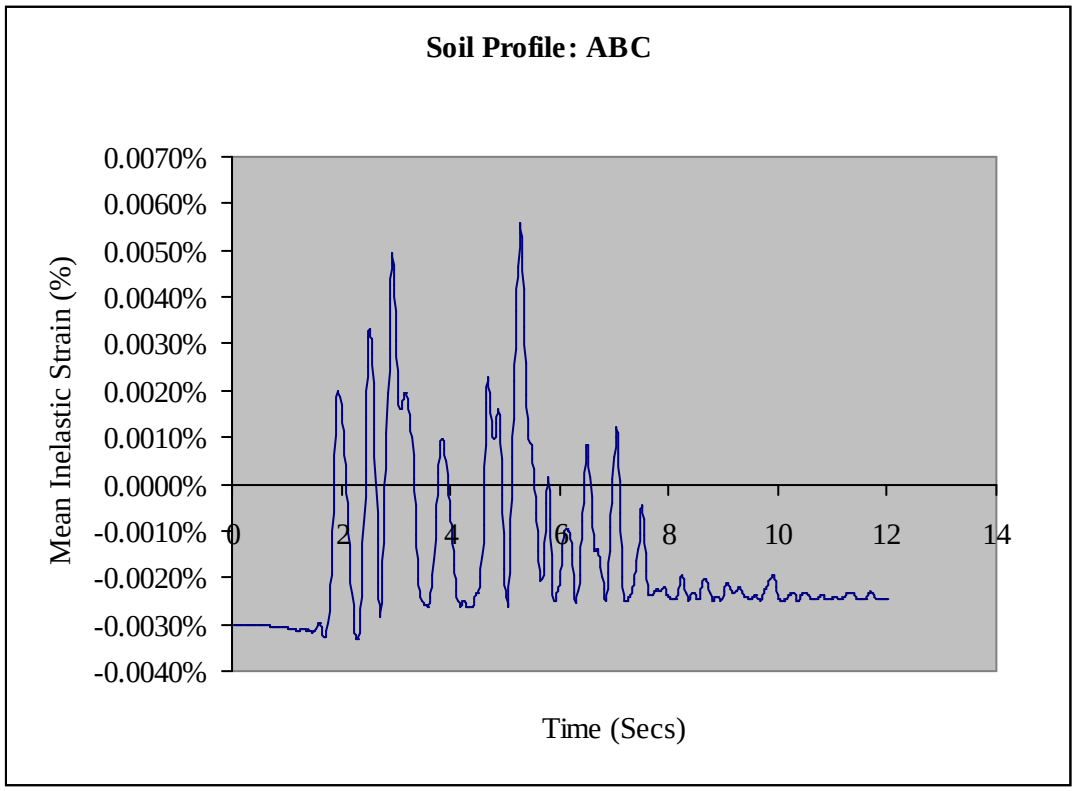
Soil Profile: ABC
0.0070%
0.0060%
0.0050%
0.0040%
0.0030%
0.0020%
0.0010%
0.0000%
-0.0010%
-0.0020%
-0.0030%
-0.0040%
Mean Inelastic Strain (%)
0
2
4
6
8
10
12
14
Time (Secs)

5.8 (a)

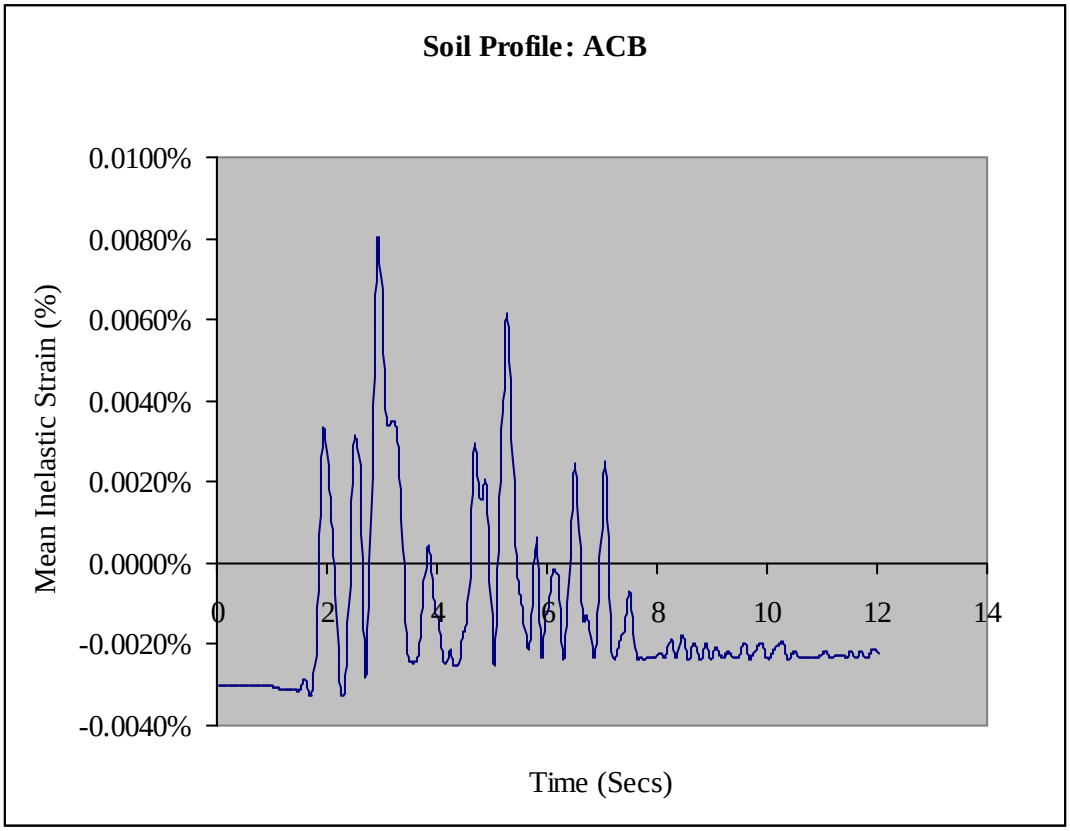
Soil Profile: ACB
0.0100%
0.0080%
0.0060%
0.0040%
0.0020%
0.0000%
-0.0020%
-0.0040%
Mean Inelastic Strain (%)
0
2
4
6
8
10
12
14
Time (Secs)

5.8 (b)

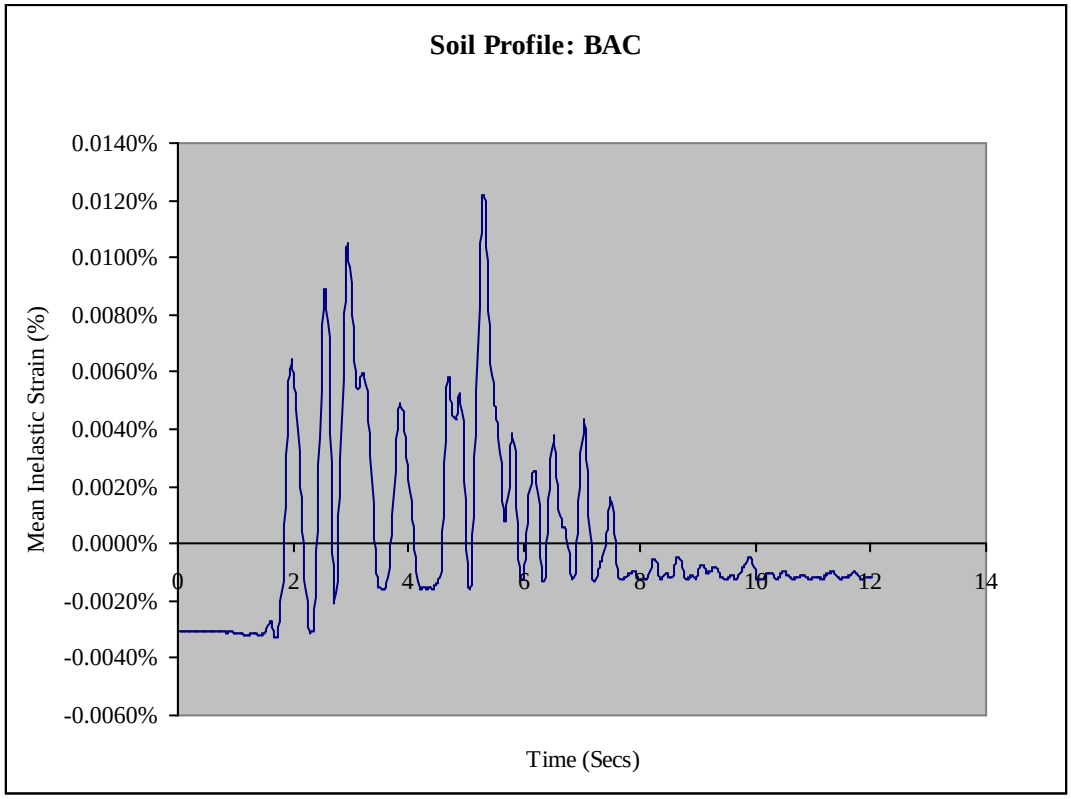
Soil Profile: BAC
0.0140%
0.0120%
0.0100%
0.0080%
0.0060%
0.0040%
0.0020%
0.0000%
-0.0020%
-0.0040%
-0.0060%
Mean Inelastic Strain (%)
0
2
4
6
8
10
12
14
Time (Secs)

5.8 (c)

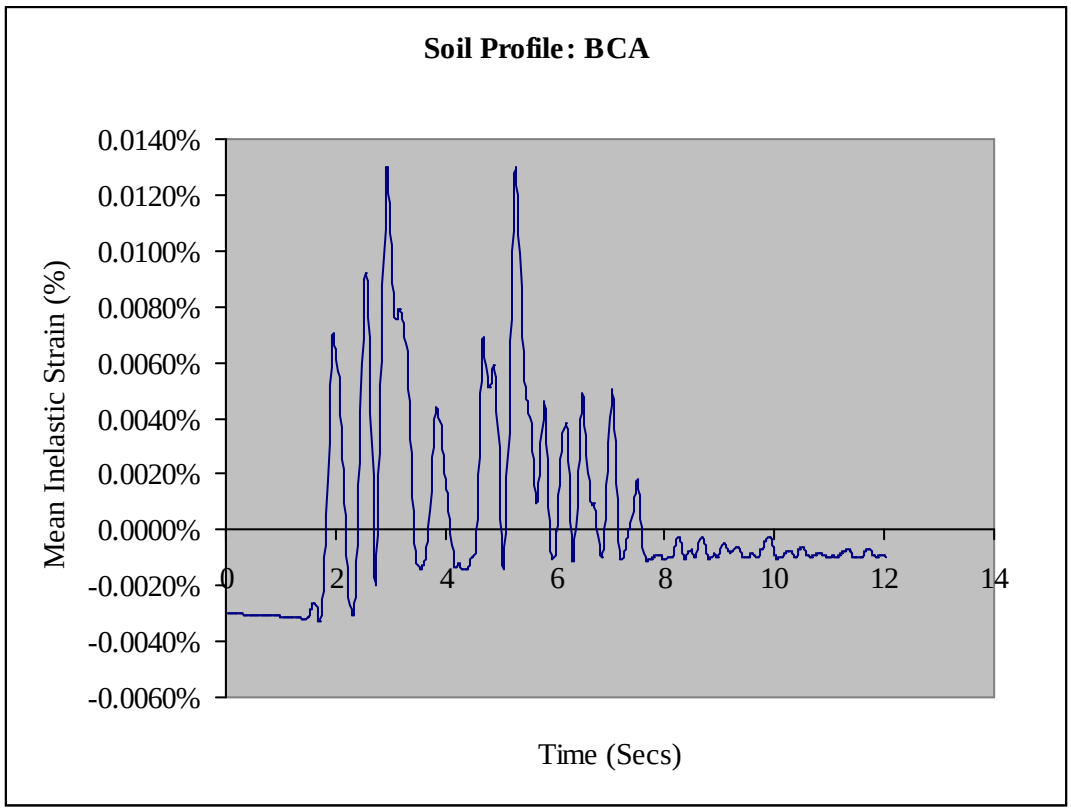
Soil Profile: BCA
0.0140%
0.0120%
0.0100%
0.0080%
0.0060%
0.0040%
0.0020%
0.0000%
-0.0020%
-0.0040%
-0.0060%
Mean Inelastic Strain (%)
0
2
4
6
8
10
12
14
Time (Secs)

5.8 (d)

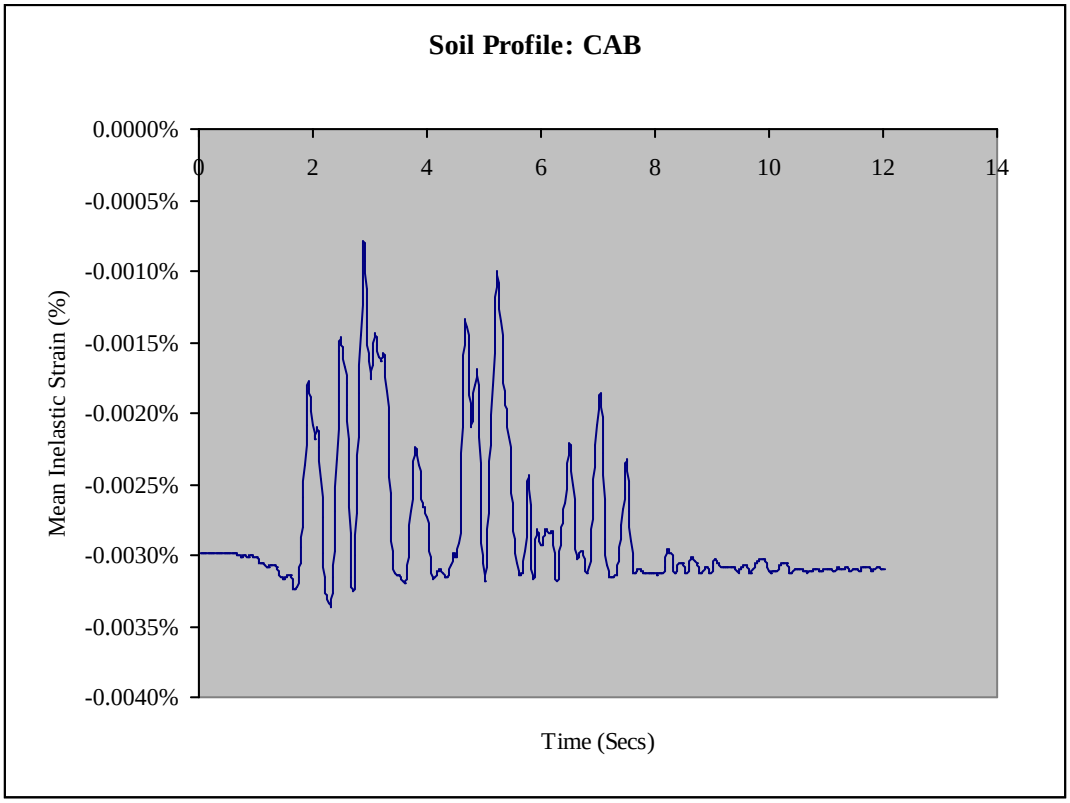

5.8 (e)

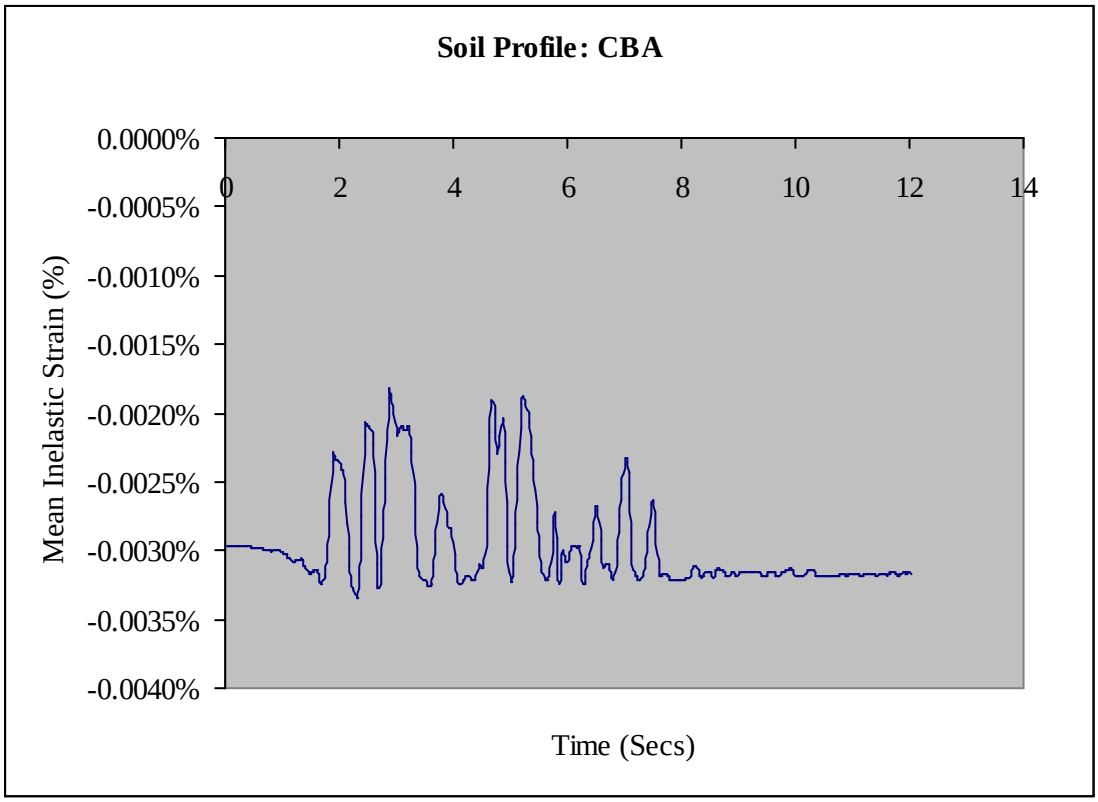

5.8 (f)

Figure 5.8 (a)-(f): Mean inelastic strain in time domain of soil profile consisting of combination of soil properties A, B, C

Among the six combinations of soil profiles, soil profiles CC_SP_CAB and CC_SP_CBA have got the least mean inelastic strain. Soil profiles CC_SP_BAC and CC_SP_BCA have got the highest mean inelastic strain level. Soil profiles CC_SP_ABC and CC_SP_ACB have got mean inelastic strain levels almost half than that of soil profiles CC_SP_BAC and CC_SP_BCA.

Soil profile: ABC-Original, ABC-Equal thickness and ABC-Middle layer small thickness

Figure 5.9 (a)-(b) shows the plots of mean inelastic strain for soil profiles CC_SP_ABC_ET and CC_SP_ABC_MLST. The mean inelastic strain of the soil profile having equal thickness layers with the underground structure completely surrounded by the middle soil layer (CC_SP_ABC_ET) is increased than that of the original soil profile. However, when the structure is embedded in the soil profile with a smaller thickness soil layer sandwiched between the two larger thickness soil layers (CC_SP_ABC_MLST) the structure showed quite different response than the other two cases. The mean inelastic strain increased considerably indicating larger damage than the other two cases.

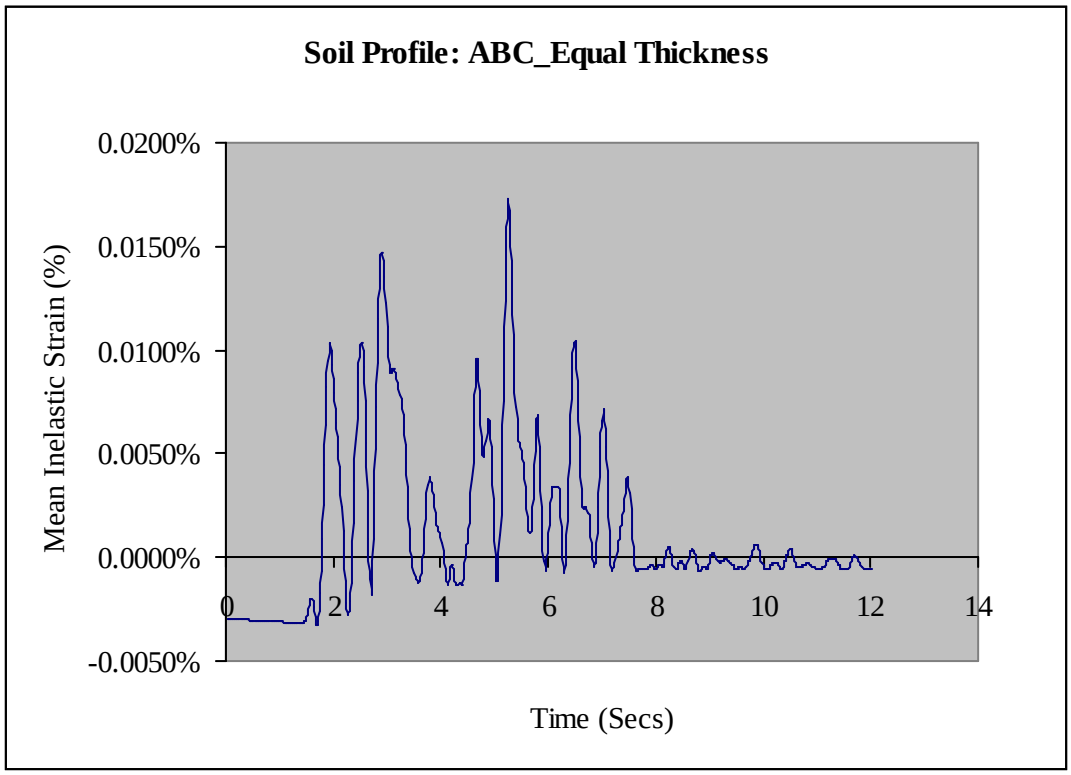

Figure 5.9.a: Plot of Mean Inelastic Strain of Soil Profile ABC of Equal thickness

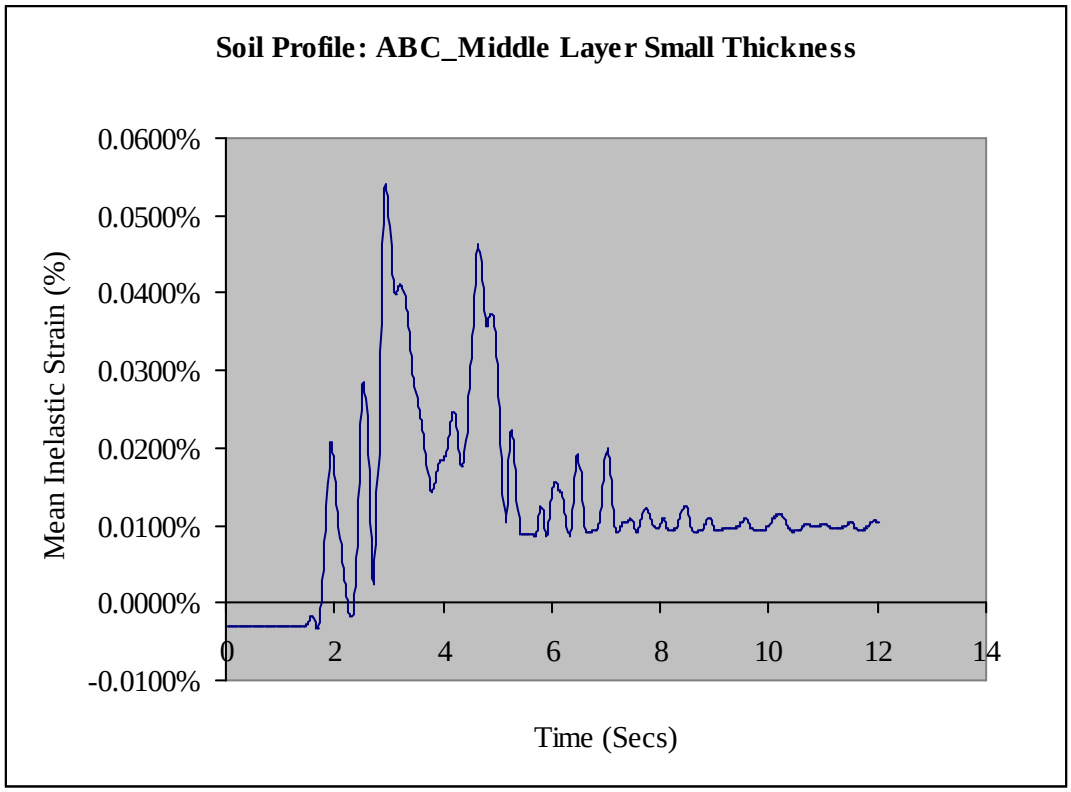

Figure 5.9.b: Plot of Mean Inelastic Strain of Soil Profile ABC with middle layer of small thickness

Comparison among the soil profiles CC_SP_A, CC_SP_ABC and CC_SP_ACB

Let us look at the plots of mean inelastic strain of figures 5.7 (a), 5.8 (a), and 5.8 (b). The plots reveal that the mean inelastic strain is almost identical among the three cases of the soil profile.

Comparison among the soil profiles CC_SP_B, CC_SP_BAC and CC_SP_BCA

Looking at the plots of mean inelastic strains in figures 5.7 (b), 5.8 (c) and 5.8 (d) we find that the mean inelastic strain of soil profiles CC_SP_BAC and CC_SP_BCA is almost identical. But, the mean inelastic strain of soil profile CC_SP_B is almost half than that of soil profiles CC_SP_BAC and CC_SP_BCA.

Comparison among the soil profiles CC_SP_C, CC_SP_CAB and CC_SP_CBA

Plots of mean inelastic strains in figures 5.7 (c), 5.8 (e) and 5.8 (f) shows that the mean inelastic strain of soil profiles CC_SP_CAB and CC_SP_CBA is drastically different than that of soil profile CC_SP_C. The mean inelastic strain of soil profiles

CC_SP_CAB and CC_SP_CBA is very low and is below zero. However, the mean inelastic strain is almost identical in both cases.

The results of these comparisons show that even when the underground structure is embedded in a homogenous soil medium at least up to depth equal to the height of the underground structure below its base, the soil layers below that depth have got effect on the performance of the underground structure. These comparisons thus give a very clear message. The soil exploration should be carried out to a considerable depth beyond the base of the underground structure, up to a depth where the soil layer can be considered as the engineering base rock.

5.5.2 Comparison of Peak Mean inelastic strain

The soil profile CC_SP_ABC is taken as the base case for comparison. The peak mean inelastic strain of soil profiles CC_SP_A and CC_SP_ACB are 1.44 times greater than that of soil profile CC_SP_ABC, i.e., the base case. Similarly, the peak mean inelastic strain of soil profiles CC_SP_B, CC_SP_BAC and CC_SP_BCA are 1.25, 2.19 and 2.33 times greater than the base case respectively. Further the peak mean in elastic strain of soil profile CC_SP_C is 2.91 times more than that of the base case. However, the peak mean inelastic strains of soil profiles CC_SP_CAB and CC_SP_CBA are very less and are equal to –0.14 and –0.33 times than the base case respectively. The peak mean inelastic strain of soil profile CC_SP_ABC_ET is slightly increased than the other soil profile cases. The peak mean inelastic strain is 3.11 times more than the base case. But, the peak mean inelastic strain of the soil profile CC_SP_ABC_MLST is drastically increased than the base case as well as other soil profile cases. The peak mean inelastic strain is 9.71 times more than the base case.

5.5.3 Damage Level

Looking at the damage results of the soil profiles, we see that the soil profiles grouped in set 1 and set 2 experienced only light damage during the entire history of the earthquake with no residual damage. However, when we look at the damage results of set 3, we find some interesting results. Even when the soil profile is changed to the one having equal thickness soil layers, the structure experienced the light damage. But when the soil profile is changed to the one having smaller thickness soil layer

sandwiched, the damage level experienced was considerable with residual light damage. It seems that when there is a presence of layered soil around the underground structure, the damage incurred becomes more. Thus, the soil properties and the soil profile around the underground structure should be accessed in detail. Similar kind of the results have been obtained by Maekawa et al. (2003). The location of damage and type of damage has been shown in figures 5.10 and 5.11.

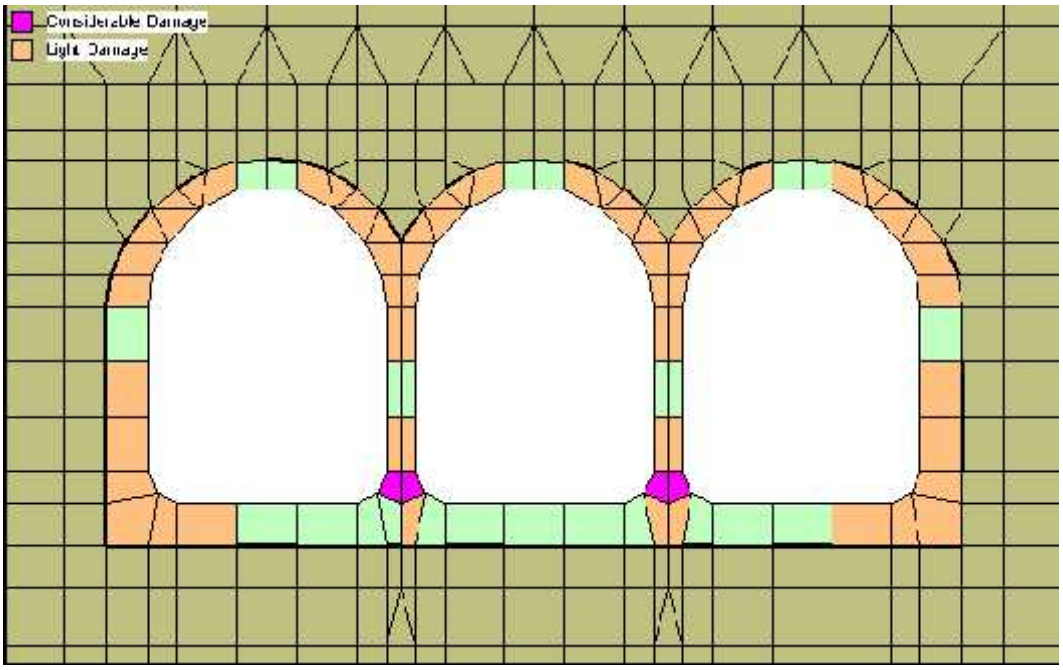

Figure 5.10: Peak damage for Soil Profile CC_SP_ABC_MLST

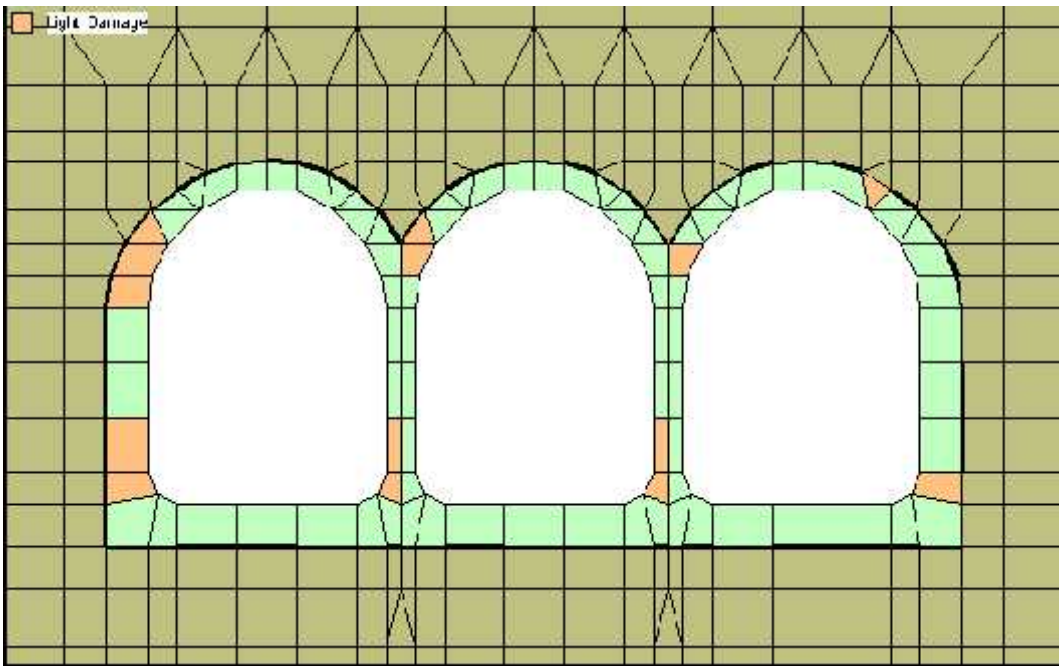

Figure 5.11: Residual damage for Soil profile CC_SP_ABC_MLST

5.5.4 Peak acceleration

Figures 5.12 shows the peak acceleration and peak displacement response at the top and bottom of the structure along the centerline of the structure.

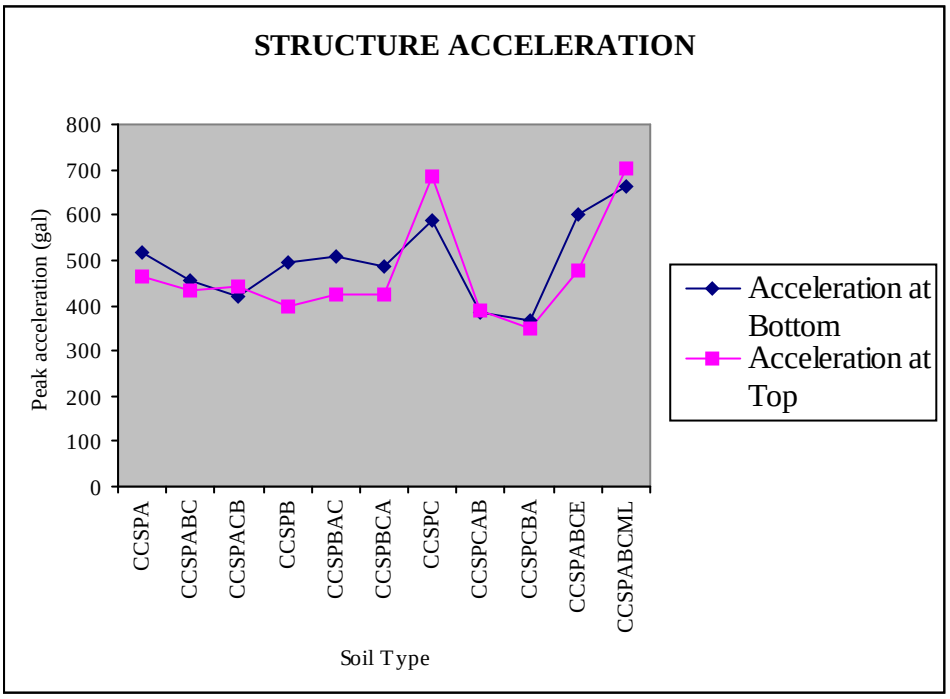

Figure 5.12: Peak acceleration at the top and bottom of the structure

The acceleration at both the top and bottom of the structure is largest for the soil profile CC_SP_ABC_MLST. The second largest acceleration at both top and bottom of the structure is for soil profile CC_SP_C. The least acceleration is for the soil profile CC_SP_CBA. In all cases of soil profiles, the acceleration value is attenuated.

5.5.5 Relative displacement

Figure 5.13 shows the relative displacement between the top and bottom of the structure along the centerline of the structure. The relative displacement is largest for the soil profile, CC_SP_ABC_MLST. Similarly, the second largest relative displacement is for the soil profile CC_SP_ABC_ET. The least relative displacement is for soil profile CC_SP_CBA. The considerable damage experienced by the structure in soil profile CC_SP_ABC_MLST can be explained through the largest deformation that occurred in the structure.

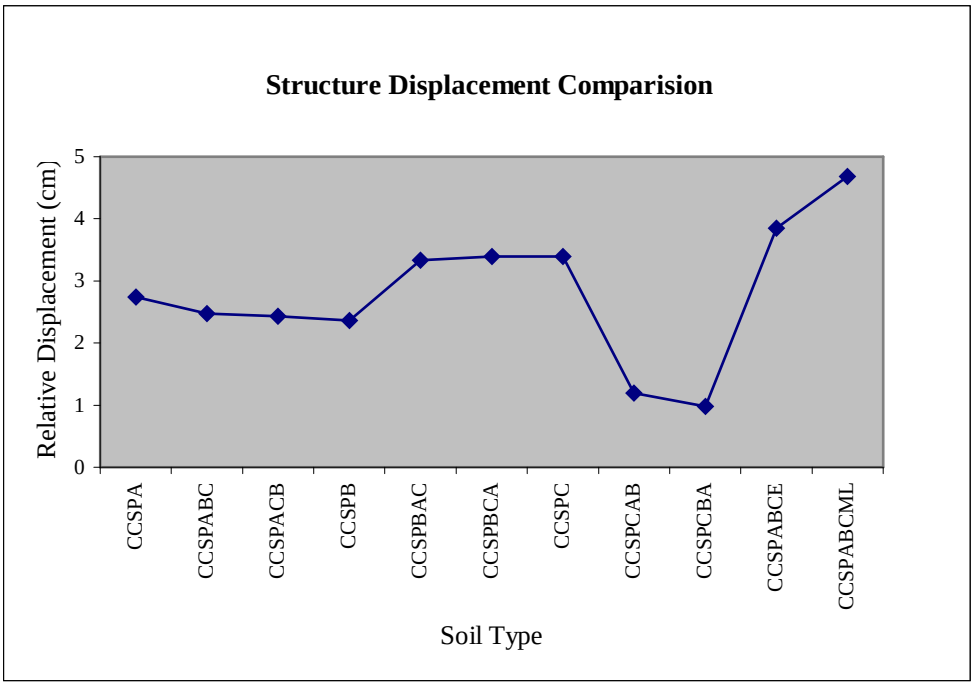

Figure 5.13: Relative displacement between the top and bottom of the structure

5.5.6 Variation of Stress and Strain in Time domain

The plots of variation of different stress and strain parameters during the entire history of the earthquake are presented herein this section. For this purpose element 465 is chosen. The variation of stress and strain history at gauss point 32 of element 465 is presented here. The element 465 along with the gauss point 32 is shown in figure 5.14. The element 465 lies at the bottom of the inner wall right to the symmetry of the covered canal. The plots of normal stress along X and Y direction (□xx and □yy) and shear stress (□xy) for the eleven cases of soil profile are presented and comparison among them is made. Similarly, the plots of normal strain along X and Y direction (□xx and □yy) and shear strain (□xy) for eleven cases of soil profile are also presented and compared.

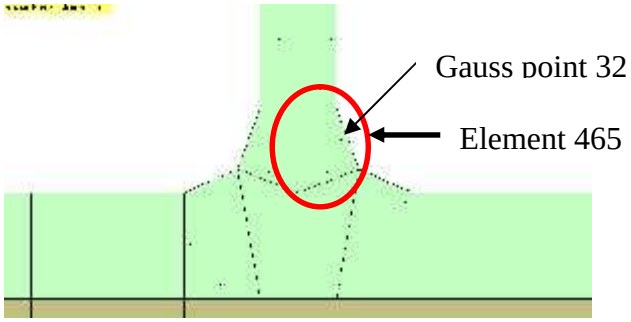

Figure 5.14: Element 465 along with gauss point 32

Variation of □xx

The plots of variation of □xx in time domain are presented in figure 5.14.

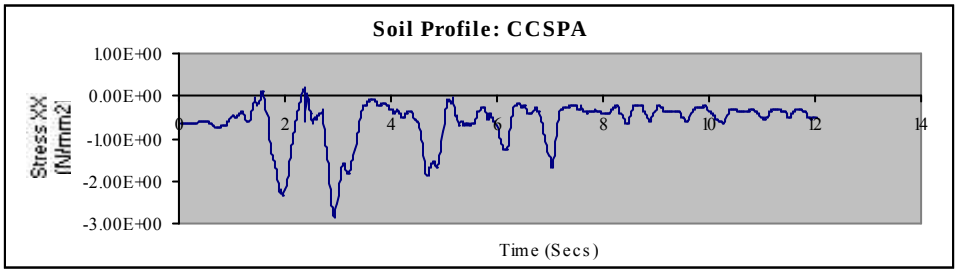

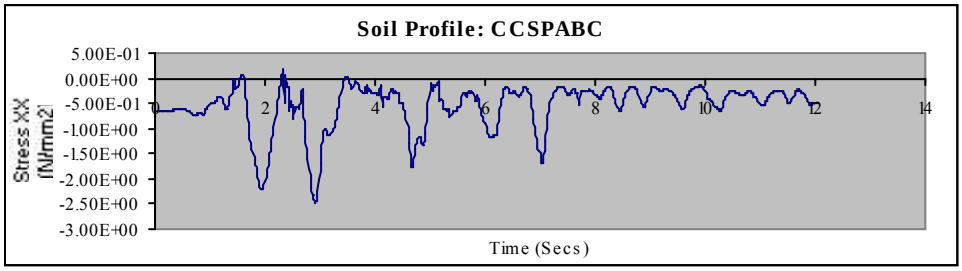

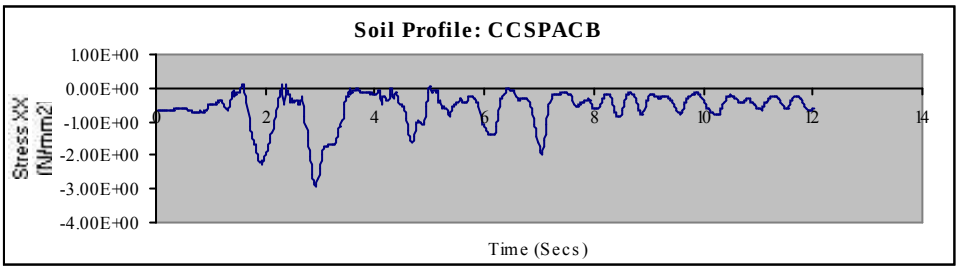

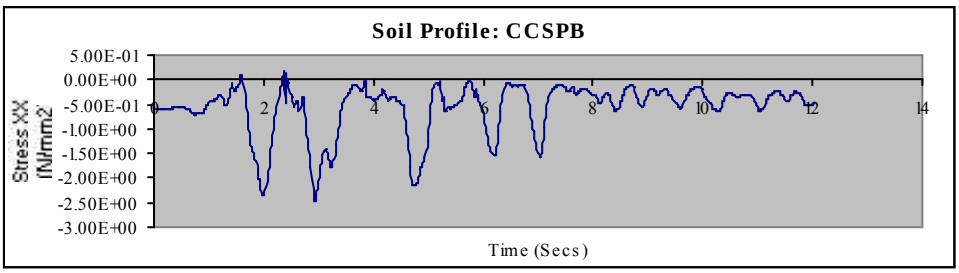

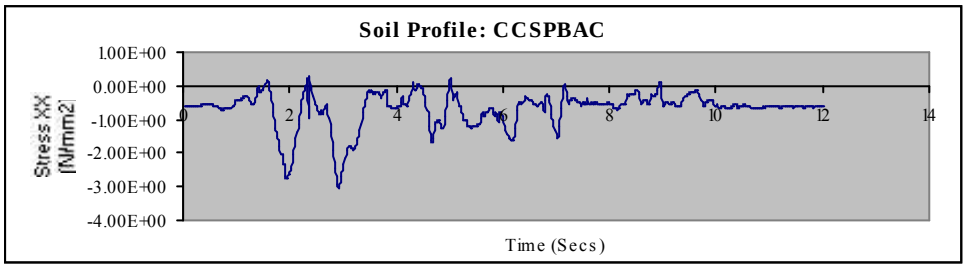

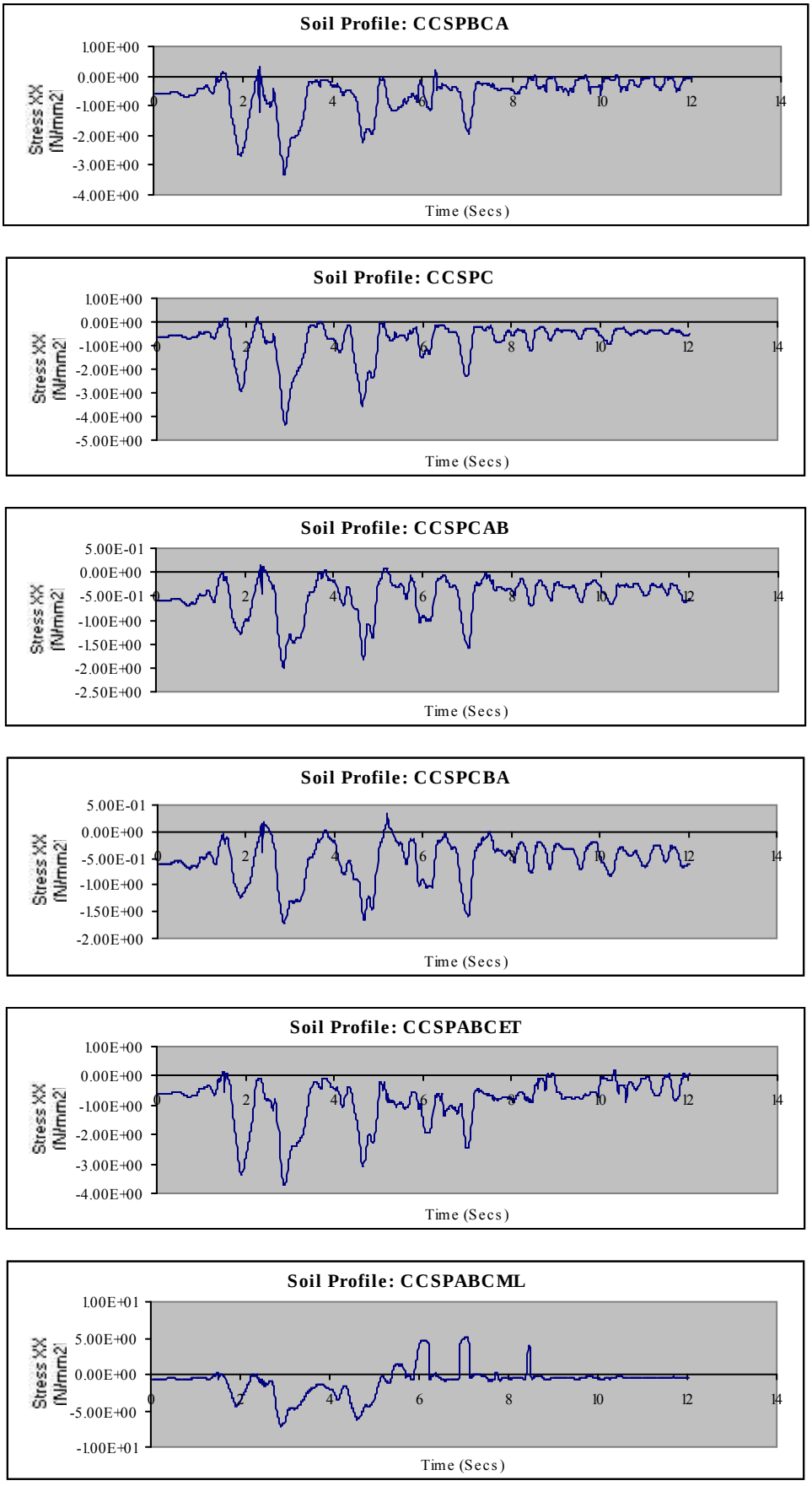

Figure 5.15: Variation of Stress XX in time domain for various soil profiles

Variation of □yy

The plots of variation of □yy in time domain are presented in figure 5.15.

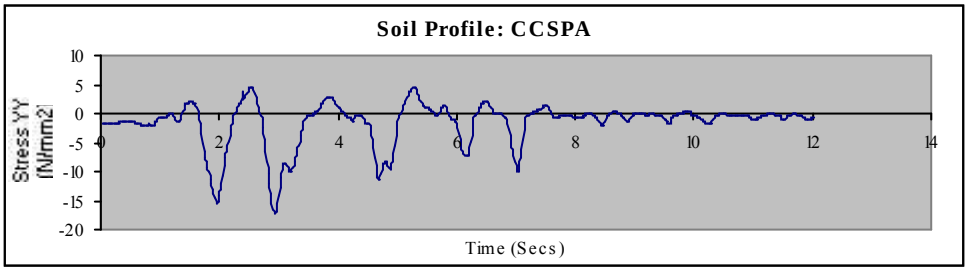

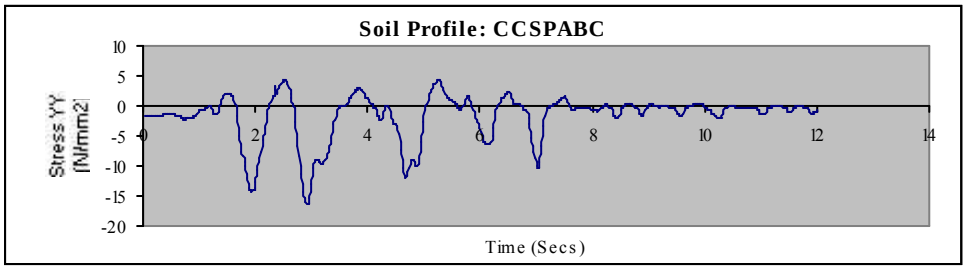

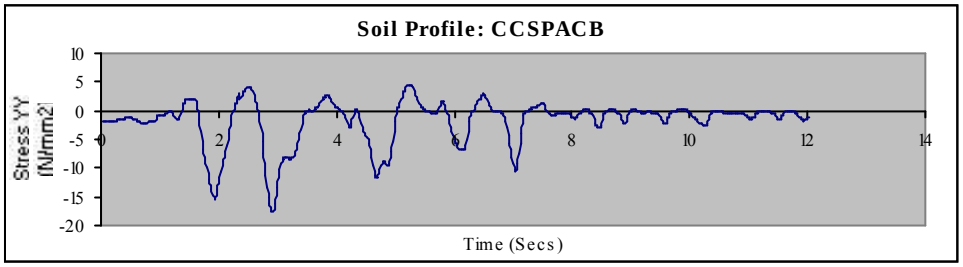

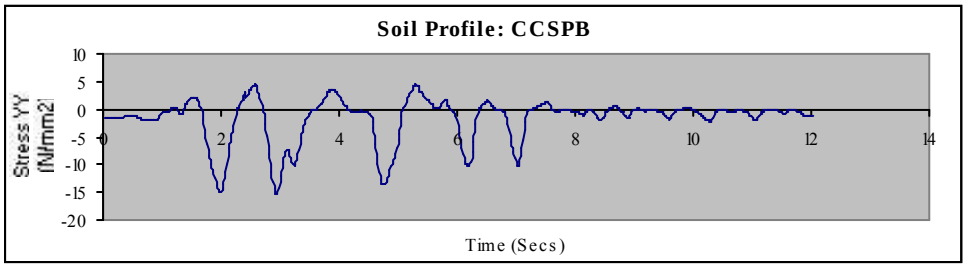

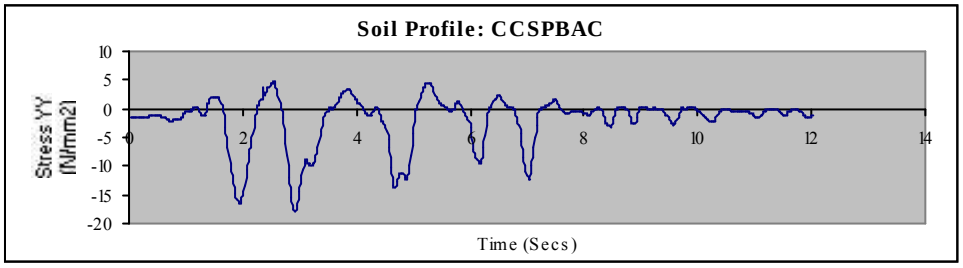

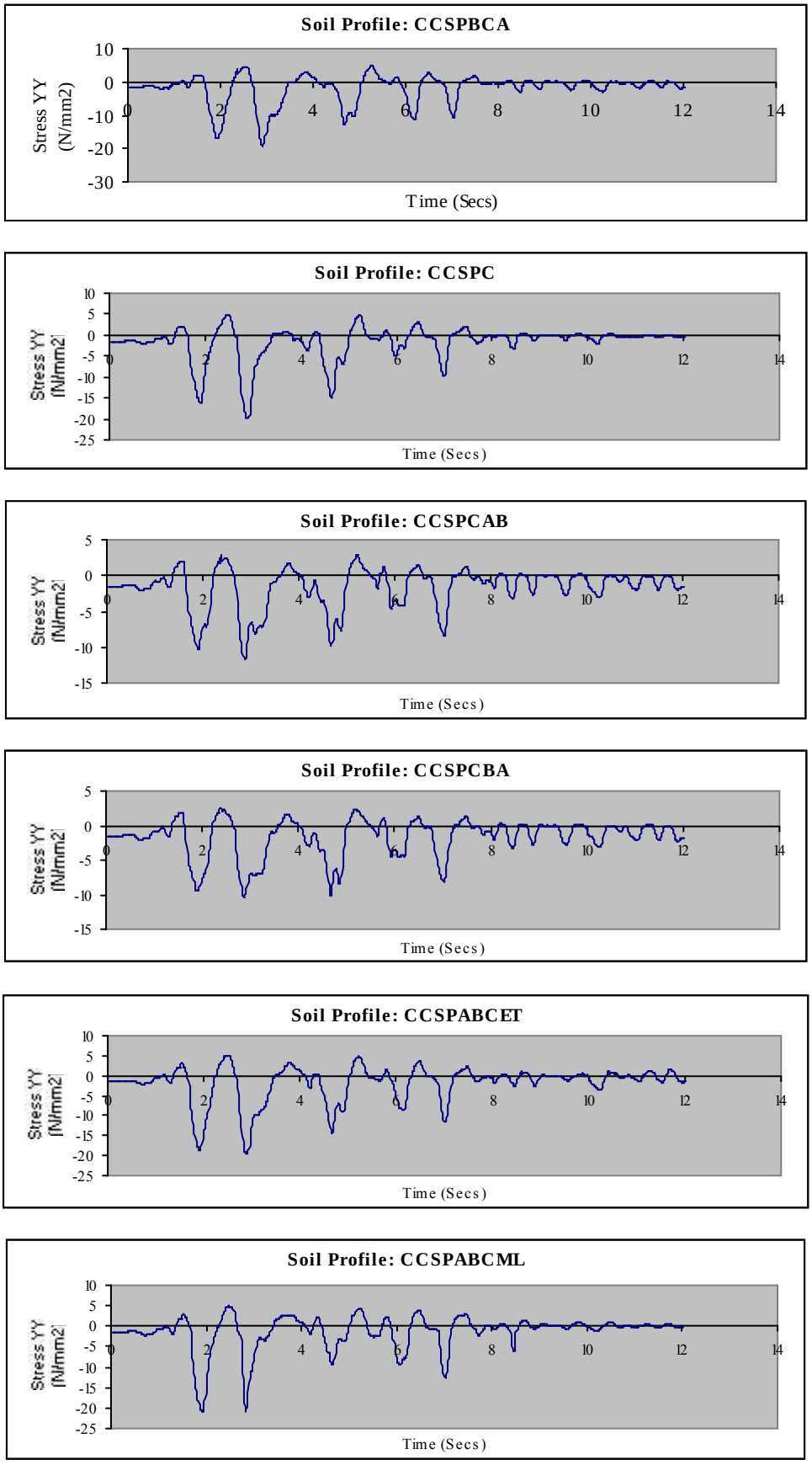

Figure 5.16: Variation of Stress YY in time domain for various soil profiles

Variation of □xy

The plots of variation of □xy in time domain are presented in figure 5.16.

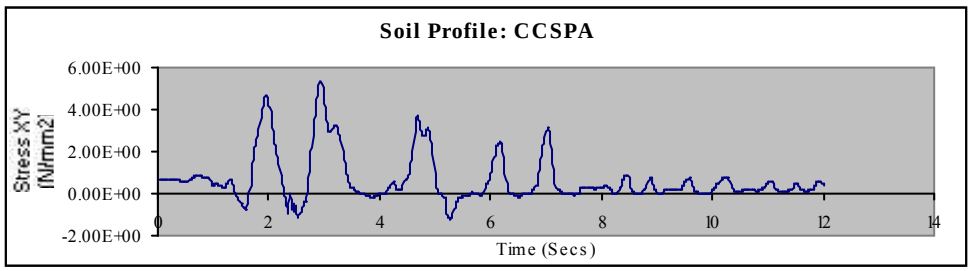

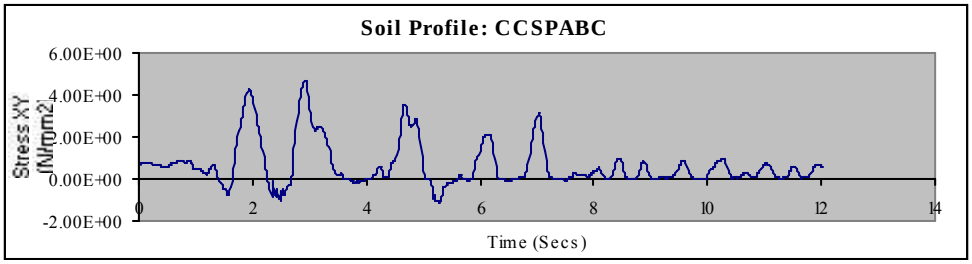

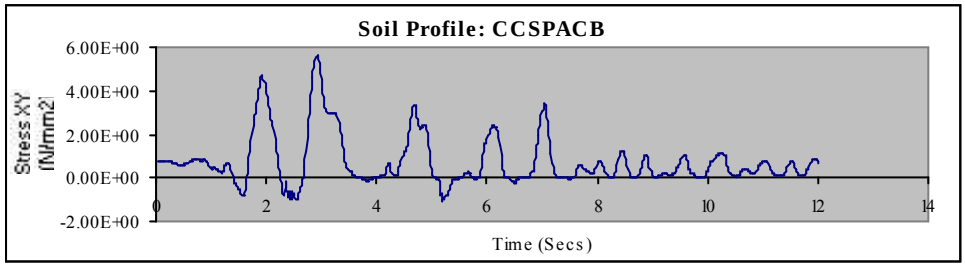

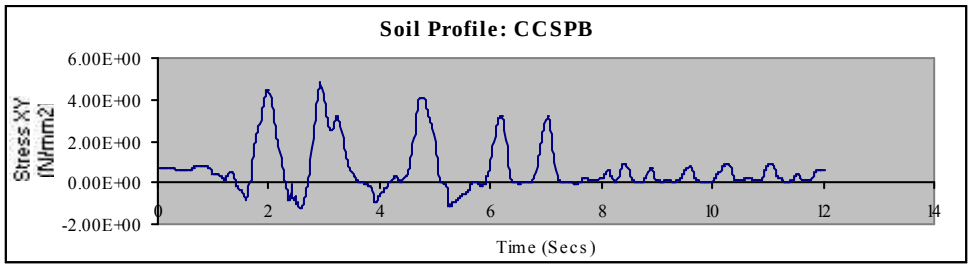

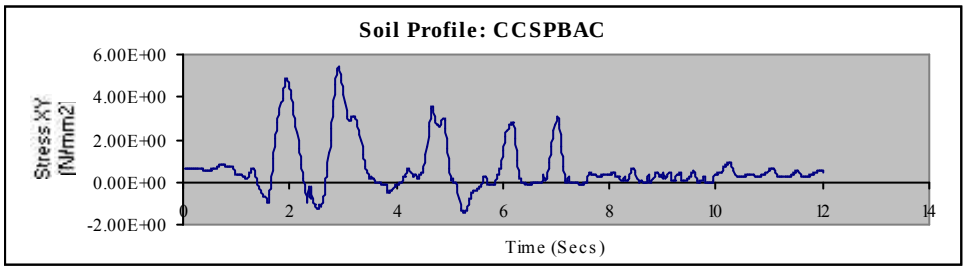

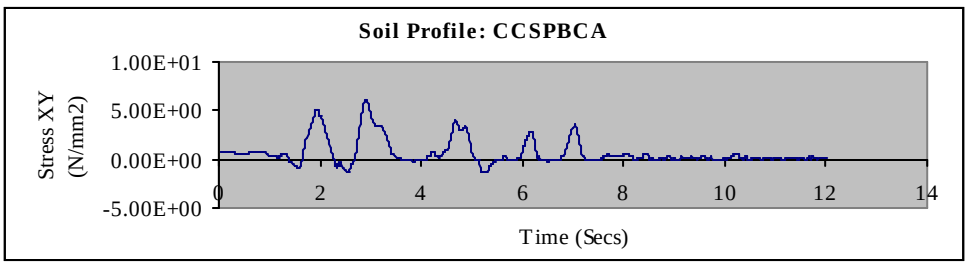

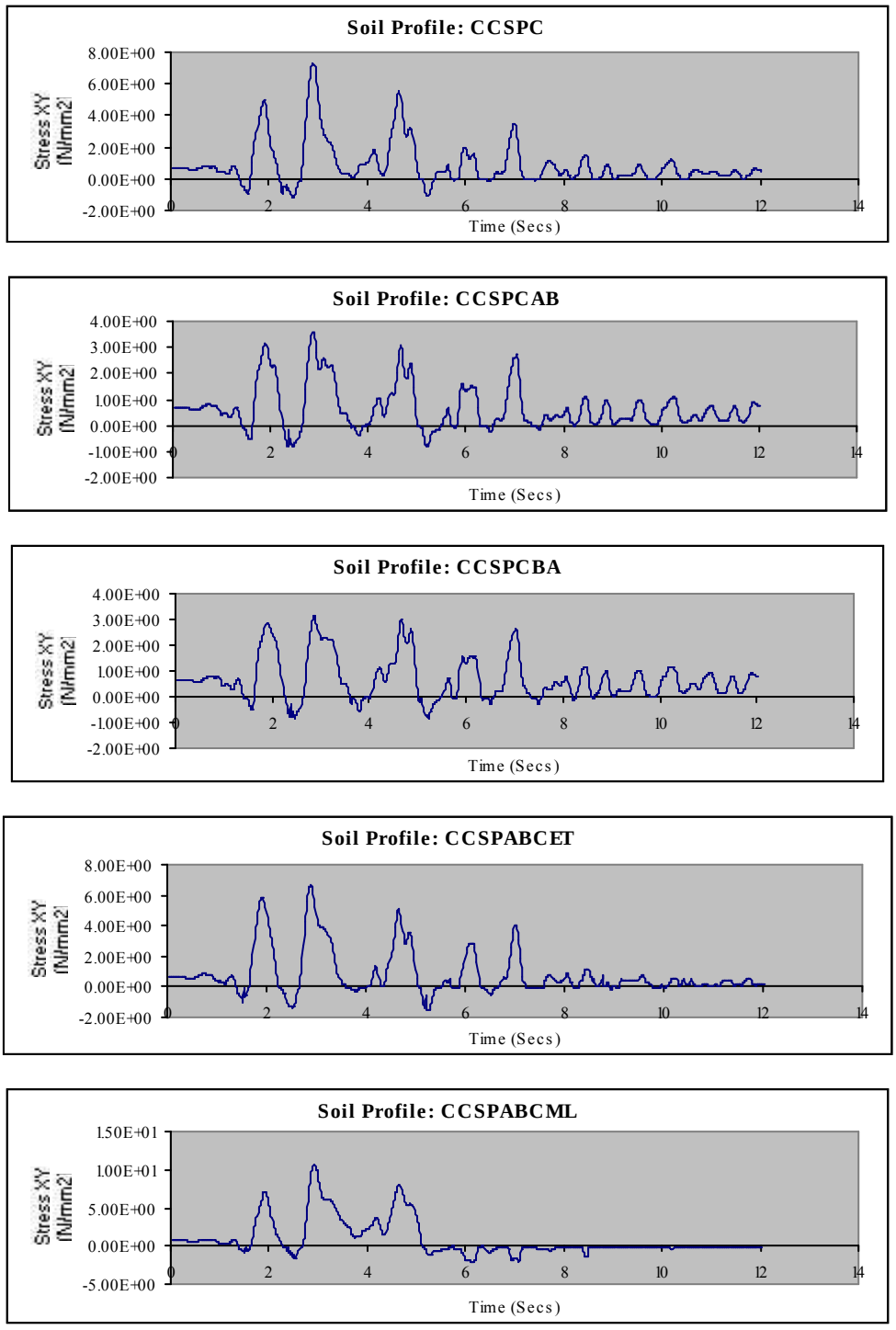

Figure 5.17: Variation of Stress XY in time domain for various soil profiles

Variation of □xx

The plots of variation of □xx in time domain are presented in figure 11.

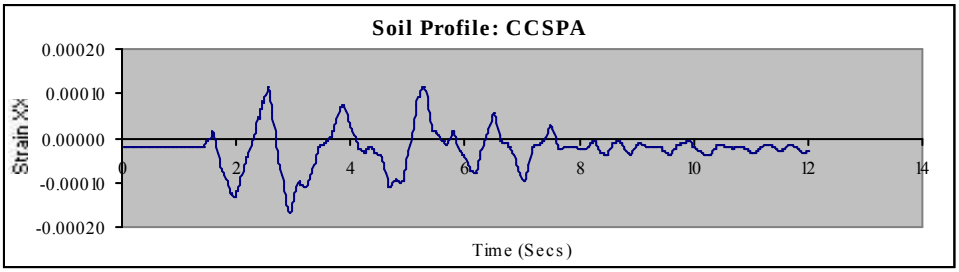
Soil Profile: CCSPA
0.00020
0.00010
0.00000
-0.00010
-0.00020
Strain XX
0
2
4
6
8
10
12
14
Time (Secs)

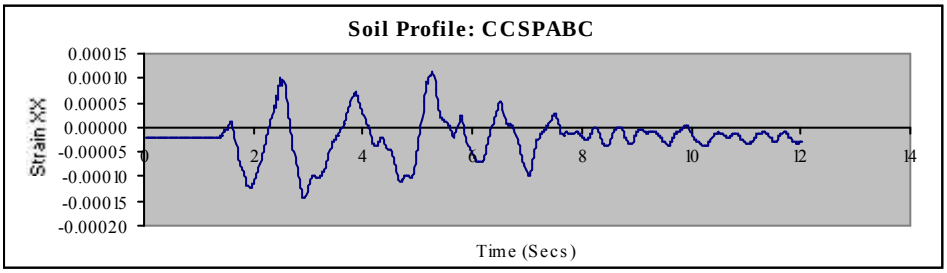
Soil Profile: CCSPABC
0.00015
0.00010
0.00005
0.00000
-0.00005
-0.00010
-0.00015
-0.00020
Strain XX
0
2
4
6
8
10
12
14
Time (Secs)

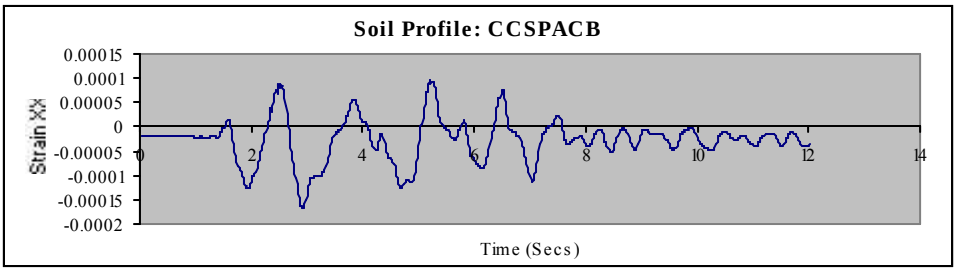
Soil Profile: CCSPACB
0.00015
0.0001
0.00005
0
-0.00005
-0.0001
-0.00015
-0.0002
Strain XX
0
2
4
6
8
10
12
14
Time (Secs)

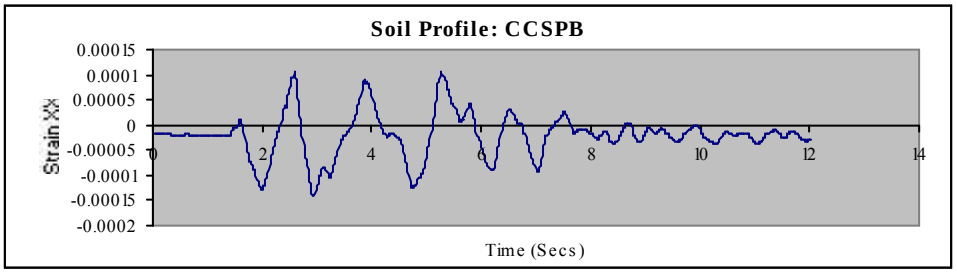
Soil Profile: CCSPB
0.00015
0.0001
0.00005
0
-0.00005
-0.0001
-0.00015
-0.0002
Strain XX
0
2
4
6
8
10
12
14
Time (Secs)

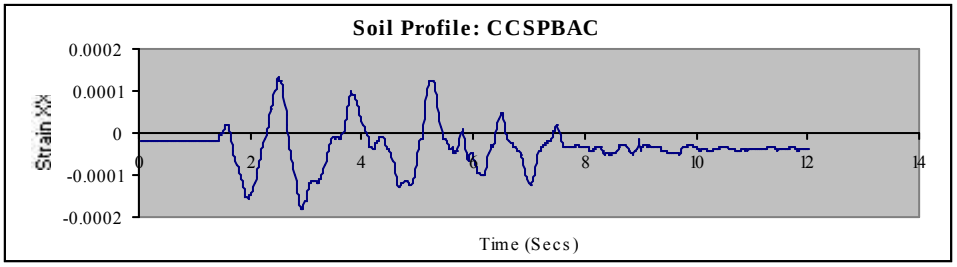
Soil Profile: CCSPBAC
0.0002
0.0001
0
-0.0001
-0.0002
Strain XX
0
2
4
6
8
10
12
14
Time (Secs)

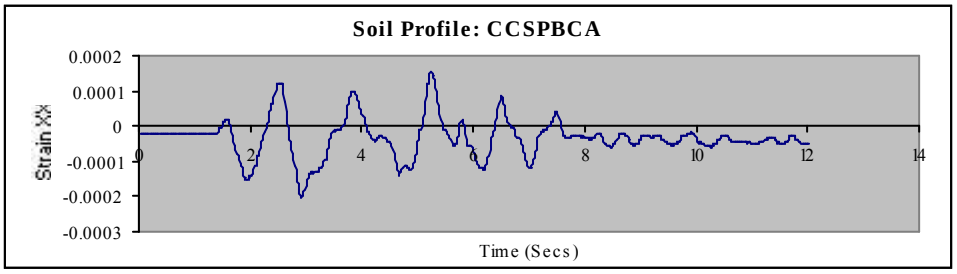
Soil Profile: CCSPBCA
0.0002
0.0001
0
-0.0001
-0.0002
-0.0003
Strain XX
0
2
4
6
8
10
12
14
Time (Secs)

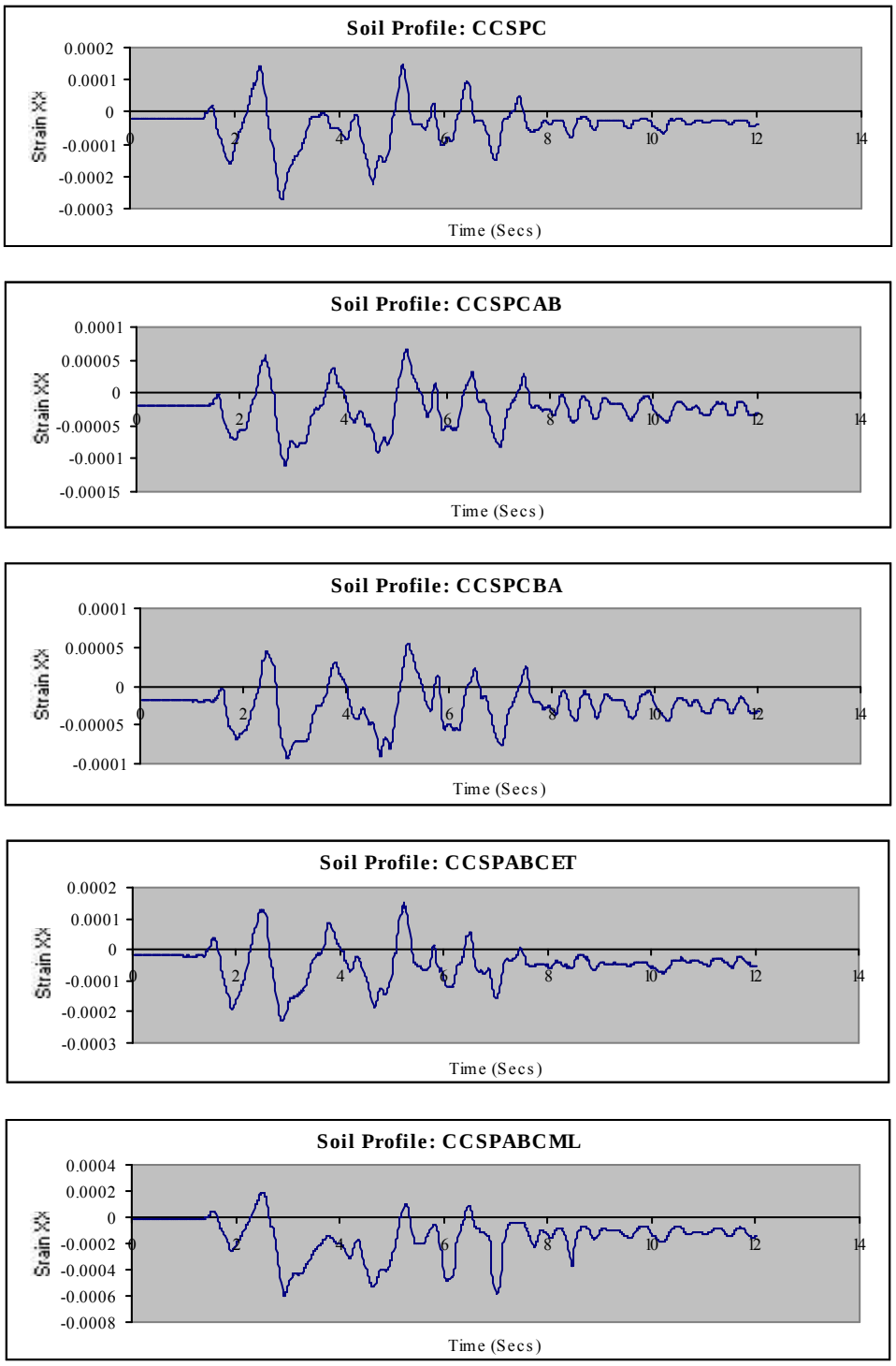

Figure 5.18: Variation of Strain XX in time domain for various soil profiles

Variation of □yy

The plots of variation of □yy in time domain are presented in figure 11.

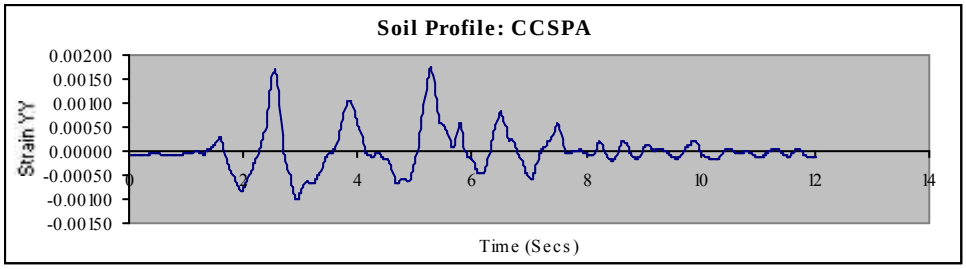
Soil Profile: CCSPA
Strain Y'Y
0.00200
0.00150
0.00100
0.00050
0.00000
-0.00050
-0.00100
-0.00150
0
2
4
6
8
10
12
14
Time (Secs)

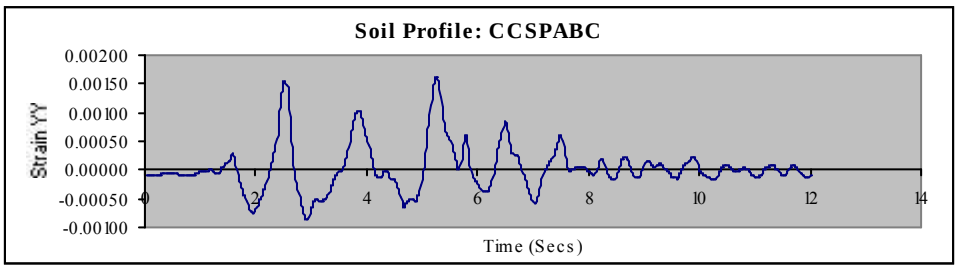
Soil Profile: CCSPABC
Strain Y'Y
0.00200
0.00150
0.00100
0.00050
0.00000
-0.00050
-0.00100
0
2
4
6
8
10
12
14
Time (Secs)

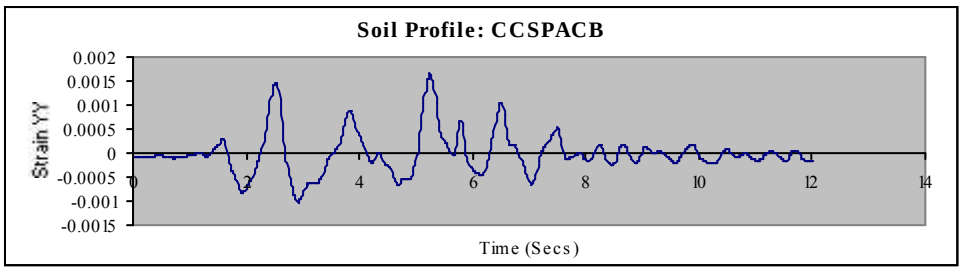
Soil Profile: CCSPACB
Strain Y'Y
0.002
0.0015
0.001
0.0005
0
-0.0005
-0.001
-0.0015
0
2
4
6
8
10
12
14
Time (Secs)

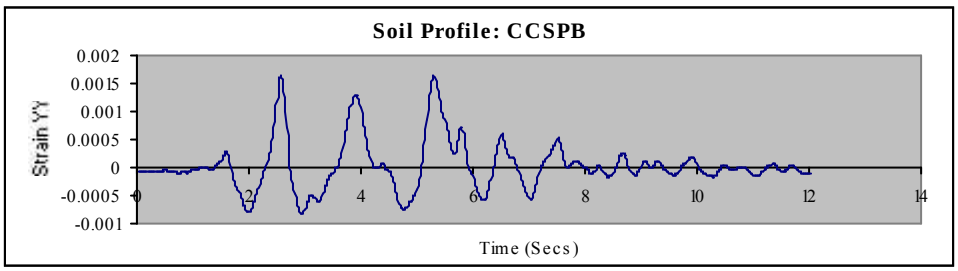
Soil Profile: CCSPB
Strain Y'Y
0.002
0.0015
0.001
0.0005
0
-0.0005
-0.001
0
2
4
6
8
10
12
14
Time (Secs)

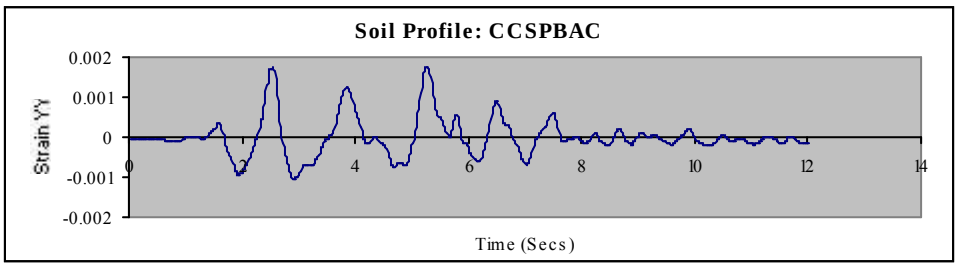
Soil Profile: CCSPBAC
Strain Y'Y
0.002
0.001
0
-0.001
-0.002
0
2
4
6
8
10
12
14
Time (Secs)

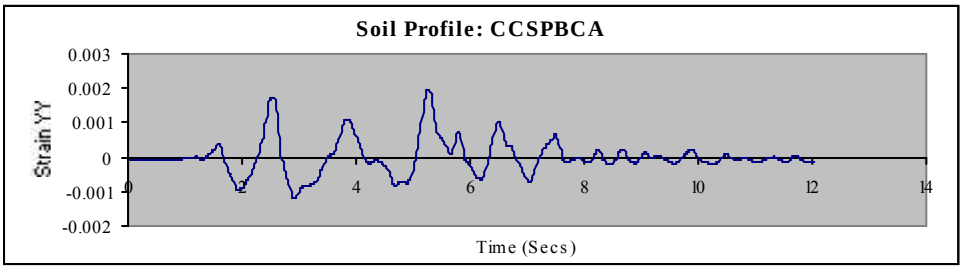
Soil Profile: CCSPBCA
Strain Y'Y
0.003
0.002
0.001
0
-0.001
-0.002
0
2
4
6
8
10
12
14
Time (Secs)

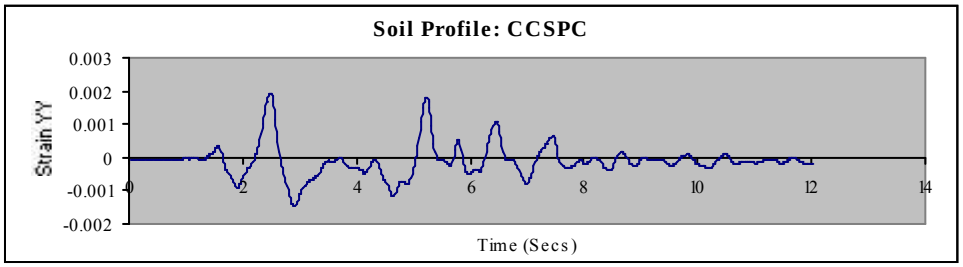

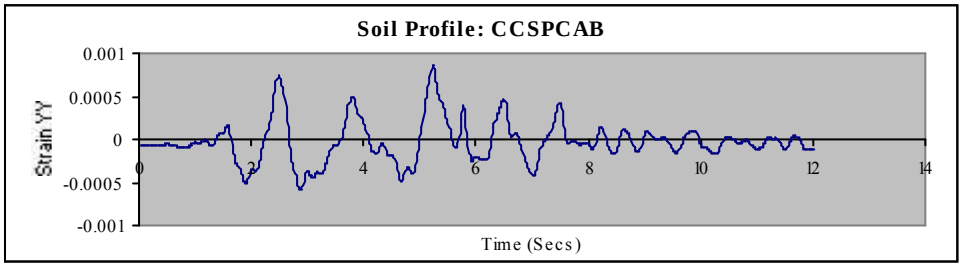

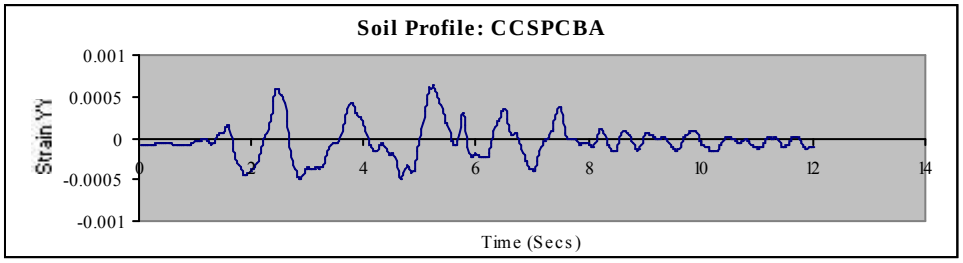

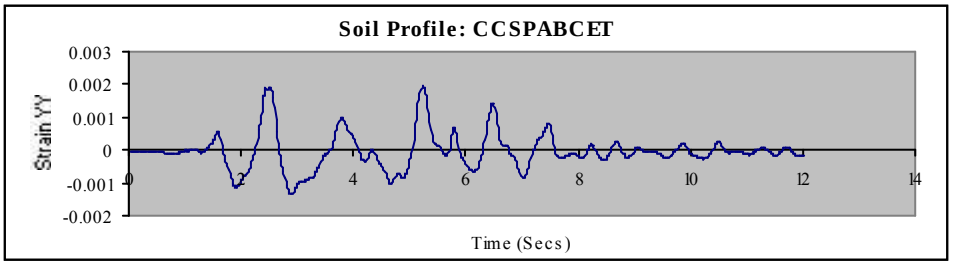

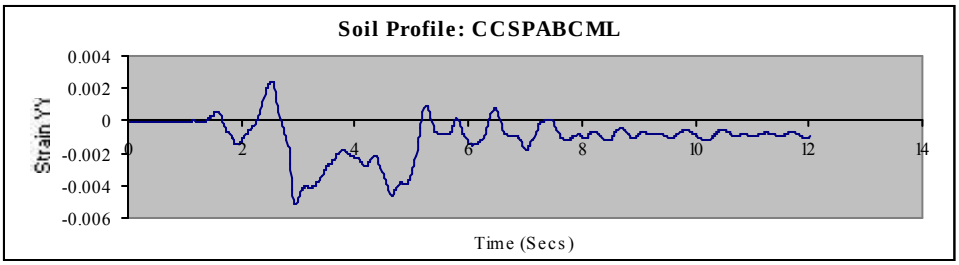

Figure 5.19: Variation of Strain YY in time domain for various soil profiles

Variation of □xy

The plots of variation of □xy in time domain are presented in figure 11.

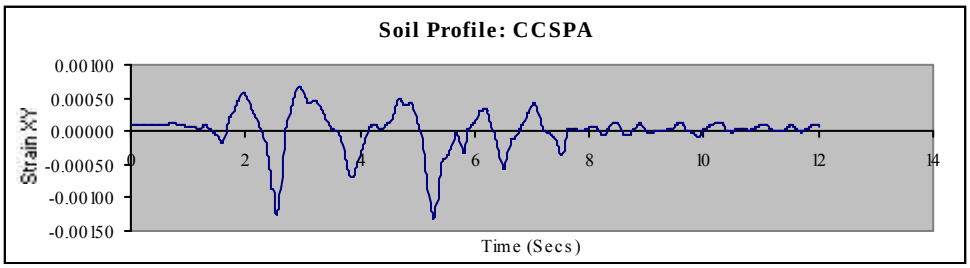
Soil Profile: CCSPA
0.00100
0.00050
0.00000
-0.00050
-0.00100
-0.00150
Strain XY
0
2
4
6
8
10
12
14
Time (Secs)

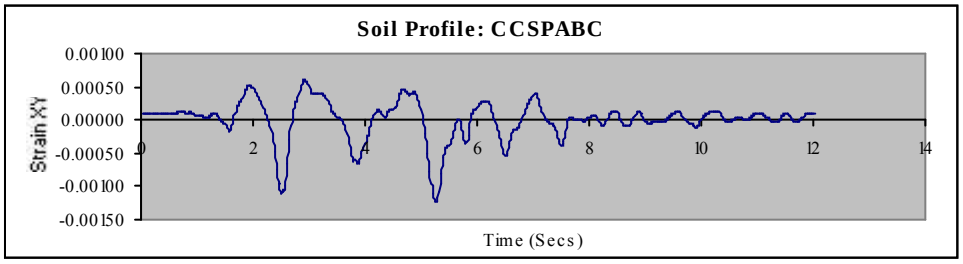
Soil Profile: CCSPABC
0.00100
0.00050
0.00000
-0.00050
-0.00100
-0.00150
Strain XY
0
2
4
6
8
10
12
14
Time (Secs)

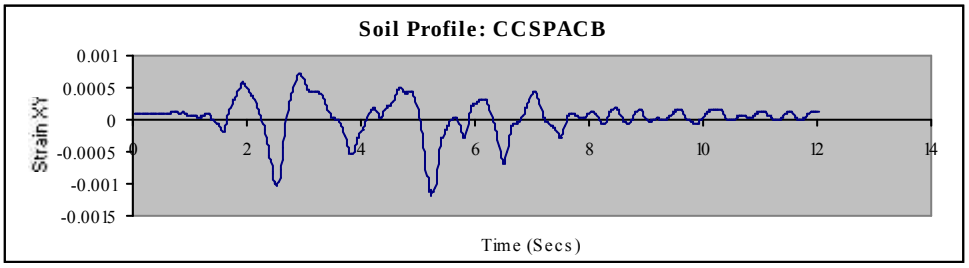
Soil Profile: CCSPACB
0.001
0.0005
0
-0.0005
-0.001
-0.0015
Strain XY
0
2
4
6
8
10
12
14
Time (Secs)

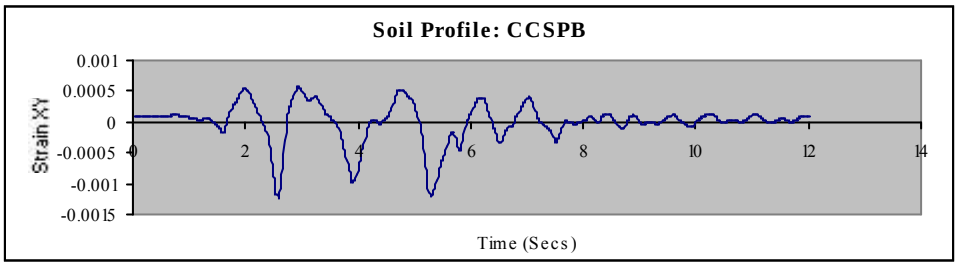
Soil Profile: CCSPB
0.001
0.0005
0
-0.0005
-0.001
-0.0015
Strain XY
0
2
4
6
8
10
12
14
Time (Secs)

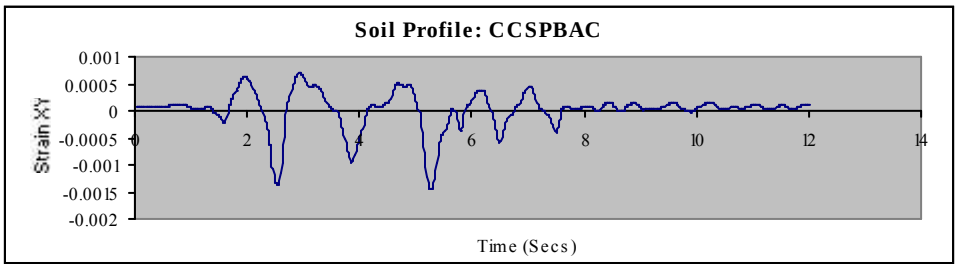
Soil Profile: CCSPBAC
0.001
0.0005
0
-0.0005
-0.001
-0.0015
-0.002
Strain XY
0
2
4
6
8
10
12
14
Time (Secs)

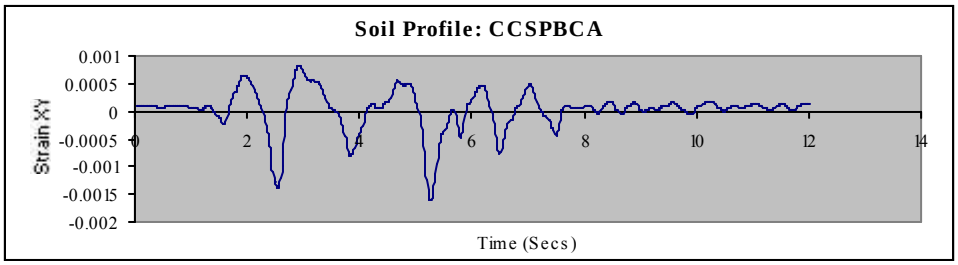
Soil Profile: CCSPBCA
0.001
0.0005
0
-0.0005
-0.001
-0.0015
-0.002
Strain XY
0
2
4
6
8
10
12
14
Time (Secs)

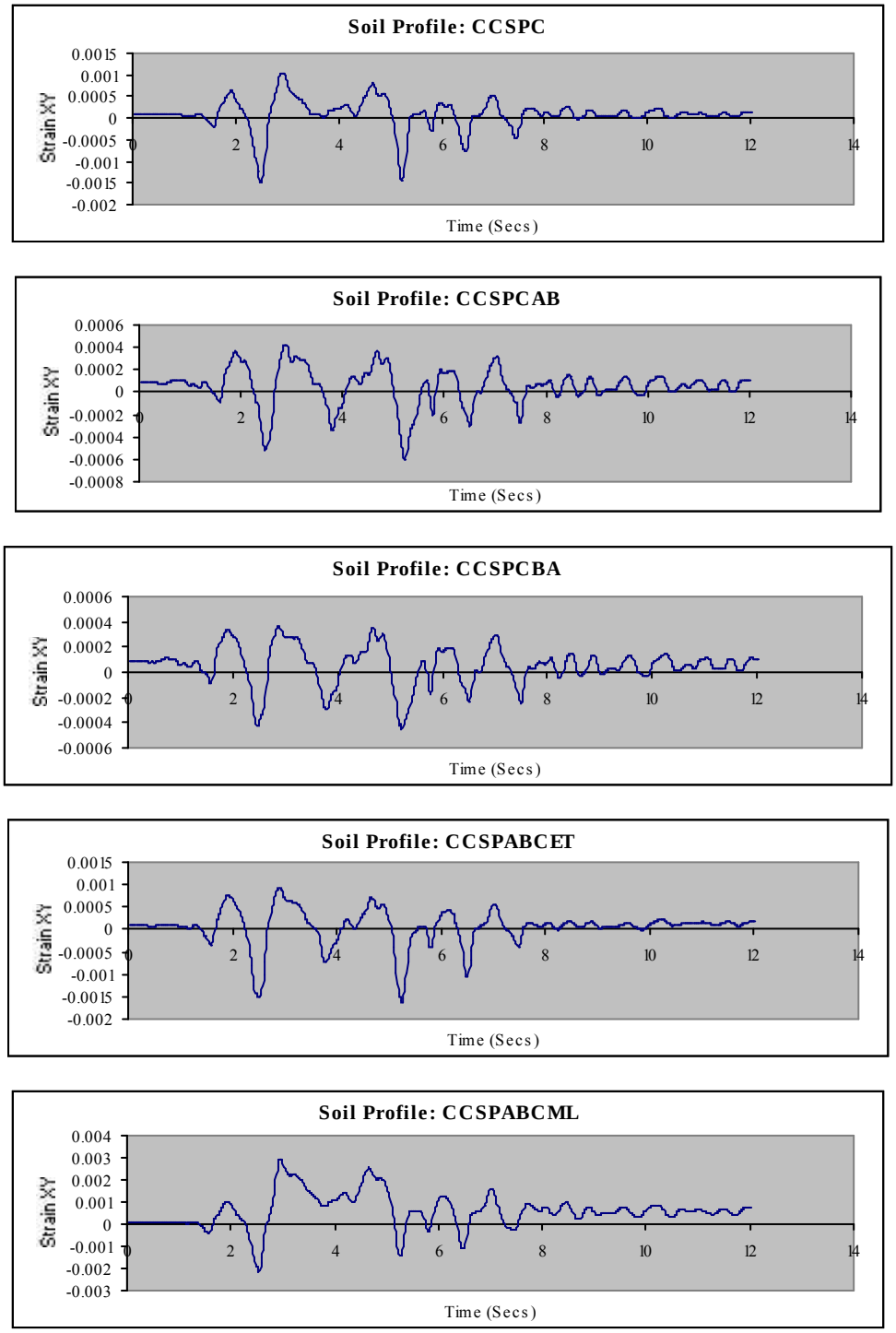

Figure 5.20: Variation of Strain XY in time domain for various soil profiles

The nature of □xx stress history of the soil profile CC_SP_ABC_MLST is quite different from the other soil profiles. Other soil profiles have got similar nature of □xx stress history. The maximum □xx of about -7.5 N/mm2 occurs in this case.

However the nature of □yy stress history is similar for all the soil profiles. Here also maximum □yy of about -20 N/mm2 occurs in case of soil profile CC_SP_ABC_MLST.

The nature of □xy stress history is different in case of soil profiles CC_SP_BCA and CC_SP_ABC_MLST. Maximum □xy stress of about 10 N/mm2 occurs in case of soil profile CC_SP_ABC_MLST.

The nature of □xx, □yy and □xy strain histories is different in case of soil profiles CC_SP_C and CC_SP_ABC_MLST.

The maximum □xx of about -0.005 occurs in case of soil profile CC_SP_ABC_MLST.

The maximum □yy of about -0.0007 occurs in case of soil profile CC_SP_ABC_MLST.

The maximum □xy of about 0.003 occurs in case of soil profile CC_SP_ABC_MLST.

6 CONCLUSIONS

This research work has been carried out to access the performance of the covered canal of the SIKTA irrigation project in particular and underground tunnel structures in general. The severe damage and collapse of the underground structures in recent earthquakes, particularly the 1995 Kobe earthquake has triggered the interest in carrying out this research. This research has revealed some thoughtful as well as interesting results regarding the performance of the covered canal. The conclusions drawn from this research is as follows.

1. Finite element method can be used effectively and efficiently to study the soil-structure interaction problems.
2. While carrying out finite element analysis, the length of the soil mass, i.e., the lateral extent of the soil mass to be considered works out to be very large. This requires considerable time and effort for carrying out the study. There is no way other than to carry out trial and error procedure to determine this length.
3. The lateral boundaries should be modeled properly to account for far field effect; otherwise the reflection of waves from these boundaries will affect the response of the underground structure.
4. The different conditions of water levels have got little affect on the overall performance of the covered canal when hydrodynamic effects of water are not considered.
5. In general, the properties and type of soil surrounding the underground structure have got considerable effect on the performance of the underground structure.
6. In reality, the soil consists of multi layered soil profile. This fact has to be taken into account properly. Analysis conducted by taking average property values won't give the realistic results. Particularly, the properties of the soil layers around the underground structure have to be accessed in detail. It has been found out that the soil profile around the underground structure has got considerable effect on the performance of it.
7. Not only the properties of soil layers, but the thickness of the soil layers also have got considerable effect on the performance of the underground structure. With the identical soil properties but the thickness of the middle layer soil made smaller and placing this middle layer around the underground structure, damage was found to be considerable.

8. The soil exploration has to be carried out to a considerable depth beyond the base of the structure up to a depth where the soil layer can be considered as the seismic bedrock.
9. The geological bedrock is generally located at several kilometers below the ground surface. So, while carrying out the finite element analysis, it becomes practically impossible to incorporate such depths. Further, at such depths soil properties cannot be accessed accurately. So, bedrock has to be assigned at shallow depths, which is accurate enough for engineering purposes. Rational methodologies for assigning the seismic bedrock have to be developed.
10. It can be felt from this study that the generalized and simplified design methodologies cannot be used for different conditions of soil profiles. Each case is different from the other and thus each of this case have to be dealt with separately. Moreover, nonlinear analysis procedures have to be employed for the analysis of the tunnel-soil interaction problems.
11. More computations are needed to fully understand the mechanism and performance of the underground structures embedded in multi-layered soils.
12. With the soil profile taken to be similar to the soil profile of the head works area, the covered canal is found to be safer under the 1995 Kobe earthquake.

7 RECOMMENDATIONS FOR FUTURE WORKS

1. The research has been carried out on a three bay arch type covered canal structure. Study can be conducted on one and two bay covered canal structures and compared with the three bay one.
2. An arch type three bay structure has been studied in the current research. Study on an equivalent three bay rectangular structure can also be made.
3. A high acceleration earthquake wave has been used in the analysis. Instead of this, a low to moderate acceleration earthquake wave can be used to study the performance of the covered canal.
4. Vertical acceleration has not been considered in the current analysis. Combination of horizontal and vertical acceleration can be used to study the performance.
5. Hydrodynamic effect can be incorporated in the study of the covered canal.
6. Coupled method utilizing finite elements and boundary elements can be used to study the performance of the covered canal.

8 REFERENCES

Rosenblueth, E. ed. (1980). Design of Earthquake Resistant Structures, Pentech Press, London: Plymouth, pp. 223-260.

Kramer, S. L. (1996). Geotechnical Earthquake Engineering, Pearson Education (Singapore) Pte. Ltd., Indian Branch, Delhi, pp. 280-303.

Kausel, E. A. M (1983, November), Soil – Structure interaction, Notes for Seminar held at the National Taiwan Institute of Technology, Taipei, Taiwan Republic of China, pp. 459-496.

An, X. (1996). Failure Analysis and Evaluation of Seismic Performance for Reinforced Concrete in Shear, Ph. D Dissertation, Department of Civil Engineering, The University of Tokyo, Japan.

Gazetas, G., Gerolymos, N., and Anastasopoulos, I. (2004). Response of three Athens metro underground structures in the 1999 Parnitha earthquake, Soil Dynamics and Earthquake Engineering, doi: 10.1016/j.soildyn.2004.11.006, pp. 617-633.

Para-Montesinos, et.al (2006, January-February). Evaluation of Soil-Structure Interaction and Structural Collapse in Daikai Subway Station During Kobe Earthquake, Technical Paper, ACI Structural Journal, Vol. 103, No. 1, pp 113-122.

Samata, S., Ohuchi, H. and Matsuda,a T. (1997). A study of the Damage of subway structures during the 1995 Hanshin-Awaji Earthquake, Cement and Concrete composites, 19, Elsevier Science Ltd., pp. 223-239.

Liu, H., and Song, E. (2005). Seismic Response of Large underground structures in liquefiable soils subjected to horizontal and vertical earthquake excitation, Computers & Geotechnics 32, doi: 10.1016/j.compgeo.2005.02.002, Elsevier Ltd., pp. 223-244.

Choi, J.S., Lee, J.S., and Kim, J.M. (2002, June). Nonlinear Earthquake Response Analysis of 2-D underground structures with Soil-structure interaction including

separation and sliding at interface, 15th ASCE Engineering Mechanics conference, Columbia University, New York, NY.

Nishioka, T. and Unjoh, S. A Simplified Seismic Design Method for Underground Structures based on the Shear Transmitting Characteristics, http://www.pwri.go.jp/eng/kokusai/conference/nishioka01.pdf.

Sarigul, N. G., (1997). Parametric studies on vertical boundary location in dynamic finite element analysis, Computers & Structures, Vol. 62, No. 3, Elsevier Science Ltd., pp. 595-601.

Hashash, Y.M.A., Hook, J.J, Schmidt, B., and Yao, J-I-C. (2001). Seismic design and analysis of underground structures, Science Direct, doi: 10.1016/S0886-7798 (01) 00051-7.

Tadanobu, S. (ed) (2000). Dynamic Analysis and Earthquake Resistant Design, Volume 2: Method of Dynamic Analysis, JSCE, Oxford & IBH Publishing Co. Pvt. Ltd., New Delhi, pp. 172-201.

Sears, F.W., Zemansky, M.W., and Young, H.D. (1985). University Physics, Narosa Publishing House, New Delhi, pp. 420-422.

Okamura, H. and Maekawa, K. (1991). Nonlinear Analysis and Constitutive Models of Reinforced Concrete, Gihado Shuppan Co., Tokyo.

Maekawa, K., Pimanmas, A., and Okamura, H. (2003). Nonlinear Mechanics of Reinforced Concrete, SPON Press, London.

Wang, J. N. (1993). Seismic Design of Tunnels, A State-of-the-art approach, Monograph 7, Parsons Brickerhoff Quade & Douglas, Inc., New York.

SIKTA Irrigation Project-Feasibility Study-Main Report (2003, October), http:// www.gitec-consult.de/IDP-Nepal/SIKTA_MR.

Dash, S. R., and Jain, S. K. (2007, July). IITK-GSDMA Guidelines for Seismic Design of Buried Pipelines: Provisions with commentary and Explanatory Examples, Indian Institute of Technology Kanpur, Kanpur.

Upreti, B. N. (2001, April). Earthquake and Earthquake Hazards in Nepal, News Bulletin of Nepal Geological Society, Vol. 18.

Geological Study (Headworks Area and Main Canal up to 15 km), Final Report, Sikta Irrigation Project, Jawalakhel, Lalitpur, May 2007.

Final Report on Soil Investigation Works of Sikta Headworks, Sikta Irrigation Project, Jawalakhel, Lalitpur, May 2006.

IS 1893 (Part 1):2002, Indian Standard Criteria for Earthquake Resistant Design of Structures, Part 1: General provisions and Buildings, fifth revision, BIS, 2002.

NBC 105:1994, Seismic Design of Buildings in Nepal, Department of Buildings, Nepal, 1994.

Cervenka, V. (2002). Computer Simulation of Failure of Concrete Structures for Practice, 1st Fib Congress 2002 concrete structures in 21st century, Osaka, Japan, Keynote lecture in session 13, pp. 289-304.